

2007

# Signaling By Protease-Activated Receptors in Gastrointestinal Smooth Muscle

Wimolpak Sriwai

*Virginia Commonwealth University*

Follow this and additional works at: <http://scholarscompass.vcu.edu/etd>

 Part of the [Physiology Commons](#)

© The Author

---

Downloaded from

<http://scholarscompass.vcu.edu/etd/656>

This Dissertation is brought to you for free and open access by the Graduate School at VCU Scholars Compass. It has been accepted for inclusion in Theses and Dissertations by an authorized administrator of VCU Scholars Compass. For more information, please contact [libcompass@vcu.edu](mailto:libcompass@vcu.edu).

© Wimolpak Sriwai 2007

All Rights Reserved

SIGNALING BY PROTEASE-ACTIVATED RECEPTORS IN GASTROINTESTINAL  
SMOOTH MUSCLE

A Dissertation submitted in partial fulfillment of the requirements for the degree of  
Doctor of Philosophy at Virginia Commonwealth University.

by

WIMOLPAK SRIWAI  
Master of Science, Virginia Commonwealth University, 2001  
Bachelor of Science, Khon Kaen University, Thailand, 1996

Director: S. Murthy Karnam, Ph.D.  
Professor, Department of Physiology

Virginia Commonwealth University  
Richmond, Virginia  
May 2007

## Acknowledgement

I would like to express my gratitude to my advisor, Dr. S. M. Karnam, who not only served as my advisor but also encouraged and challenged me throughout my academic program. I am indebted to him for the warmth, great insights, perspectives, guidance and sense of humor. This dissertation could not have been written without him.

My sincere thanks also to Dr. J. R. Grider who patiently guided and assisted me through the studies and dissertation process. Also thanks to my committee members, Dr V. Lyall, Dr. R. J. Witorsch, Dr. S. A. Gudas and Dr. D. V. Simpson, who offered guidance and support and also read my numerous revisions and helped make some sense of the confusion.

My thanks go to Dr. G. M. Makhlouf and Dr. G. D. Ford for helping in various ways to clarify the things related to my academic works and to my living in the Virginia in time with excellent guidance. Thanks again to Dr. S. M. Karnam, Dr. J. R. Grider, and the Department of Physiology for providing me with the financial means during my graduate studies and research over the past years.

I am most especially grateful to my parents, Tongmee and Kanpech Sriwai, for their eternal love and support. I would like to extend sincere gratitude to the School of Allied Health Sciences of Thammasat University, for providing me the scholarships and opportunity for me to pursue my graduate studies.

Lastly, I would like to thank many individuals, friends and colleagues who have not been mentioned here personally and endured this long process with me, always offering support and love in making this educational process a success. I thank them all.

## Table of Contents

	Page
<b>Acknowledgement .....</b>	<b>ii</b>
<b>List of Tables .....</b>	<b>viii</b>
<b>List of Figures.....</b>	<b>ix</b>
<b>List of Abbreviations .....</b>	<b>xii</b>
<b>List of Symbols .....</b>	<b>xvii</b>
<b>Protease-Activated Receptors (PARs) and Their Ligands.....</b>	<b>1</b>
<b>1.1 Introduction .....</b>	<b>1</b>
<b>1.2 Molecular Organization of PARs.....</b>	<b>2</b>
<b>1.3 Signal Transduction Pathways Activated by PARs .....</b>	<b>6</b>
<b>1.3.1 Signaling by PAR1 .....</b>	<b>7</b>
<b>1.3.2 Signaling by PAR2 .....</b>	<b>11</b>
<b>1.3.3 Signaling by PAR3 and PAR4 .....</b>	<b>12</b>
<b>1.4 Desensitization of PARs .....</b>	<b>12</b>
<b>PARs in Inflammation .....</b>	<b>14</b>
<b>2.1 PARs in Neurons and Neuronal Inflammation .....</b>	<b>14</b>

2.2	Role of PARs in Tissue Repair .....	17
<b>Function of PARs in Gastrointestinal Tract.....</b>		<b>22</b>
3.1	Protective Roles of PARs in Gastric Mucosa .....	22
3.2	Role of PARs in Neurotransmission .....	24
3.3	Role of PARs in Ion Transport .....	25
3.4	Role of PARs in Exocrine Secretion .....	28
3.5	Roles of PARs in Regulation of Gastric Mucosal Circulation.....	28
3.6	PARs Modulate Gastrointestinal Tract Smooth Muscle Contractility	29
<b>Review of Signaling Pathways Mediating Contraction .....</b>		<b>32</b>
<b>Significance.....</b>		<b>37</b>
<b>Hypothesis and Specific Aims .....</b>		<b>38</b>
6.1	Hypothesis .....	38
6.2	Specific Aims .....	38
<b>MATERIALS AND METHODS .....</b>		<b>40</b>
7.1	Materials.....	40
7.2	Methods .....	42
7.2.1	Collection of tissue .....	42
7.2.2	Preparation of dispersed gastric smooth muscle cells .....	42
7.2.3	Preparation of cultured gastric smooth muscle cells .....	43
7.2.4	Minigene construction .....	43

7.2.5	Transfection of dominant negative mutants and minigene constructs into cultured smooth muscle cells .....	44
7.2.6	Identification of PAR1- and PAR2-activated G proteins .....	47
7.2.7	Assay for Phosphoinositide (PI) hydrolysis (PLC- $\beta$ activity) .	47
7.2.8	Assay for Rho Kinase activity .....	49
7.2.9	Assay for adenylyl cyclase activity .....	50
7.2.10	Phosphorylation of G <sub>12</sub> and G <sub>13</sub> .....	50
7.2.11	Western blot analysis .....	51
7.2.12	Measurement of contraction in dispersed smooth muscle cells	52
<b>Statistical Analysis .....</b>		<b>53</b>
<b>Experimental Approach .....</b>		<b>54</b>
<b>Results .....</b>		<b>58</b>
10.1	Co-expression of PAR1 and PAR2 in Gastric Smooth Muscle .....	58
10.2	Distinctive Patterns of G-protein Activation by PAR1 and PAR2 in Smooth Muscle.....	58
10.3	Signaling Pathways Activated by PAR1 and PAR2 in Smooth Muscle	61
<b>Discussion.....</b>		<b>129</b>
11.1	Co-expression of PAR1 and PAR2 in Gastric Smooth Muscle .....	130
11.2	Distinctive Pattern of G protein-dependent Signaling by PAR1 and PAR2 in Smooth Muscle .....	130
11.3	Stimulation of PI Hydrolysis by PAR1 and PAR2 .....	131



<b>11.4</b>	<b>Inhibition of Adenylyl Cyclase by PAR1 and PAR2 .....</b>	<b>133</b>
<b>11.5</b>	<b>Activation of RhoA-dependent Pathways by PAR1 and PAR2 .....</b>	<b>134</b>
<b>11.6</b>	<b>PAR1 and PAR2 Mediated Contraction in Gastric Smooth Muscle.</b>	<b>136</b>
<b>11.6.1</b>	<b>Signaling pathways mediating the initial muscle contraction by PAR1 and PAR2 in smooth muscle .....</b>	<b>138</b>
<b>11.6.2</b>	<b>Signaling pathways mediating the sustained muscle contraction by PAR1 and PAR2 in smooth muscle .....</b>	<b>139</b>
<b>11.7</b>	<b>Feedback Inhibition of RhoA by G<sub>12</sub>-coupled PAR1 and G<sub>13</sub>-coupled PAR2 in Smooth Muscle .....</b>	<b>142</b>
	<b>Conclusion .....</b>	<b>155</b>
	<b>List of References .....</b>	<b>158</b>
	<b>Vita .....</b>	<b>172</b>

## List of Tables

	Page
<b>Table 1. Protease-activated receptor pharmacology.....</b>	<b>3</b>
<b>Table 2. Sequences of expressed G protein COOH-terminal peptides.....</b>	<b>45</b>
<b>Table 3. Pharmacological inhibitors of signaling molecules.....</b>	<b>55</b>

## List of Figures

	Page
<b>Figure 1.</b> Activating proteases cleave PARs to expose the tethered ligand domains. ....	8
<b>Figure 2.</b> Signaling by muscarinic m3 receptors via G <sub>q</sub> - and/or G <sub>13</sub> -coupled receptors during the sustained phase of contraction.....	33
<b>Figure 3.</b> Selective expression of protease-activated receptor 1 (PAR1) and PAR2 in rabbit gastric smooth muscle cells.....	59
<b>Figure 4.</b> Distinct pattern of pertussis toxin-sensitive G proteins activated by PAR1-AP and PAR2-AP in rabbit gastric smooth muscle cells. ....	62
<b>Figure 5.</b> Distinct pattern of pertussis toxin-insensitive G proteins activated by PAR1-AP and PAR2-AP in rabbit gastric smooth muscle cells. ....	64
<b>Figure 6.</b> PAR1-AP and PAR2-AP did not activate G <sub>α<sub>s</sub></sub> and G <sub>α<sub>z</sub></sub> in rabbit gastric smooth muscle cells.....	66
<b>Figure 7.</b> Concentration-dependent stimulation of PI hydrolysis (PLC-β activity) by PAR1-AP and PAR2-AP. ....	69
<b>Figure 8.</b> Selective inhibition of PAR2-AP-stimulated PI hydrolysis by pertussis toxin.....	71
<b>Figure 9.</b> Inhibition of PAR1-AP- and PAR2-AP-stimulated PI hydrolysis by G <sub>α<sub>q</sub></sub> minigene or G <sub>α<sub>i</sub></sub> minigene. ....	74
<b>Figure 10.</b> PI hydrolysis stimulated by PAR1-AP and PAR2-AP was regulated by RGS4.....	77
<b>Figure 11.</b> Inhibition of forskolin-stimulated cAMP formation by PAR1-AP and PAR2-AP.....	79

<b>Figure 12.</b>	<b>Inhibition of PAR1-AP- and PAR2-AP-stimulated Rho kinase activity by the selective Rho kinase inhibitor Y27632. ....</b>	<b>82</b>
<b>Figure 13.</b>	<b>Inhibition of PAR1-AP- and PAR2-AP-stimulated Rho kinase activity in muscle cell expressing dominant negative RhoA. ....</b>	<b>84</b>
<b>Figure 14.</b>	<b>Inhibition of PAR1-AP- and PAR2-AP-stimulated Rho kinase activity by G<math>\alpha</math><sub>12</sub> minigene or G<math>\alpha</math><sub>13</sub> minigene, respectively. ....</b>	<b>86</b>
<b>Figure 15.</b>	<b>Time course of PAR1-AP- and PAR2-AP-induced contraction in dispersed gastric smooth muscle cells. ....</b>	<b>89</b>
<b>Figure 16.</b>	<b>Concentration-response curves for the contractile effect of PAR1-AP and PAR2-AP in dispersed gastric smooth muscle cells. ....</b>	<b>91</b>
<b>Figure 17.</b>	<b>Phosphorylation of MYPT1, CPI-17, and MLC<sub>20</sub> by PAR1-AP and PAR2-AP in dispersed muscle cells. ....</b>	<b>94</b>
<b>Figure 18.</b>	<b>Blockade of PAR1-AP-induced initial contraction by inhibitors of phospholipase C and MLC kinase. ....</b>	<b>96</b>
<b>Figure 19.</b>	<b>Blockade of PAR2-AP-induced initial contraction by inhibitors of phospholipase C, MLC kinase, and pertussis toxin. ....</b>	<b>98</b>
<b>Figure 20.</b>	<b>Blockade of PAR1-AP-induced sustained contraction by the inhibitor of PKC. ....</b>	<b>101</b>
<b>Figure 21.</b>	<b>Blockade of PAR2-AP-induced sustained contraction by the inhibitor of Rho kinase. ....</b>	<b>103</b>
<b>Figure 22.</b>	<b>Sequential activation of RhoA and NF-<math>\kappa</math>B pathways by PAR1-AP. ....</b>	<b>106</b>
<b>Figure 23.</b>	<b>Sequential activation of RhoA and NF-<math>\kappa</math>B pathways by PAR2-AP and PKA-mediated phosphorylation of RhoA. ....</b>	<b>108</b>
<b>Figure 24.</b>	<b>Feedback inhibition of PAR1-AP-stimulated Rho kinase activity by PKC. ....</b>	<b>111</b>
<b>Figure 25.</b>	<b>Feedback inhibition of PAR1-AP-stimulated Rho kinase activity by PKA derived from NF-<math>\kappa</math>B pathway and by PKC. ....</b>	<b>113</b>

<b>Figure 26.</b>	<b>PKC-mediated phosphorylation of <math>G\alpha_{12}</math> and PKA-mediated phosphorylation of RhoA by PAR1-AP in freshly dispersed muscle cells. ....</b>	<b>115</b>
<b>Figure 27.</b>	<b>Feedback inhibition of PAR1-AP-stimulated Rho kinase activity by PKA via phosphorylation of RhoA at Ser<sup>188</sup> .....</b>	<b>118</b>
<b>Figure 28.</b>	<b>Feedback inhibition of PAR2-AP-stimulated Rho kinase activity by PKA derived from NF-<math>\kappa</math>B pathway and by PKC.....</b>	<b>120</b>
<b>Figure 29.</b>	<b>Feedback inhibition of PAR2-AP-stimulated Rho kinase activity by PKA via phosphorylation of RhoA at Ser<sup>188</sup> .....</b>	<b>123</b>
<b>Figure 30.</b>	<b>PKA-mediated phosphorylation of RhoA by PAR2-AP.....</b>	<b>125</b>
<b>Figure 31.</b>	<b>Pathways mediating initial and sustained contraction by PAR1. ....</b>	<b>143</b>
<b>Figure 32.</b>	<b>Pathways mediating initial and sustained contraction by PAR2. ....</b>	<b>145</b>
<b>Figure 33.</b>	<b>Feedback inhibition of PAR1-stimulated RhoA by cAMP-independent PKA derived from activation of canonical NF-<math>\kappa</math>B pathway and by PKC.....</b>	<b>148</b>
<b>Figure 34.</b>	<b>Feedback inhibition of PAR2-stimulated RhoA by cAMP-independent PKA derived from activation of canonical NF-<math>\kappa</math>B pathway.....</b>	<b>150</b>

## List of Abbreviations

5-HT	5-hydroxytryptamine
ACh	acetylcholine
ATP	adenosine triphosphate
bp	base pair
BSA	bovine serum albumin
CaM	calmodulin
cAMP	cyclic adenosine 3',5'-monophosphate
CCK	cholecystokinin
cDNA	complementary deoxyribonucleic acid
cGMP	cyclic guanosine 3',5'-monophosphate
CGRP	calcitonin gene-related peptide
cmp	count per minute
COX-1	cyclooxygenase-1
CPI-17	PKC-potentiated inhibitor 17-kDa protein
DAG	diacylglycerol
DMEM	Dulbecco's modified Eagle's medium
dNTP	deoxynucleotidetriphosphates
DRG	dorsal root ganglia

DTT	dithiotreitol
ECM	extracellular matrix
EDHF	endothelium-derived hyperpolarizing factor
EGFR	epidermal growth factor receptor
ErbB2	v-erb-b2 erythroblastic leukemia viral oncogene homolog 2
ERK	extracellular signal-regulated kinases
ET	endothelin
FXa	blood coagulation factor Xa
GAPDH	glyceraldehydes-3-phosphate dehydrogenase
GEF	guanosine exchange factor
GI	gastrointestinal
GMBF	gastric mucosal blood flow
GRKs	G protein-coupled receptor kinases
GTP	guanosine triphosphate
h	hour
HBEC	human bronchial epithelial cells
HEPES	N-2-hydroxyethylpiperazine-N'-2-ethane- sulfuric acid
IBMX	3-isobutyl-1-methyl xanthine
ICAMs	intracellular adhesion molecules
I $\kappa$ B $\alpha$	NF- $\kappa$ B inhibitor

IKK2	I $\kappa$ B $\alpha$ kinase
IKK $\beta$	I $\kappa$ B $\beta$ kinase
IL	interleukin
IP <sub>3</sub>	inositol-1,4,5-triphosphate
kDa	10 <sup>3</sup> Dalton
L-NAME	N <sup>ω</sup> -nitro-L-arginine methyl ester
M	Molar
MAPK	mitogen-activated protein kinases
MCP-1	monocyte chemoattractant protein-1
MEF	mouse embryonic fibroblasts
min	minute
MLC <sub>20</sub>	20 kD regulatory light chain of myosin II
MLCK	Ca <sup>2+</sup> /calmodulin-dependent myosin light chain kinase
MLCP	myosin light chain phosphatase
mM	millimolar
MMPs	matrix metalloproteinases
mRNA	messenger ribosomal nucleic acid
MYPT1	myosin phosphatase target subunit 1
NK1 receptor	tachykinin receptor
nM	nanomolar
NO	nitric oxide



PAR1	protease-activated receptor-1
PAR2	protease-activated receptor-2
PAR3	protease-activated receptor-3
PAR4	protease-activated receptor-4
PAR-AP	protease-activated receptor activating peptide
PARs	protease-activated receptors
PBS	phosphate buffer saline solution
PCR	polymerase chain reaction
PGE <sub>2</sub>	prostaglandin E <sub>2</sub>
PGF <sub>1α</sub>	prostaglandin F <sub>1α</sub>
PH	pleckstrin homology domain
PI	phosphatidylinositol
PI3K	phosphatidylinositol 3-kinase
PIP <sub>2</sub>	phosphatidylinositol bisphosphate
PKC	protein kinase C
PLA <sub>2</sub>	phospholipase A <sub>2</sub>
PLC	phospholipase C
PLC-β	phospholipase C beta
PLC-γ	phospholipase C gamma
PLD	phospholipase D
PP1δ	protein phosphatase delta isoform

PTx	pertussis toxin
RGS	regulators of G protein signaling
RNAi	RNA interference
RT-PCR	reverse-transcriptase polymerase chain reaction
S1P <sub>2</sub>	sphingosine-1-phosphate receptors
sec	seconds
Shc	Src homology
SLIGRL	H-Ser-Leu-Ile-Gly-Arg-Leu-NH <sub>2</sub>
SP	substance P
TCA	trichloroacetic acid
TFLLR	H-Thr-Phe-Leu-Leu-Arg-NH <sub>2</sub>
TGF	tumor growth factor
VEGF	vascular endothelial growth factor
VIP	vasoactive intestinal peptide

## List of Symbols

$\text{Ca}^{2+}$	calcium
$[\text{Ca}^{2+}]_i$	cytosolic free calcium
$\text{CaCl}_2$	calcium chloride
$\text{Cl}^-$	chloride
COOH-terminus	carboxy terminus
$\text{EC}_{50}$	effective concentration <sub>50</sub>
$\text{K}^+$	potassium
N-terminus	amino-terminus

## Abstract

### SIGNALING BY PROTEASE-ACTIVATED RECEPTORS IN GASTROINTESTINAL SMOOTH MUSCLE

By Wimolpak Sriwai, Ph.D.

A Dissertation submitted in partial fulfillment of the requirements for the degree of  
Doctor of Philosophy at Virginia Commonwealth University.

Virginia Commonwealth University, 2007

Major Director: S. Murthy Karnam  
Professor, Department of Physiology

In the present study, we have examined the expression of protease-activated receptors (PARs) and characterized their signaling pathways in rabbit gastric muscle cells. Immunoblot analysis revealed expression of PAR1 and PAR2 but not PAR3 or PAR4 in smooth muscle. The PAR1 agonist TFLLR activated  $G_q$ ,  $G_{12}$ , and  $G_{13}$ , but not  $G_{i1}$ ,  $G_{i2}$ ,  $G_{i3}$ ,  $G_s$  or  $G_z$ , whereas the PAR2 agonist SLIGRL activated  $G_q$ ,  $G_{13}$ ,  $G_{i1}$ , and  $G_{i2}$ , but not  $G_{i3}$ ,  $G_{12}$ ,  $G_s$ , or  $G_z$ . Both PAR1 and PAR2 agonists stimulated PI hydrolysis and Rho kinase activity and inhibited cAMP formation. PAR1-stimulated PI hydrolysis was abolished in cells expressing  $G\alpha_q$  minigene, but was not affected in cells expressing  $G\alpha_i$  minigene or in cells treated with pertussis toxin (PTX). PAR2-stimulated PI

hydrolysis was partially inhibited in cells expressing  $G\alpha_q$  or  $G\alpha_i$  minigene and in cells treated with PTx. PAR1- and PAR2-stimulated Rho kinase activity was abolished in cells expressing  $G\alpha_{12}$  or  $G\alpha_{13}$  minigene, respectively. Both PAR1 and PAR2 agonists induced a transient initial contraction that was selectively blocked by the inhibition of PI hydrolysis with U73122 and MLC kinase activity with ML-9. PAR1-induced sustained contraction was preferentially inhibited by the PKC inhibitor bisindolylmaleimide and to a minor extent by the Rho kinase inhibitor Y27632, whereas PAR2-induced sustained contraction was preferentially inhibited by Y27632. Activation of both PAR1 and PAR2 induced MLC20 phosphorylation, whereas phosphorylation of MYPT1 and CPI-17 are receptor-specific: only PAR1 induced CPI-17 phosphorylation and only PAR2 induced MYPT1 phosphorylation.

Activation of PAR1 and PAR2 also induced  $I\kappa B\alpha$  degradation and NF- $\kappa B$  activation; the effects were abolished by the blockade of RhoA activity by *Clostridium botulinum* C3 exoenzyme suggesting NF- $\kappa B$  is downstream of RhoA. PAR1- and PAR2-stimulated Rho kinase activity was significantly augmented by the inhibitors of PKA (PKI), IKK2 (IKKIV), or NF- $\kappa B$  (MG132), and in cells expressing dominant negative mutants of IKK (IKK(K44A),  $I\kappa B\alpha$  ( $I\kappa B\alpha$ (S32A/S36A)), or phosphorylation-deficient RhoA (RhoA(S188A)). In addition, activation of PAR1 induced  $G\alpha_{12}$  phosphorylation, which was abolished by bisindolylmaleimide, suggests that phosphorylation was mediated by PKC derived from the activation of RhoA. Only PAR1-stimulated Rho kinase activity was significantly augmented by the PKC inhibitor. The effect of PKC inhibitor was additive to that of the PKA inhibitor.

## **Protease-Activated Receptors (PARs) and Their Ligands**

### **1.1 Introduction**

Proteases comprise two percent of the human genome. They possess a wide spectrum of biological activities from degradation of proteins to regulation of cell growth. Accumulating evidence indicates that certain serine protease cleave membrane-bound receptors, known as protease-activated receptors (PARs), to initiate a variety of cellular actions. The PARs belong to the G protein-coupled receptor family and have a common mechanism of activation that is very distinct from that of the other G protein coupled receptors. Proteases hydrolyze a specific cleavage site within the extracellular N-terminus domain of the receptor in order to expose a new N-terminus that acts as a ligand. Since the ligand region is attached to the receptor itself, it is called a “tethered ligand”. The tethered ligand binds intramolecularly to regions in the second extracellular loop of the cleaved receptor to activate G proteins and initiate cellular signaling. Thus, these receptors essentially activate themselves via exposure of their tethered ligand. Support for this mechanism of G protein activation came from studies using synthetic peptides as short as 5-6 amino acids, corresponding to the amino acid sequence of the exposed tethered ligand, that mimic the effect of the proteases independent of the proteolytic cleavage of the receptor. Four PARs have been identified and cloned thus far: PAR1, PAR2, PAR3, and PAR4 (132, 167). A large number of proteases can activate all

four identified types of PARs (Table 1), although it remains to be tested whether all of these enzymes will activate PARs under physiological condition. Thrombin activates PAR1, PAR3 and PAR4, whereas trypsin activates PAR2. Thus, pharmacologically, the PARs can be distinguished on the basis of their relative susceptibility to activation by proteases.

## 1.2 Molecular Organization of PARs

Protease-activated receptors were first described as thrombin receptors. Prior to molecular cloning of thrombin receptor cDNAs, the primary method used to determine a number of thrombin-binding proteins and the location of thrombin receptors in different cell types was the analysis of radiolabeled ligand binding to functional thrombin receptors (83). However, due to the discrepancies of ligand binding to existing thrombin-binding proteins and the functional response, such studies were not considered to be conclusive.

Vu et al (164) and Rasmussen et al (140) identified PAR1 using an expression cloning of messenger RNA of thrombin from humans and hamsters in oocytes of *Xenopus*. A single cDNA species that encoded a protein with a 425-amino-acid sequence and an extracellular amino-terminal domain of 75 residues was isolated. It contained a potential thrombin-cleavage site at LDPR<sup>41</sup>/S<sup>42</sup>FLLR within the amino terminus. The PAR1 gene is located on human chromosome 5q13 and contains two exons with one intron interrupting its amino terminus (46).

PAR2 was identified by hybridization screening of a mouse genomic library using a bovine substance K receptor probe (132). PAR2 consists of a 395-amino-acid sequence

**Table 1. Protease-activated receptor pharmacology.**



Receptor	Chromosomal location (human)	Structure	Effector	Selective Ligand			Expression in GI System
				Agonist		Antagonist	
				Protease	Peptide		
PAR1	5q13	<sup>425 aa</sup> LDPR <sup>41</sup> /S <sup>42</sup> FLLR	Gq, G <sub>13</sub> , G <sub>12</sub>	Thrombin Trypsin Plasmin FXa	TFLLRN	SCH 79797 (IC <sub>50</sub> 70 nm)	Esophagus, gastric, intestine, nervous system
PAR2	5q13	<sup>395 aa</sup> SKGR <sup>34</sup> /S <sup>35</sup> LIGRL	Gq, G <sub>11</sub> , G <sub>12</sub> , G <sub>13</sub>	Tryptase Trypsin	SLIGRL		Exocrine gland, gastric, duodenum, ileum, nervous system, pancreas
PAR3	5q13	<sup>374 aa</sup> LPIK <sup>38</sup> /T <sup>39</sup> FRGAP		Thrombin Trypsin			
PAR4	19p12	<sup>385 aa</sup> PAPR <sup>47</sup> / <sup>48</sup> GYPGQV		Thrombin Trypsin	AYPGKFN, GYPGKFN	tc-YPGKFN- NH <sub>2</sub>	GI tract, nervous system

with an extracellular amino-terminus of 46 residues. It contains a trypsin cleavage site at SKGR<sup>34</sup>/S<sup>35</sup>LIGRL. PAR2 is highly sensitive to trypsin treatment and fails to respond to  $\alpha$ -thrombin. Mouse PAR2's amino acid sequence has 30% amino acid homology with that of human PAR1 and 28% amino acid homology with that of mouse PAR1. PAR2 is located on human chromosome 5q13 and consists of two exons (133).

PAR3 was cloned using degenerated primers based on conserved domains of PAR1 and PAR2 to screen RNA from rat platelets (57). Human PAR3 has 27% and 28% sequence homology to human PAR1 and PAR2, respectively. Human PAR3 is 374-amino-acids in length and has a thrombin cleavage site within the extracellular amino terminus at LPIK<sup>38</sup>/T<sup>39</sup>FRGAP. Human PAR3 has two exons and is located proximal to the same locus as PAR1 and PAR2 (145).

PAR4 was identified by searching expressed sequence tag libraries (61). Human PAR4 has an open reading frame encoding a 385-amino-acid protein. A cleavage site for thrombin and trypsin is in the amino terminus at PAPR<sup>47</sup>/<sup>48</sup>GYPGQV. Human PAR4 has 33% amino acid sequence homology with PAR1, PAR2, and PAR3. The human PAR4 gene is located on chromosome 19p12 (167).

Each PAR has a unique N-terminal tethered ligand sequence. The physiological function of each receptor was discerned by the development of receptor-selective synthetic peptides. These peptides are referred to as PAR-activating peptides (PAR-AP) and are found to be surrogate activators of the receptor. These PAR-APs have been very useful in determining the effects of activating PARs in bioassay models *in vivo* and *in vitro*.

### 1.3 Signal Transduction Pathways Activated by PARs

PAR1 is sensitive to activation by thrombin. PAR1 contains a cluster of negatively charge residues in the extracellular domain, which resemble the thrombin-binding site of hirudin. This hirudin-like domain appears to be important for thrombin affinity. The second extracellular loop and the amino terminus of PAR1 are important for tethered ligand interaction and receptor activation (43, 127). Specific serine proteases cleave PAR1 at the R<sup>41</sup>/S<sup>42</sup>FLLRN site to expose a new extracellular N-terminus that acts as a tethered activating ligand (21, 164). The tethered activating ligand binds to the extracellular loop of the cleaved receptor, thereby initiating signaling. The short synthetic 5-6 amino acid peptide, SFLLRN, resembles the receptor-activating sequence of the ordinary receptor that activates PAR1 without having to cleave the actual receptor (164). Besides thrombin, other serine protease enzymes such as trypsin, plasmin, and blood coagulation factor Xa (Fxa) can also activate PAR1.

Unlike PAR1, the PAR2 sequence lacks the hirudin-like domain present in PAR1 (165), thus it is not activated by thrombin. However, PAR2 is activated by trypsin and other trypsin-like enzymes including mast cell tryptase, coagulation factor, and unknown proteases (41). Trypsin cleaves PAR2 at R<sup>34</sup>/S<sup>35</sup>LIGRL to reveal the tethered ligand (100) , which bind to the second extracellular loop thereby initiating signaling (89). Synthetic peptides that mimic the tethered ligand, such as SLIGRL, activate mouse PAR2 without the need of proteolytic activity (10).

Like PAR1, PAR3 contains a thrombin cleavage site at K<sup>38</sup>/T<sup>39</sup>FRGAP and is followed by a hirudin-like domain (57). In contrast to PAR1 and PAR2, synthetic

peptides corresponding to the PAR3-tethered ligand, such as TFRGAP, do not activate PAR3. In addition, mouse PAR3 is unable to signal when expressed alone, but when co-expressed with PAR4, it augments PAR4 responses, suggesting that PAR3 functions as a cofactor for PAR4 (125).

PAR4 has a protease cleavage site but lacks a hirudin-like domain (61). It is activated by thrombin, trypsin, coagulation factor, and unknown proteases (15, 98). In mouse, PAR4 is cleaved by specific serine proteases at R<sup>47</sup>/G<sup>48</sup>YPGKF in the amino terminus to reveal the tethered ligand, which acts as a tethered activating ligand (21, 165).

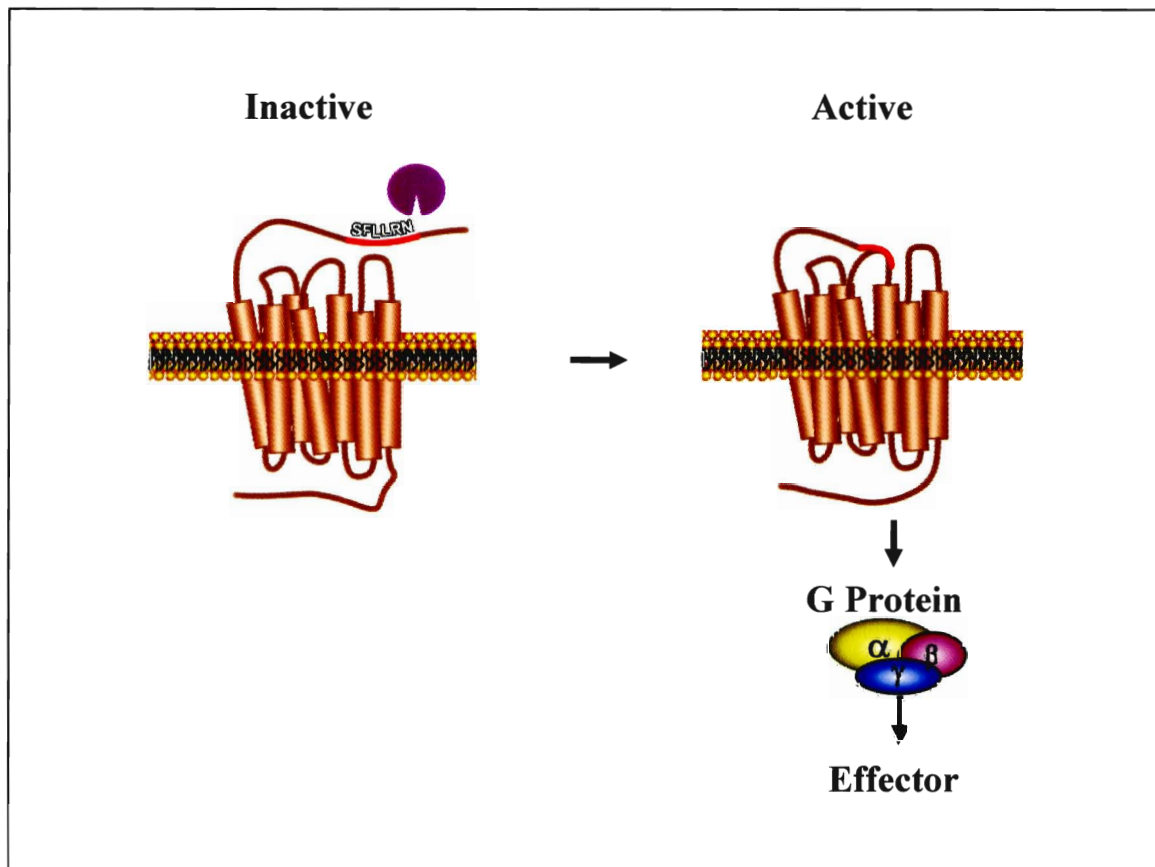
### 1.3.1 Signaling by PAR1

The signal transduction pathways of PARs involve the binding of tethered ligands and activation of several G proteins, tyrosine kinase and serine/threonine kinase molecules. After the selective agonist or tethered ligand binds to the extracellular loop of the receptor, PAR is activated resulting in the receptor conformational changes that permit interaction of receptors with heterotrimeric G proteins leading to G-protein activation and activation of a substantial network of signaling pathways (164) (Fig. 1).

PAR1 couples to several G proteins such as G $\alpha_q$ , G $\alpha_i$ , and G $\alpha_{12/13}$ . Activated PAR1 stimulates several signaling enzymes including phospholipase C beta (PLC- $\beta$ ), PLC- $\gamma$ , p38 MAP kinase, extracellular signal-regulated kinases (ERK) and mitogen-activated protein kinases (MAPK).

Binding of PAR1 to G $\alpha_q$  stimulates PLC- $\beta$  to generate inositol-1,4,5-triphosphate (IP<sub>3</sub>) and diacylglycerol (DAG) (55). IP<sub>3</sub> formation increases intracellular calcium

**Figure 1. Activating proteases cleave PARs to expose the tethered ligand domains.** Proteases (purple circle) generated during inflammation, injury or from the coagulation cascade, inflammatory cells, or bacteria can cleave PARs on a variety of different cells types to expose a tethered ligand domain (red box) that binds to conserved region in second extracellular loop of the cleaved receptor. This in turn initiates the signal transduction.



release from an intracellular storage pool.  $\text{Ca}^{2+}$  mobilization activates  $\text{Ca}^{2+}$ -regulated protein kinases, such as calcium-dependent calmodulin and calcium/calmodulin-activated kinase II. Activation of myosin light chain kinase permits  $\text{G}\alpha_q$  to mediate control of cell contraction.  $\text{Ca}^{2+}$  also binds to the C2 region of protein kinase C (PKC) and this enzyme is subsequently translocated to the plasma membrane where DAG activates it. PKC activation stimulates the ERK/MAP kinase pathway (36). This PKC activation is transient and rapid; therefore, a more pronounced activation of PKC is required for its growth stimulatory effects.

PAR1 is also coupled to the  $\text{G}\alpha_{12/13}$  family and leads to the activation of monomeric G protein RhoA (81). Activation of RhoA results in the stimulation of phospholipase D (PLD) activity. PLD hydrolyzes phosphatidylcholine to choline and phosphatidic acid that is then converted to DAG by phosphomonoesterase. This long-term generation of DAG by PLD causes sustained-activation of PKC and induces its mitogenic effects.

RhoA also stimulates phosphorylation of the regulatory subunits of MLC phosphatase at Thr<sup>696</sup> or Thr<sup>850</sup> via Rho kinase resulting in the inhibition of MLC phosphatase. Thus, activation of Rho kinase permits Rho-mediated control of cell shape, contraction, migration, and cytoskeletal reorganization (45, 62).  $\text{G}\alpha_{12}$  also has been shown to be involved in the activation of Shc-mediated mitogenic signaling (25).

Furthermore, PAR1-mediated  $\text{G}\alpha_q$  activation also induces the activation of PKC- $\delta$  (139). In parallel, activated  $\text{G}_{\beta\gamma}$  subunits released from this same activation induce  $\text{IP}_3$  formation,  $\text{Ca}^{2+}$  mobilization, and phosphatidylinositol 3-kinase (PI3K) activation. Both

PI3-K and PKC- $\delta$  activate the down stream effector Akt that in turn activates I $\kappa$ B $\beta$  kinase (IKK $\beta$ ) resulting in serine phosphorylation of I $\kappa$ B $\alpha$  in NF- $\kappa$ B/I $\kappa$ B $\alpha$  complex. Phosphorylated I $\kappa$ B $\alpha$  is targeted for ubiquitination and degradation by proteosomes. Degradation of I $\kappa$ B $\alpha$  releases NF- $\kappa$ B and thus, activates NF- $\kappa$ B. Upon release, NF- $\kappa$ B migrates to the nucleus where it binds to various gene promoters including ICAM-1 promoter. Both G $\alpha_q$  and G $\beta\gamma_q$  are important in signaling of PAR1-induced NF- $\kappa$ B activation (139).

Because thrombin-induced Ca<sup>2+</sup> mobilization is inhibited by pertussis toxin in some types of cells (56), thrombin receptors have been described as coupling via G $\alpha_i$  to inhibit of adenylyl cyclase and suppress intracellular cAMP formation (116).

### **1.3.2 Signaling by PAR2**

Since pertussis toxin treatment blocked PAR2-induced IP<sub>3</sub> generation and Ca<sup>2+</sup> immobilization, it is suggested that activated PAR2 likely couples to G $\alpha_q$ /G $\alpha_o$ /G $\beta\gamma_i$  and thus activates PLC- $\beta$ 1 and/or PLC- $\beta$ 3 isoforms. PAR2 was also reported to activate the protein tyrosine phosphatase SHP<sub>2</sub> and the tyrosine kinase pathway (40, 168). Other studies also showed that the PAR2 agonist activates ERK1/2 and p38 MAP kinase in the Caco-2 cell line (40).

Downstream signaling of PAR2 also leads to activation of c-Jun-N-terminal kinase (JNK) and p38 MAP kinase in PAR2 expressing keratocyte cell line (63). These could contribute to PAR2-mediated cytokine production and mitogenic signaling (40, 168). Activated PAR2 stimulates prostaglandin E<sub>2</sub> (PGE<sub>2</sub>) and F1 $\alpha$  (PGF<sub>1 $\alpha$</sub> ) generation, suggesting the activation of phospholipase A<sub>2</sub> (PLA<sub>2</sub>) and cyclooxygenase-1 (COX-1)



(79). Additionally, the effects of trypsin as well as PAR2 agonists on the activation of nuclear transcriptional factors have recently been demonstrated (147).

### **1.3.3 Signaling by PAR3 and PAR4**

Little is known about the signal transduction pathways of PAR3 and PAR4. In vascular smooth muscle cells of the human saphenous vein, PAR3 activating peptides induce ERK1/2 activation and  $[Ca^{2+}]_i$  and slightly increase PGE<sub>2</sub> release (11). On the other hand, PAR4 activating peptides mediate p38 MAPK, PLC, and Src protein activation. Further studies implicate that thrombin phosphorylates EGFRs and ErbB2 via a Src kinase inhibitor, a PP1-sensitive pathway in PAR1<sup>-/-</sup> cells that stably overexpress PAR4 (142). In addition, AYPGKF, a selective PAR4 agonist, enhances PGE<sub>2</sub> production,  $[Ca^{2+}]_i$  (3), thromboxane production, and platelet aggregation (47).

### **1.4 Desensitization of PARs**

Unlike the other G-protein coupled receptors in which agonists can diffuse away from the receptors, the catalytic irreversible tethered ligand cannot diffuse away. PARs are disposable “one-shot” receptors, as they are activated in an irreversible manner and then degraded. After proteolytic activation, the tethered ligand of a PAR is always available to interact with the cleaved receptor. PAR signaling, however, is rapidly terminated by mechanisms similar to those classical pathways used by other G protein coupled receptors involving phosphorylation of activated receptors by G protein-coupled receptor kinases (GRKs) (9, 37). Overexpression of GRK3 and GRK5 enhances PAR1 phosphorylation and markedly inhibits inositol phosphate accumulation (58, 156). Activated PARs induce membrane translocation of GRKs, and GRK-mediated

termination of PAR1 usually phosphorylates within the C-terminus or the third intracellular loop (58). In consistence with this finding, Paing et al (136) have shown that mouse embryonic fibroblasts (MEF) transfected with PAR1 mutant C-tail, which has defects in agonist-induced phosphorylation, fail to induce PAR1 internalization from the plasma membrane, suggesting that phosphorylation of the PAR1 cytoplasmic tail is required for internalization.

The  $\beta$ -arrestin isoforms 1 and 2 are widely expressed and bind to phosphorylated G-protein coupled receptors to mediate desensitization and internalization (82). Phosphorylated PARs promote membrane translocation of  $\beta$ -arrestins. Interaction between  $\beta$ -arrestins and phosphorylated PARs mediate dissociation of G-proteins from activated PARs and terminates the signal (136). Desensitization of PAR1 signaling is markedly diminished in MEFs lacking both  $\beta$ -arrestin 1 and  $\beta$ -arrestin 2 isoforms compared with wild-type cells. In cells lacking only  $\beta$ -arrestin 1, PAR1 desensitization is also impaired compared with  $\beta$ -arrestin 2-lacking or wild type cells, suggesting that  $\beta$ -arrestin 1 functions as the predominant regulator of PAR1 desensitization. Surprisingly, in cells lacking both  $\beta$ -arrestin 1 and 2, activated PAR1 is internalized through a dynamin- and clathrin-dependent pathway at a similar rate as compared to wild type cells, indicating that PAR1 internalization is independent of  $\beta$ -arrestins (136).

Little is known about the desensitization of PAR2, PAR3 and PAR4. Dery et al (37) have shown that trypsin induces redistribution of  $\beta$ -arrestin 1 to the plasma membrane and internalization of  $\beta$ -arrestin 1 and PAR2 to the early endosomes.

## **PARs in Inflammation**

### **2.1 PARs in Neurons and Neuronal Inflammation**

The events where PARs mediate neurogenic inflammation have been extensively investigated in recent years. Although initially detected in platelets, endothelial cells, and fibroblasts, it is now recognized that all four PAR subtypes are differentially expressed and regulated in the nervous system (150, 173). PAR1, PAR2, PAR3 and PAR4 have been detected on neurons in many parts of the brain, such as the hippocampus and cortex (135, 150). The four members of PARs have been detected in adult rat dorsal root ganglia and on rat astrocytes (166, 173).

Reverse-transcriptase polymerase chain reaction (RT-PCR) and immunohistochemical studies have revealed the expression of PAR1 and PAR2 in isolated dorsal root ganglion of rat neurons (149, 159). In addition, PAR1 and PAR2 expression has been detected in guinea pig myenteric neurons and submucosal neurons (29, 44, 141). The results of double labeling analysis with CGRP and PAR1 mRNA indicate that about 77% of PAR1 mRNA expressing neurons are CGRP positive. PAR1 mRNA is distributed in both small-unmyelinated neurons and in large-myelinated neurons, suggesting a nociceptive role for PAR1. The same studies report that 16% of DRG neurons express PAR2 mRNA and 77% of PAR2-mRNA-labeled neurons express CGRP. Forty percent of DRG neurons express PAR3 mRNA and 84% of PAR3-mRNA-

labeled neurons express CGRP. These results suggest the involvement of PAR3 in the nociceptive mechanism in periphery. Finally, the data shows a lack of PAR4 mRNA in DRG neurons which may indicate that PAR3 can act independently of PAR4 (173). PAR1 was also found to be present on sensory neurons (35). In cultured rat dorsal root ganglia, thrombin or PAR1 agonists stimulated cultured neurons to release substance P (SP) through PAR1.

Neurogenic inflammatory effects mediated by PARs include vasodilatation, increased vascular permeability, and cellular adhesion and infiltration by chemotaxis. Since PAR2 coexists with proinflammatory neuropeptides such as SP and CGRP in sensory neurons (149), it is possible that PAR2 activation on sensory nerves might be involved in neurogenic inflammatory mechanisms. *In vivo* studies have shown that paw edema has been observed after intraplantar injection with a selective PAR2 agonist and was significantly inhibited by ablation of spinal afferent C-fibers, antagonists of CGRP<sub>1</sub> receptors and NK<sub>1</sub> receptors. These results suggest that activation of PAR2 causes the release of SP and CGRP from primary spinal afferent neurons, which in turn interacts with NK<sub>1</sub> receptors and CGRP<sub>1</sub> receptors, respectively, to induce plasma extravasation leading to paw edema (149, 161). However, PAR2-induced edema was not completely abolished by the disruption of sensory nerves, antagonists of NK<sub>1</sub> and CGRP<sub>1</sub> receptors, and did not prevent neutrophil infiltration. Thus, it is likely that agonists of PAR2 stimulate granulocyte infiltration and paw edema at least in part by non-neurogenic mechanisms. The same study also showed that injection of thrombin or PAR2 agonists into a rat paw induces a noticeable increase of myeloperoxidase in the paw. Histological

examination of the paw indicated that PAR2 activation causes infiltration of neutrophils into the dermis (149). The elevation of neutrophils at sites of vascular injury and inflammation results in the release of neutrophil-derived serine proteases, such as cathepsin G, causing further morphological and functional changes in endothelial cells and leading to additional permeability (101, 137). In addition, tryptase or PAR2 agonists stimulate the release of granulocyte potent chemotactic and proadhesive mediator IL-8, up-regulates expression of ICAM-1 on epithelial cells (14), and induces the expression of mRNA for IL-1 $\beta$  (27), which in turn intensifies the inflammatory reaction.

In a similar manner, activation of PAR1 on primary spinal afferent neurons induces release of SP, which activates the NK1 receptors on endothelial cells to stimulate edema. de Garavilla et al (35) have shown that administration of thrombin or selective PAR1 agonists induces gap formation, extravasation of plasma proteins, and edema. Although, an NK1 receptor antagonist and ablation of sensory nerves with capsaicin significantly inhibited PAR1 agonist induced edema, these responses were not completely abolished (35). These results indicate that thrombin or PAR1 agonists, at least in part, cause neurogenic inflammation by directly stimulating sensory neurons to release SP and also indirectly by stimulating cells other than neurons leading to inflammation.

It has been shown that both PAR1 and PAR2 have been localized to plasma membrane and intracellular granules of human mast cells (32). Dery et al (36) have shown that PAR1 is expressed on endothelial cells and fibroblasts. PAR1 agonists can directly signal endothelial cells to induce gap formation and macromolecule

transmigration across monolayers of endothelial cells (16, 35, 149), and stimulate the expression of chemoattractants (26) and adhesion molecules (138, 151) that promote the adhesion and infiltration of granulocytes. Colotta et al (26) have shown that thrombin activates PAR1 on endothelial cells leading to the production of monocyte chemoattractant protein-1 (MCP-1).

In conclusions, stimulation of PAR1 and PAR2 on nerve fibers results in the release of SP and/or CGRP from primary sensory neuron endings in peripheral tissues by a  $Ca^{2+}$ -dependent mechanism. Neuropeptides released from sensory neurons initiate vasodilatation, plasma protein extravasation, and adhesion of leukocytes to the tissues. These results reveal the proinflammatory effects of PAR1 and PAR2 mediated by neurogenic mechanisms.

## **2.2 Role of PARs in Tissue Repair**

Tissue repair requires several steps including recruitment of inflammatory cells, migration and proliferation of endothelial and epithelial cells, synthesis of an extracellular matrix, and collagen deposition. Recent studies have demonstrated that PARs contribute to each of these events.

Early in tissue injury or inflammation, PARs-mediated secretion of growth factors and/or cytokines is an essential part for tissue repair (86). PARs-mediated coagulation mediators (FIIa, FXa, and FVIIa) signal inflammatory cells to the sites of injury. Bachli et al (4) showed that FXa and thrombin induce IL-6, IL-8, and MCP-1 expression in primary human dermal fibroblast cells. The experiment with human vascular wall cells showed that signaling by FXa is mediated by both PAR1 and PAR2 and the responses

included increased cell proliferation, increased production of the proinflammatory cytokine IL-6, and increased production of prothrombotic tissue factor (96). In addition, PAR1 mediates the induction of chemoattractant proteins and cytokines release from numerous cells, which are involved in proinflammation, cellular proliferation and angiogenesis. PAR1-dependent FXa or thrombin action elicits the production of IL-6, IL-8, or MCP-1 (4, 49, 96), whereas thrombin or its agonist peptide mediates IL-1, MCP-1, or ICAM-1 production (139).

The ability of leukocytes to recognize vascular endothelium, to adhere to the vessel wall and to transmigrate into the site of inflammation are crucial for tissue repair (86). The rolling of leukocytes on the endothelium is mainly mediated by the cell surface adhesion molecule, P-selectin (60). The up-regulation of P-selectin promotes the adherence of inflammatory cells to the vessel wall before they migrate into the tissue. Thrombin induces P-selectin expression on the surface of endothelial cells, which contribute to the rolling of neutrophils on the endothelial surface. Selective activating peptides for PAR2 and thrombin have been shown to cause a significant increase in rolling and adhesion of leukocytes to the vascular endothelium and vessel wall (157, 161, 162). The effects are mediated by the release of platelet-activating factor but are independent of mast cell activation.

Besides the effect on leukocyte rolling, selective PAR1 activating peptides and thrombin stimulate the expression of adhesion molecule ICAM-1 (138, 151). Thrombin mediates endothelial ICAM-1 binding to beta 2-integrins present on the surface of neutrophils induced by inflammation. This step provides additional stronger adhesion

between leukocytes and endothelial cells. Koo et al (80) have shown that PAR2 mediates FXa signaling by inducing the expression of IL-6, PDGF or MCP-1 as well as ERK 1/2 activation. Consistent with further study in PAR2 deficient mice, PAR2 is responsible for the induction of IL-6, ICAM-1, and E-selectin expression (146). PAR3 activation by thrombin or FXa induces the expression of IL-6, IL-8, or MCP-1 (4). PAR4 activating peptide induces IL-6, IL-8, or PGE<sub>2</sub> production in the A459, BEAS-2B cell lines, and primary human bronchial epithelial cells (HBEC) (3). These results suggest that PARs play essential roles in leukocyte adhesion and transmigration into the site of inflammation.

After the recruitment of inflammatory cells, new small blood vessels permeate into the site of injury, a process called angiogenesis. Angiogenesis from pre-existing vessels have several steps including vasodilatation and an increased permeability of the existing vessels, a degradation of ECM, and a migration of endothelial cells to distal sites (86). Recent studies have demonstrated that PARs contributes to a number of these events. It has been known that PAR1 and PAR2 mediated nitric oxide-dependent vascular relaxation, and increased both vasodilatation and vascular permeability (16, 17, 20, 35, 149). In addition to that PARs can induce increased expression and secretion of vascular endothelial growth factor (VEGF) in platelets (93) and fibroblasts (54). Roles of activated-PAR2 in angiogenesis have been studied recently using a canine myocardial infarction model (148). It has been shown that mast cell tryptase or PAR2 agonist-induced endothelial expression of the angiogenic chemokines, MCP-1 and IL-8 mediated by PAR2. Another *in vivo* study has shown that trypsin or PAR2 agonists induce



angiogenesis in skeletal muscle (97). Additionally, *in vivo* studies have shown that thrombin induces neoangiogenesis in the chick chorioallantoic membrane and is accompanied by the induction of VEGF and angiopoietin-2 (Ang-2) (18). PARs also have been reported to mediate proteolytic degradation of the basement membrane of the parent vessel by metalloproteinases (8, 92) and disruption of cell-to-cell contact between endothelial cells of the vessel by plasminogen activators. Thrombin also facilitated migration of endothelial cells toward the angiogenic stimulus (160). PAR1 mRNA is known to be expressed in monocytes, whereby activated PAR1 is capable of inducing IL-1 and IL-6 production (126). These cytokines are known to be proangiogenic, suggesting a role of PAR1 in angiogenesis and tissue repair.

Despite the diversity of PARs that may participate at various steps in angiogenesis, PARs emerge as an important factor promoting cell proliferation at the site of injury. Frungieri et al (39) showed that the proliferative effects of tryptase and PAR2 activating peptide in human fibroblasts are inhibited by a cyclooxygenase-2 inhibitor and a peroxisome proliferator activated receptor- $\gamma$  antagonist, suggesting a role of cyclooxygenase-2 and peroxisome proliferator-activated receptor- $\gamma$  in the proliferative response (39). Darmoul et al. (33) identified PAR1 mRNA in human cancer cell line HT29 using RT-PCR. Upon activation by thrombin or PAR1 activating peptide, the receptor induces an increase in intracellular calcium accompanied by an increase in the cell proliferation rate and motility. Further studies have shown that activation of PAR1 by thrombin or peptide agonist causes MMP induced release of TGF- $\alpha$  leading to TGF- $\alpha$  mediated ERK1/2 phosphorylation, and cell proliferation by EGFR-dependent and Src

kinase-dependent pathways (34).

As repair continues, collagen synthesis by fibroblasts begins within 3 to 5 days after injury and continues for several weeks, depending on the size of the wound (86). Chambers et al (19) showed that thrombin or PAR1 activating peptide stimulates procollagen production and increases newly procollagen synthesis rates in human fetal lung fibroblasts (HFL-1). Fang et al (38) have shown that thrombin and PAR1 agonist mediate collagen gel contraction through PAR1. The contraction was partially inhibited by expression of PAR1 RNAi. Taken together, thrombin might influence the deposition of connective tissue proteins and stimulate collagen contraction through activation of PAR1 during normal wound healing and remodeling.

## **Function of PARs in Gastrointestinal Tract**

### **3.1 Protective Roles of PARs in Gastric Mucosa**

The gastrointestinal tract is exposed to the widest array of proteases in both normal situations and during diseases (10, 29, 131, 132). The availability of endogenous ligands, thrombin and mast cell tryptase during intestinal inflammation or hemorrhage has suggested the involvement of PARs in the digestive system (98). The mechanisms by which the gastric mucosa protects itself against luminal acid and other injurious agents present in its lumen are not fully understood. Several mechanisms such as the secretion of mucus (132), secretion of bicarbonate(1), restraining of tight junctions (22, 59), manipulation of cell proliferation and restitution, and modulation of blood flow have been shown to participate in gastric mucosal defense. Work by several investigators has indicated the crucial role of PARs in maintaining the ability of gastric mucosa to withstand noxious injury.

Protective roles of PAR1 in gastric mucosa appear to be associated with the production of endogenous prostanoids (153). In a rat gastric injury model, selective PAR1 agonists, administered systemically, exert gastric mucosal protection, partly by decreasing acid secretion and maintaining the mucosal integrity under such conditions. The protective effect of PAR1 agonist is abolished by indomethacin, and COX-1 inhibitor, but not by COX-2 inhibitor and sensory nerve ablation by capsaicin, suggesting

the involvement of endogenous prostanoids in gastric mucosal protection (153). Involvement of endogenous prostanoids is also suggested by other studies in cultured RGM1 cells in which thrombin and PAR1 agonist SFLLRNP stimulate PGE<sub>2</sub> secretion in a dose-dependent manner (158). Taken together, the PAR1-activating peptide induces gastric mucosal protection involving endogenous prostanoid formation, but not neurally mediated protection.

There is evidence that PAR2 also plays a protective role in the gut through several mechanisms. Unlike PAR1, PAR2 involves the activation of capsaicin-sensitive sensory neurons, calcitonin gene-related peptide (CGRP), and tachykinins (66). In the rat, PAR2 agonist, when administered systemically, triggers secretion of gastric mucus (95, 152) that is abolished by pretreatment with capsaicin, CGRP<sub>1</sub> receptor antagonist, or NK<sub>2</sub> receptor antagonist. The data also shows that exogenous application of CGRP and both neurokinin A and substance P induces gastric mucus secretion via CGRP<sub>1</sub> and NK<sub>2</sub> receptor, respectively. The same study shows that PAR2 agonists systemically administered increases gastric mucosal blood flow as detected by a laser Doppler flow meter. Another important finding is that PAR2 also inhibits gastric acid secretion induced by carbachol, pentagastrin, or 2-deoxy-D-glucose (131). The inhibitory effect by PAR2 agonists was not reduced by pretreatment with indomethacin or capsaicin. These findings suggest that PAR2-mediated gastric acid secretion is independent of endogenous prostanoid formation or sensory neurons (131). In addition, several studies (65, 66, 128) have shown that PAR2 triggers a release of neuropeptides from capsaicin-sensitive sensory neurons, leading to mucus secretion via CGRP<sub>1</sub> and NK<sub>2</sub> receptors, and resulting

in mucosal cytoprotection.

There is evidence that mRNA for both PAR1 and PAR2 is abundantly expressed in rat gastric mucosa (131). Although, immunoreactive PAR1 is not clearly detectable in gastric epithelial cells (75, 130), repeat administration of PAR1-activating peptide facilitates pepsinogen secretion in the rat model (76). It is possible that a certain level of PAR1 might be present in rat gastric mucosa, but not enough to be detected in the immunohistochemical studies. Electron microscopic and immunohistochemical study of human gastritis biopsy specimens demonstrate that immunoreactive PAR1 is present on the superficial mucous epithelial layer and in the oxyntic gastric gland on parietal cells (158). The fact that parietal cells are hydrochloric acid-secreting cells led to the hypothesis that PAR1 could modulate the secretion of both mucin and hydrochloric acid suggesting an important role of PAR1 in gastric defense mechanism.

In contrast to PAR1, immunoreactive PAR2 is abundantly expressed in gastric mucosa, especially in chief cells (77). The fact that chief cells are pepsin/pepsinogen-secreting cells suggests that PAR2 could modulate pepsin secretion. Kawao and colleagues have shown that repeatedly administering the PAR2 agonist, SLIGRL-NH<sub>2</sub>, facilitated pepsin secretion in pylorus ligation rats. PAR2-mediated pepsin secretion was not secondary to acid secretion and was independent of nitric oxide formation, sensory neurons and muscarinic receptors. Therefore, according to these findings, PAR2 expressed in chief cells may have a significant role in pro-inflammation (77).

### **3.2 Role of PARs in Neurotransmission**

Both PAR1 and PAR2 are expressed within both excitatory and inhibitory motor

transmitters (41). Recent studies showed that thrombin, trypsin, filtrates from degranulated mast cells, or peptide agonists for PAR1, PAR2, or PAR4 evoke slowly activating excitatory responses in the guinea pig enteric nervous system. PARs-mediated depolarizing responses involve stimulation of PLC and intraneuronal calcium mobilization, but not prostanoid formation. In the myenteric glia of guinea pig PAR2-mediated calcium mobilization involves PLC and sphingosine kinase while PAR1-mediated responses involve PLC activity only (42). Another finding is that, in intact myenteric plexus of the longitudinal smooth muscle of guinea pig ileum, PAR2 agonist or trypsin elicits a prolonged depolarization and an increased excitability in individual myenteric plexus neurons, suggesting the role of PAR2 in neuronal transmissions which may contribute to intestinal motility (90).

### **3.3 Role of PARs in Ion Transport**

The effects of PAR activation on electrolyte secretion have been examined using a modified Ussing chamber technique, which allows detection of ion transport in small sections of tissue biopsies (87, 94). This technique also allows the application of agonists to apical (luminal) and basolateral surface.

PAR1 mRNA is expressed in mouse colon, including the mucosa. PAR1 immunoreactivity is also detected on both epithelial cells and neurons in submucosal ganglia (13), suggesting that direct activation of PAR1 on enterocytes in mouse colon might evoke ion transport.

Application of thrombin or PAR1 agonist on the basolateral side of SCBN cells, nontransformed duodenal epithelial crypt cells lines from human, stimulates an apical Cl<sup>-</sup>

secretion and increase in short-circuit current ( $I_{sc}$ ) by a  $Ca^{2+}$ -dependent mechanism. PAR1-mediate the change in  $I_{sc}$  blocked by the COX inhibitor, suggesting that the secretory response of SCBN cells to PAR1 activation is COX-1 and COX-2 dependent. In addition, Src kinase inhibitor significantly reduces the chloride secretory response upon activation by PAR1. Activation of PAR1 induces stimulation of cytosolic phospholipase A<sub>2</sub> (cPLA<sub>2</sub>) phosphorylation. The phosphorylation is inhibited by MEK inhibitor, which suggests the involvement of the ERK1/2 MAP kinase pathway in cPLA<sub>2</sub> activation.

Furthermore, PAR1 activation in SCBN cells results in a significant increase in PGE<sub>2</sub> and PGF<sub>2 $\alpha$</sub>  release in response to thrombin and PAR1 activating peptides as measured in media and in cell lysate. Since pretreatment with either PGE<sub>2</sub> or PGF<sub>2 $\alpha$</sub>  intensifies rather than reduces the PAR1-mediate response, it is implied that PGE<sub>2</sub> and PGF<sub>2 $\alpha$</sub>  are not the primary PGs mediating response. These results suggest that PAR1-induces apical directed Cl<sup>-</sup> secretion in SCBN cells involving Src stimulation and EGF receptor transactivation and subsequently stimulates the ERK1/2 MAP kinase pathway, cPLA<sub>2</sub> phosphorylation, and COX activation, but not PGE<sub>2</sub> and PGF<sub>2 $\alpha$</sub>  activation (12).

Recent studies have shown that intracolonic infusion with PAR1 agonists increases colonic permeability in mice and PAR1 agonists induce tight junctional zonula-occludens (ZO)-1 disruption (22). Another study has shown that thrombin causes rapid and transient contraction of endothelial cell cultures, resulting in gap formation and increase permeability of confluent cells (88). Similar to PAR1, PAR2 activation by trypsin, mast cell tryptase, and peptide agonists increases permeability of T84 colonic

epithelial cells and induces redistribution of tight junction ZO-1, occludin, and perijunctional F-actin (59). These results suggest the involvement of PAR1 and PAR2 in ion transport across the epithelial layer of intestinal lumen.

Application of trypsin or selective PAR2 agonists to the basolateral side of human intestinal epithelial colonic biopsy stimulates a transient increase in luminal-negative voltage ( $V_{te}$ ) and an increase in  $I_{sc}$ , but no response in mouse colonic epithelium (87, 94). In the presence of amiloride, to block electrogenic  $Na^+$  absorption, PAR2 agonist induces a transient increase in luminal-negative  $V_{te}$  and  $I_{sc}$  (94), suggesting that  $Cl^-$  secretion cause an increase in  $V_{te}$  and  $I_{sc}$ . Green et al (44) have also shown that application of PAR2 agonists to the basolateral side of the pig ileum stimulates  $Cl^-$  secretion, which is strongly suppressed by treatment with the neuronal conduction blocker saxitoxin and  $\delta$ -opoid agonist. Therefore, PAR2-mediated  $Cl^-$  secretion depends on functional innervations of submucosal neurons and is mediated by  $\delta$ -opoid-sensitive enteric neurons (44).

Furthermore, the colocalization of PAR2 immunoreactivity with the neuronal marker within the submucosal plexus supports the functional observations that PAR2 is present on enteric neurons. The administration of PAR2 agonist and trypsin to the basolateral side of a rat jejunal preparation in an Ussing chambers causes a prompt change in active ion transport (163). Indomethacin, but not a selective COX-2 inhibitor, completely inhibits the PAR2-induced response.  $PGE_2$  causes a sustained activation of ion transport. Application of tetrodotoxin did not block the short circuit current response to PAR2 agonist. Thus, PAR2-induced ion secretion is acting directly on the basolateral



side of enterocytes via COX-1-derived prostaglandins and not by neuronal release of stored neurotransmitters (163).

### **3.4 Role of PARs in Exocrine Secretion**

PARs are also involved in digestive exocrine function. PAR2 is highly expressed in the pancreas, both in pancreatic acinar cells (70) and duct epithelium (129). Activation of PAR2 administered intraperitoneally in combination with amastatin triggers exocrine secretion of pancreatic amylase in the conscious mouse in a dose-dependent manner. Similarly, PAR2 agonists, but not selective PAR1 agonists, administered intravenously, increase salivary secretion in the mouse or rat *in vivo* as well as *in vitro* (74). PAR2 is highly expressed in the pancreatic duct system. The fact that pancreatic duct cells are responsible for production of bicarbonate and fluid secreted into pancreatic juices, suggests that PAR2 may play a role in bicarbonate secretion.

### **3.5 Roles of PARs in Regulation of Gastric Mucosal Circulation**

It has been shown that systemic administration of PAR1 or PAR2 agonists cause a prompt increase in gastric mucosal blood flow (GMBF) in anesthetized rats, as measured by a laser Doppler flow meter (66, 75). In rat aorta, PAR1 and PAR2 are present in the vascular endothelium, and, upon activation, produce NO-dependent relaxation (69, 143). However, in the rat model, the GMBF increase produced by either PAR1 or PAR2 agonist is resistant to pretreatment with an NO synthase inhibitor. It is likely that PARs-mediated GMBF depends on two mechanisms. One is that PARs elicit release of endothelial nitric oxide, leading to vascular relaxation (73). PAR1 mediates nitric oxide secretion from endothelial cells leading to the relaxation of precontracted tissues (73). In

the absence of endothelium, PAR1 directly mediates vascular smooth muscle contraction that requires extracellular  $\text{Ca}^{2+}$ , whereas PAR2 causes neither contraction nor relaxation. However, in the presence of endothelium, PAR2 induces relaxation of the isolated rat gastric artery. The other mechanism is that PAR2 agonist elicits endothelium-dependent relaxation, leading to increased GMBF involving endothelium-derived hyperpolarizing factor (EDHF). Pretreatment of epithelial cells with L-NAME prior to addition of PAR2 agonists inhibits vascular relaxation. Further addition of apamin/charybdotoxin abolishes these relaxation effects. Thus, PAR2 mediates GMBF depending on both nitric oxide and EDHF pathways (67).

Kawabata et al demonstrated that endothelial PAR1 and PAR2, upon activation, dilate the gastric mesenteric artery via NO and prostanoid formation and also stimulate EDHF mechanisms including gap junctions, which would enhance GMBF (73). Besides the effects on endothelial cells, PAR1 can also promote other cell types, such as platelets and mast cells, to release serotonin and histamine, respectively, both of which have vasodilatation effects.

### **3.6 PARs Modulate Gastrointestinal Tract Smooth Muscle Contractility**

Apart from their effects in mucosal cytoprotection, PAR1 and PAR2, upon activation, produces gastric longitudinal smooth muscle contractile responses in guinea pigs and rats (143, 144). The contractility actions in the gastric preparation are entirely dependent on extracellular calcium. The contractile responses are inhibited by L-type calcium channel blocker, nifedipine, genistein and indomethacin (143, 144). However, in longitudinal strips of mouse gastric fundus, contractility mediated by both PAR1 and

PAR2 causes biphasic responses, relaxation followed by contraction in which the relaxation is involved in both ryanodine-sensitive and ryanodine-insensitive activations of  $\text{Ca}^{2+}$ -dependent small-conductance  $\text{K}^+$  channels (24).

In the rat duodenal longitudinal smooth muscle, PAR1 activation evokes relaxation followed by contraction, while PAR2 activation induces only a small contraction on the same muscle (72). PARs-induced contractile responses of the duodenal strips are mediated, in part, by activation of L-type calcium channels, protein kinase C and tyrosine kinase. In addition, apamin, but not charybdotoxin, completely abolishes the PAR1-mediated duodenal relaxation, and significantly enhances the PAR1-mediated contraction. These results suggest that duodenal smooth muscle relaxation is mediated in part by endothelium-derived hyperpolarizing factor (EDHF). The relaxation in the PAR1-mediated activation is suppressed by the combined administration of GF109203X and genistein suggesting the synergistic involvement of both protein kinase C and tyrosine kinase in this mechanism. Taken together PAR1, but not PAR2, activates apamin-sensitive  $\text{K}^+$  channels, resulting in relaxation of isolated rat duodenal smooth muscle. Both PAR1- and PAR2-mediated gastric contractions occur through activation of L-type calcium channel, PKC, and tyrosine kinase, but are independent of cyclooxygenase.

Similarly, in rat colonic circular muscle, PAR1 activation produces an inhibitory effect on the spontaneous rhythmic contraction. While in longitudinal muscles, PAR1 activation produces contractile effects at low PAR1 agonist concentrations or dual effects, relaxation followed by contraction, at high PAR1 agonist concentrations (over 1

$\mu\text{M}$ ). PAR2, upon activation, causes similar effects, a concentration-dependent reduction of the spontaneous phasic contraction in the circular muscle and contractile effects in the colonic longitudinal muscle (102). The suppression of contractility in the circular muscle mainly occurs via activation of  $\text{Ca}^{2+}$ -dependent small-conductance  $\text{K}^+$  channels. In this experiment, responses to PAR1 and PAR2 are independent of the propagation of neural action potentials and the production of cyclooxygenase. Taken together, PAR1 and PAR2 play a dual role in the control of rat colonic motility, producing suppression of contractility in the circular muscle and contraction of the longitudinal muscle.

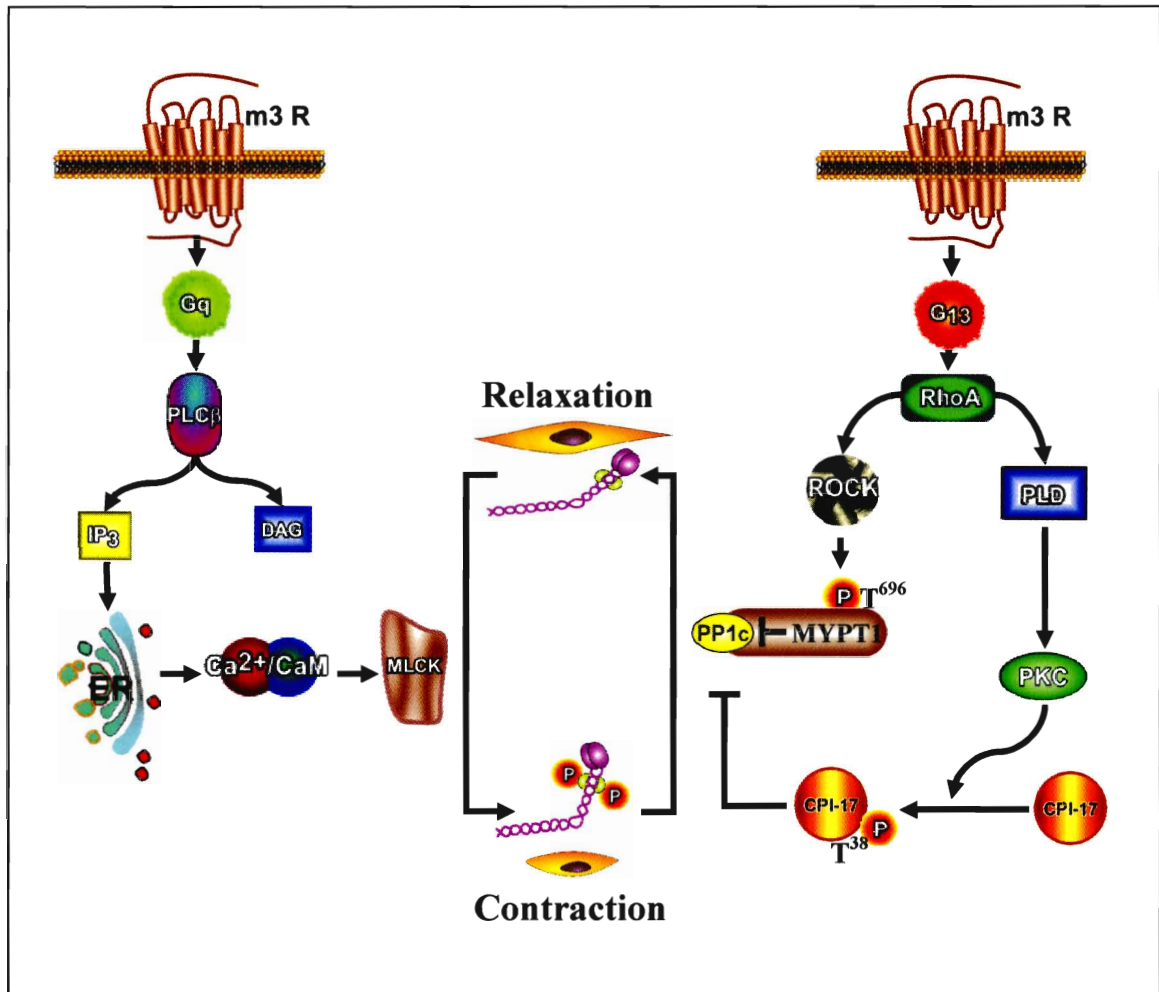
In summary, these studies indicate the difficulties in identifying the signaling pathways activated by PARs *in vivo* and in innervated *in vitro* preparations. The effect of PAR activation may vary in different specific regions of the gut depending on whether the activated receptor is present predominantly on smooth muscle cells or enteric neurons. Transmitters released from the enteric neurons, in turn, modulate the intrinsic electrical and mechanical activities of the gastrointestinal smooth muscle. To avoid the confounding effects of neural activation by PARs, the present study focuses on characterizing PARs and the signaling pathways to which these receptors are coupled in freshly dispersed and cultured smooth muscle cells of the gut.

## Review of Signaling Pathways Mediating Contraction

In smooth muscle, contractile agonists elicit a transient increase in cytosolic calcium concentrations ( $[Ca^{2+}]_i$ ), which are responsible for initial contraction. Increased  $[Ca^{2+}]_i$  results in activation of  $Ca^{2+}$ /calmodulin-dependent myosin light chain kinase (MLCK) through calmodulin (CaM). CaM is a cofactor required for the activation of MLCK and is bound to four  $Ca^{2+}$  ions. The regulatory  $Ca^{2+}$ /CaM subunit binds to and activates the catalytic subunit of MLCK in order to phosphorylate the 20-kDa regulatory subunit of myosin, called myosin light chain 20 (MLC<sub>20</sub>), on the primary phosphorylation sites of Ser<sup>19</sup> and Thr<sup>18</sup>. Phosphorylation of MLC<sub>20</sub> activates myosin ATPase activity, increases the actin and myosin crossbridge, and subsequently initiates smooth muscle contraction (Fig. 2).

Previous studies in circular smooth muscle have shown that G<sub>q</sub>-coupled receptor agonists induce initial MLC<sub>20</sub> phosphorylation and contraction via PLC-β1 activation by (104, 112) Gα<sub>q</sub> binding to PLC-β1's COOH-terminal tail. G<sub>i</sub>-coupled receptor agonists induce initial MLC<sub>20</sub> phosphorylation and contraction via PLC-β3 activation by Gβγ<sub>i</sub> binding to PLC-β3's NH<sub>2</sub>-terminal pleckstrin homology (PH) domain (5, 78). Both PLC-β1 and PLC-β3 hydrolyzes PIP<sub>2</sub> to generate IP<sub>3</sub> and DAG. Sarcoplasmic reticulum contains the high-affinity IP<sub>3</sub> receptor/ $Ca^{2+}$  channel, IP<sub>3</sub>R-I. An increase in IP<sub>3</sub> leads to the binding of IP<sub>3</sub> to IP<sub>3</sub>R-I and releases  $Ca^{2+}$  from sarcoplasmic reticulum. Stimulation

**Figure 2. Signaling by muscarinic m3 receptors via G<sub>q</sub>- and/or G<sub>13</sub>-coupled receptors during the sustained phase of contraction.**



of PLC- $\beta$  activity and increases in  $[Ca^{2+}]_i$  are rapid and transient. Calcium is efficiently removed by  $Ca^{2+}$  extrusion from the cell and reuptake into the sarcoplasmic reticulum. When  $[Ca^{2+}]_i$  is removed, myosin light chain phosphatase activity is continued, resulting in a rapid decline in the level of MLC<sub>20</sub> phosphorylation reflecting the transient phase of initial contraction.

However, subsequent studies have shown that despite the removal of  $[Ca^{2+}]_i$  and the rapid decline in MLCK activity, agonist-induced contractile forces and MLC<sub>20</sub> phosphorylation are well maintained suggesting the possibility of sustained contraction by the inhibition of MLC phosphatase activity (Fig. 2). MLC phosphatase is a holoenzyme consisting of three subunits: a catalytic subunit that is a 38-kDa-type 1-protein phosphatase delta isoform (PP1c $\delta$ ) and two regulatory subunits consisting of a small 20-kDa subunit and a 110- to 130-kDa subunit (myosin phosphatase target subunit 1, MYPT1). The interactions of the three subunits are required to form the functional enzyme. MYPT1 contains a PP1c-binding motif occurring at amino acids 35-38, followed by seven NH<sub>2</sub>-terminal ankyrin repeats. Binding of PP1c $\delta$  with MYPT1 alters substrate specificity and enhances catalytic activity.

Phosphorylation of the MYPT1 subunit is thought to regulate the activity of MLC phosphatase. The major regulatory phosphorylation sites of MLC phosphatase are Thr<sup>696</sup>, Thr<sup>853</sup> and Ser<sup>695</sup>. Phosphorylation of Thr<sup>696</sup> in MYPT1 by Rho kinase dissociates the enzyme from PP1c $\delta$  and inhibits activity of the catalytic subunit of MLC phosphatase. Phosphorylation of Thr<sup>853</sup> by Rho kinase within the myosin-binding domain on MYPT1 dissociates the enzyme from myosin and decreases efficiency of the enzyme by



decreasing availability of the substrate. While Rho kinase can phosphorylate both Thr<sup>696</sup> and Thr<sup>853</sup>, several other kinases have also been shown to phosphorylate the Thr<sup>696</sup> site such as ZIP kinase, a Ca<sup>2+</sup>-independent MLCK associated with MYPT1, and p21-activated protein kinase. On the other hand, phosphorylation at the Ser<sup>695</sup> site of MLC phosphatase by PKA or PKG blocks the ability of Rho kinase to phosphorylate nearby Thr<sup>696</sup> and thus increases MLC phosphatase activity. In addition to the inhibition of phosphorylation at the Thr<sup>696</sup> and Thr<sup>853</sup> sites, the inhibition of MLC phosphatase can occur via PKC or arachidonic acid-mediated pathways. PKC activated by either phorbol ester or DAG leads to phosphorylation of a 17-kDa PKC-potentiated inhibitor protein (CPI-17), which directly or indirectly inhibits MLC phosphatase. Arachidonic acid directly interacts with MLC phosphatase leading to the dissociation of the holoenzyme thus inhibiting catalytic activity. In addition, arachidonic acid activates Rho kinase and PKC, which in turn inhibits phosphatase activity.

## Significance

PAR1 and PAR2 are involved in modulating the motility of smooth muscle. *In vivo* studies have demonstrated PAR1 and PAR2's role in increasing gastrointestinal transit, whereas *in vitro* studies using isolated muscle strips have shown PAR1 and PAR2's affects on both contraction and relaxation (2, 169). The effects of PAR activation on gut motility depend on whether the activated receptor is present predominantly on smooth muscle cells or enteric neurons. However, the expression of PARs and the signaling pathways coupled to these receptors in smooth muscle are unknown. Identification of PARs in smooth muscle and characterization of receptor-specific pathways should lead to a better understanding of the role of proteases in the control of smooth muscle contraction.

## **Hypothesis and Specific Aims**

### **6.1 Hypothesis**

6.1.1 PARs expressed in smooth muscle are variously coupled to G proteins and downstream signaling pathways mediate muscle contraction.

6.1.2 Phosphorylation of RhoA by cAMP-independent PKA mediates feedback inhibition of PAR1 and PAR2 signaling.

### **6.2 Specific Aims**

6.2.1 To determine the expression of PARs in rabbit gastric muscle cells.

Receptor expression will be examined by RT-PCR and Western blot analysis in smooth muscle cells.

6.2.2 To characterize the receptor-specific signaling that mediates muscle contraction.

G protein activation, phosphoinositide-specific phospholipase C (PLC) activity, Rho kinase activity, phosphorylation of signaling intermediates, and smooth muscle contraction will be measured in smooth muscle cells. Various steps in the signaling pathways will be identified by using selective inhibitors in dispersed smooth muscle cells and by the expression of dominant negative mutants in cultured smooth muscle cells.

6.2.3 To characterize the canonical NF- $\kappa$ B pathway in the feedback inhibition of RhoA via cAMP-independent PKA.

The role of the IKK2/ I $\kappa$ B $\alpha$ /NF- $\kappa$ B pathway in the feedback inhibition of RhoA will be examined using inhibitors of IKK2 (IKK IV), I $\kappa$ B degradation (MG-132) and PKA (myristoylated PKI) in dispersed smooth muscle cells and by the expression of dominant negative mutants of IKK2 and I $\kappa$ B and phosphorylation site-specific mutants of RhoA in cultured smooth muscle cells.

## MATERIALS AND METHODS

### 7.1 Materials

PAR1-activating peptide (TFLLRN) and PAR2-activating peptide (SLIGRL) were obtained from Bachem (Torrance, CA); [ $^{125}$ I]cAMP, [ $\gamma$ - $^{32}$ P]ATP, [ $^{32}$ P]P<sub>i</sub>, [ $^{35}$ S]GTP $\gamma$ S, and [ $^3$ H]myo-inositol were obtained from PerkinElmer Life Sciences (Boston, MA); Collagenase CLS type II and soybean trypsin inhibitor were obtained from Worthington Biochemical Corporation (Lakewood, NJ); Western blotting supplies, Dowex AG-1 X 8 resin (100-200 mesh in formate form), chromatography materials, protein assay kits, and 10% Tris-HCl Ready Gels were obtained from Bio-Rad Laboratories (Hercules, CA); antibodies to G $\alpha_q$ , G $\alpha_{i1}$ , G $\alpha_{i2}$ , G $\alpha_{i3}$ , G $\alpha_{12}$ , G $\alpha_{13}$ , G $\alpha_s$ , G $\alpha_z$ , phospho-specific MYPT1 (Thr<sup>696</sup>), MLC<sub>20</sub> (Ser<sup>19</sup>), CPI-17 (Thr<sup>38</sup>), Rho kinase, IKK2(Ser<sup>177/181</sup>), and I $\kappa$ B $\alpha$ , p65 subunit were all obtained from Santa Cruz Biotechnology (Santa Cruz, CA); myelin basic protein (MBP) was obtained from Upstate USA, Inc. (Charlottesville, VA); ML-9 was obtained from Biomol International (Plymouth Meeting, PA); bisindolylmaleimide, Y27632, pertussis toxin, cAMP; *Clostridium botulinum* C3 exoenzyme, IKK-2 Inhibitor IV (IKK IV), MG-132, myristoylated PKI and U73122 were obtained from Calbiochem (San Diego, CA); RNAqueous<sup>TM</sup> Kit was obtained from Ambion (Austin, TX); Effectene Transfection

Reagent, QIAEX®II Gel Extraction Kit and QIAprep®Spin Miniprep Kit were obtained from QIAGEN Inc. (Valencia, CA); PCR reagents were obtained from Applied Biosystems (Foster City, CA); SuperScript™ II Reverse Transcriptase and TOPO TA Cloning® Kit Dual Promoter were obtained from Invitrogen Corporation (Carlsbad, CA); EcoR I was obtained from New England BioLabs ( Ipswich, MA); Dulbecco's Modified Eagle's Medium (DMEM) was obtained from Fisher Scientific (Pittsburgh, PA). All other chemicals were obtained from Sigma-Aldrich (St. Louis, MO).

New Zealand white rabbits (weight: 4-5 lbs) were purchased from RSI Biotechnology (Clemmons, NC) and killed by sodium pentobarbital overdose (100 mg/kg) as approved by the Institutional Animal Care and Use Committee at Virginia Commonwealth University. The animals were housed in the animal facility administered by the Division of Animal Resources, Virginia Commonwealth University. All procedures were conducted in accordance with the Institutional Animal Care and Use Committee at Virginia Commonwealth University.

## **7.2 Methods**

### **7.2.1 Collection of tissue**

Rabbits were sacrificed by injection of Euthasol (100 mg/kg body weight) into the ear vein. The stomach was rapidly removed, emptied of its contents and placed in cold smooth muscle buffer (pH 7.4) with the following composition: NaCl 120 mM, KCl 4 mM,  $\text{KH}_2\text{PO}_4$  2.6 mM,  $\text{CaCl}_2$  2.0 mM,  $\text{MgCl}_2$  0.6 mM, HEPES (N-2-hydroxyethylpiperazine-N' 2-ethanesulfonic acid) 25 mM, glucose 14 mM, and essential amino mixture 2.1%.

### **7.2.2 Preparation of dispersed gastric smooth muscle cells**

The antrum was separated from the rest of the stomach and the mucosal layer was removed by sharp dissection. Smooth muscle cells from the circular muscle layer of the antrum were isolated by sequential enzymatic digestion of the muscle strips followed by filtration and centrifugation as described previously (123). The antrum was cut into thin slices using a Stadie-Riggs tissue slicer and then the slices were incubated for 30 min at 31°C in smooth muscle buffer containing 0.1% collagenase (300 U/ml) and 0.01% soybean trypsin inhibitor (w/v). The tissues were continuously gassed with 100% oxygen during the entire isolation procedure. The partly digested tissues were washed twice with 50-ml of collagenase-free smooth muscle buffer and the muscle cells were allowed to disperse spontaneously for 30 min in collagenase-free medium. Cells were harvested by filtration through 500  $\mu\text{m}$  Nitex and centrifuged twice at 350 g for 10 min to eliminate broken cells and organelles. The cells were counted in a hemocytometer and it was estimated that 95% of the cells excluded trypan blue. The experiments were done within

2-3 h of cell dispersion.

### **7.2.3 Preparation of cultured gastric smooth muscle cells**

Dispersed muscle cells isolated from the antrum were resuspended in DMEM containing penicillin (200 U/ml), streptomycin (200  $\mu\text{g/ml}$ ), gentamycin (100  $\mu\text{g/ml}$ ), amphotericin B (2.5  $\mu\text{g/ml}$ ) and 10% fetal bovine serum (DMEM-10). The muscle cells were plated at a concentration of  $5 \times 10^5$  cells/ml and incubated at 37°C in a CO<sub>2</sub> incubator. DMEM-10 medium was replaced every three days for 2-3 weeks until confluence was attained. The muscle cells in confluent primary cultures were trypsinized (0.5 mg trypsin/ml), re-plated at a concentration of  $2.5 \times 10^5$  cells/ml and cultured under the same conditions. All experiments were done on cells during the first passage. Previous studies have determined the purity of cultured muscle cells using smooth muscle-specific  $\gamma$ -actin (154). Cultured muscle cells were starved in serum-free medium for 24 hours before each use.

Many measurements were done in both cultured muscle cells and freshly dispersed muscle cells. In spite of the limitations with the limitations with the cell cultures, the use of cultured muscle cells is essential for molecular studies involving expression of dominant negative and other cDNA constructs.

### **7.2.4 Minigene construction**

The cDNA sequences encoding the last 11 amino acids at the COOH-terminal of mouse  $G\alpha_q$ ,  $G\alpha_{12}$ , and  $G\alpha_{13}$ , and human  $G\alpha_i$  were amplified by PCR and verified by DNA sequencing as previously described (52, 172). The 5'-end of the sense primers contained a BamHI site followed by the ribosome binding consensus sequence (5'-GCCGCCACC-



3'), a methionine (ATG) start code, a glycine (GGA) to protect the ribosome binding site during translation, and the nascent peptide against proteolytic degradation. An *EcoRI* site was synthesized at the 5'-end of the antisense primers immediately after the stop codon (TGA). The purified PCR products were subcloned into the mammalian expression vector pcDNA3.1(+). The oligonucleotide sequence corresponding to the 11 amino acid residuals at the COOH-terminal of  $G\alpha_i$  were synthesized in random order and ligated into pcDNA3.1(+) as a control minigene. All  $G\alpha$  minigene constructs used for transfection experiments were purified using a Endotoxin-Free Maxiprep Kit (Qiagen) following the manufacturer's protocol. The sequences of expressed minigene peptides are listed in Table 2.

#### **7.2.5 Transfection of dominant negative mutants and minigene constructs into cultured smooth muscle cells**

Wild type RGS4, dominant negative RGS4 (RGS4[N88S]), IKK2 (IKK2[K44A]),  $I\kappa B$  ( $I\kappa B\alpha$ [S32A/S36A]), and phosphorylation-site deficient RhoA (RhoA[S188A]) were subcloned into the multiple cloning site (*EcoRI*) of the eukaryotic expression vector pEXV. Recombinant plasmid DNAs were transiently transfected into primary cultured muscle cells using Effectene Transfection Reagent (QIAGEN) for 48 h. Cells were co-transfected with 2  $\mu$ g of pEXV vector and 1  $\mu$ g of pGreen Lantern-1 DNA. Transfection efficiency was monitored by the expression of the green fluorescent protein using FITC filters. Control cells were transfected with vector alone (53, 121, 170). Analysis by fluorescence microscopy showed that approximately 80% of the cells were transfected.

**Table 2. Sequences of expressed G protein COOH-terminal peptides.**

<b>G Protein</b>	<b>Peptide sequences</b>
G <sub>q</sub>	MGLQLNLKEYNLV
G <sub>i</sub>	MGIKNNLKDCGLF
G <sub>12</sub>	MGLQENLKDIMLQ
G <sub>13</sub>	MGLHDNLKQLMLQ
G <sub>iR</sub>	MGNNGIKCLFNDKL

### 7.2.6 Identification of PAR1- and PAR2-activated G proteins

G proteins selectively activated by PAR1-AP and PAR2-AP were identified from the increase in G $\alpha$  binding to the [<sup>35</sup>S]GTP $\gamma$ S (5'-O-3-thiotriphosphate) using the method of Okamoto et al (134) as described previously (99, 112, 113, 115, 172). Ten milliliters of muscle cell suspension (3 X 10<sup>6</sup> cells/ml) were homogenized in 20 mM HEPES medium (pH 7.4) containing 2 mM MgCl<sub>2</sub>, 1 mM EDTA and 2 mM DTT. After centrifugation at 30,000 g for 15 min, the crude membranes were solubilized for 60 min at 4 °C in 20 mM HEPES medium (pH 7.4) containing 2 mM EDTA, 240 NaCl, 0.5% CHAPS (3-[(3-cholamidopropyl) dimethylammonio]-1-pro-panesulfonate), 2 mM PMSF, 20  $\mu$ g/ml aprotinin, and 20  $\mu$ M leupeptin. The membrane was incubated for 20 min at 37°C with 60 nM [<sup>35</sup>S]GTP $\gamma$ S in the presence or absence of PAR1-AP and PAR2-AP in a solution containing 10 mM HEPES (pH 7.4), 100  $\mu$ M EDTA and 10 mM MgCl<sub>2</sub>. The reaction was terminated with 10 volumes of 100 mM Tris-HCl medium (pH 8.0) containing 10 mM MgCl<sub>2</sub>, 10 mM NaCl and 10  $\mu$ M GTP. The mixtures were placed in wells precoated with specific antibodies to G $\alpha_q$ , G $\alpha_{i1}$ , G $\alpha_{i2}$ , G $\alpha_{i3}$ , G $\alpha_{12}$ , G $\alpha_{13}$ , G $\alpha_s$  and G $\alpha_z$ . Coating with G protein antibodies (1:1000) was done after the wells were first coated with anti-rabbit IgG (1:1000) for 2 h on ice. After incubation for 2 h on ice, the wells were washed three times with phosphate buffer saline solution (PBS) containing 0.05% Tween-20. The radioactivity from each well was counted by liquid scintillation. The amount of [<sup>35</sup>S]GTP $\gamma$ S bound to the activated G $\alpha$  subunit was expressed as counts per minute (cpm) per milligram of protein.

### 7.2.7 Assay for Phosphoinositide (PI) hydrolysis (PLC- $\beta$ activity)

Total inositol phosphates were measured in rabbit gastric circular muscle cells by anion exchange chromatography using the method of Berridge et al (6) as described previously (117, 121). Ten milliliters of cell suspension ( $2 \times 10^6$  cells/ml) were labeled with myo-2- $^3\text{H}$ inositol ( $15 \mu\text{Ci/ml}$ ) for 90 min at  $31^\circ\text{C}$ . Cells were centrifuged at  $350 \text{ g}$  for 10 min to remove excess  $^3\text{H}$ inositol then the cells were resuspended in 10 ml of fresh medium. Lithium was added to a final concentration of 10 mM and the suspension was incubated for another 10 min. PAR1-AP or PAR2-AP was added at different concentrations ( $0.01 \text{ nM} - 10 \mu\text{M}$ ) to 0.5 ml of cell suspension and the mixture was incubated in a shaking water bath for 1 min. Cultured smooth muscle cells were labeled with myo-2- $^3\text{H}$ inositol ( $0.5 \mu\text{Ci/ml}$ ) for 24 h in inositol-free DMEM medium. The cultures were washed with phosphate-buffered saline (PBS) and treated with PAR1-AP ( $1 \mu\text{M}$ ) or PAR2-AP ( $1 \mu\text{M}$ ) for 1 min in HEPES medium (pH 7.4). The reaction was terminated by the addition of chloroform:methanol:HCl (50:100:1 v/v/v). After chloroform ( $310 \mu\text{l}$ ) and water ( $310 \mu\text{l}$ ) were added, the samples were vortexed and the phase was separated by centrifugation at  $1000 \text{ g}$  for 15 min. The upper aqueous phase was applied to a column containing 1 ml of a 1:1 slurry of Dowex AG-1 X8 resin (100-200 mesh in formate form) and distilled water.

The column was washed with 10 ml of water followed by 10 ml of 5 mM sodium tetraborate-60 mM ammonium formate solution to remove  $^3\text{H}$  glycerophosphoinositol. Total inositol phosphates were eluted with 6 ml of 0.8 M ammonium formate-0.1 M formic acid. The eluates were collected into scintillation vials and counted in gel phase

after addition of 10 ml of scintillant. The results were expressed as counts per minute per mg protein.

### **7.2.8 Assay for Rho Kinase activity**

Rho kinase activity was measured using an immunokinase assay as previously described (48, 50, 52, 172). Cultured cells were washed one time with PBS, and then lysed with lysis buffer containing 50 mM Tris-HCl (pH 7.5), 150 mM NaCl, 0.1 % SDS, 0.5% sodium deoxycholate, 1% NP-40, 10 mM sodium pyrophosphate, and protease inhibitor cocktail (2  $\mu$ l/ml, BD Biosciences). The homogenates were centrifuged at 10,000 rpm for 10 min at 4 °C. The supernatant containing cytosolic protein was transferred to a fresh tube and 5  $\mu$ l of Rho kinase antibody was added to each tube followed by a 2 h incubation at 4 °C.

At the end of two hours, Protein A/G agarose was added to each tube and the mixture was reincubated at 4 °C overnight then washed 3 times with lysis buffer. The pellets were re-suspended in 50  $\mu$ l of kinase buffer containing 100 mM Tris-HCl (pH 7.4), 1 M KCl, 50 mM MgCl<sub>2</sub>, 10 mM EDTA, and 1 mM DTT. Twenty microliters of Rho kinase immunoprecipitates were added to the reaction mixture containing 100 mM Tris-HCl (pH 7.4), 1 M KCl, 50 mM MgCl<sub>2</sub>, 1 mM DTT, 1 mM ATP, and 10  $\mu$ Ci of [ $\gamma$ -<sup>32</sup>P] ATP (3,000 Ci/mol) along with 5  $\mu$ g of myelin basic protein. The mixtures were incubated at 37 °C for 15 min. Phosphorylation of myelin basic protein was absorbed onto phosphocellulose disks, and free radioactivity was removed by washing 3 times with 75 mM H<sub>3</sub>PO<sub>4</sub>. The amount of radioactivity on the disks was measured by liquid scintillation. The results were expressed as counts per minute per milligram protein per

minute.

### **7.2.9 Assay for adenylyl cyclase activity**

Adenylyl cyclase activity was measured by the formation of cAMP in response to agonists. Cyclic AMP production was measured by radioimmunoassay using [<sup>125</sup>I]cAMP (108, 113, 118, 155). The effects of PAR1-AP and PAR2-AP were studied by measuring forskolin-stimulated cAMP levels. One milliliter ( $3 \times 10^6$  cells/ml) of cell suspension was treated for 60 s with forskolin (10  $\mu$ M) in the presence of 100  $\mu$ M isobutylmethyl xanthine, either alone or in combination with PAR1-AP (1  $\mu$ M) or PAR2-AP (1  $\mu$ M). The reaction was terminated with cold 6% trichloroacetic acid (v/v) and vortexed vigorously. After centrifugation, the supernatants were extracted three times with water-saturated diethyl ether to remove the trichloroacetic acid and then lyophilized and frozen at -20°C. The samples were reconstituted for radioimmunoassay in 50  $\mu$ l of 50 mM sodium acetate (pH 6.2) and acetylated with triethylamine/acetic anhydride (2:1 v/v) for 30 min. Cyclic AMP was measured in duplicates using 100  $\mu$ l aliquots and the results were computed from a standard curve using the Prizm<sup>®</sup> GraphPad program. The results were expressed as pmol of cAMP/mg protein.

### **7.2.10 Phosphorylation of G<sub>12</sub> and G<sub>13</sub>**

Protein phosphorylation was determined from the amount of <sup>32</sup>P incorporated into each protein after immunoprecipitation with specific antibodies to G<sub>12</sub>, G<sub>13</sub>, or RhoA as previously described (53, 103, 114, 121). Freshly dispersed cells were incubated with [<sup>32</sup>P] orthophosphate for 4 h. One milliliter samples were incubated with PAR1-AP (1  $\mu$ M) or PAR2-AP (1  $\mu$ M) for 10 min and the reaction was terminated by rapid

centrifugation. The pellet was homogenized in lysis buffer containing 50 mM Tris-HCl (pH 7.5), 150 mM NaCl, 0.1 % SDS, 0.5% sodium deoxycholate, 1% NP-40, 10 mM sodium pyrophosphate, and protease inhibitor cocktail (2  $\mu$ l/ml). Cell lysates were separated by centrifugation at 13,000 g for 10 min at 4 °C, precleared with 40  $\mu$ l of protein A-Sepharose, and incubated with G $\alpha_{12}$ , G $\alpha_{13}$ , or RhoA antibody for 2 h at 4 °C then with 40  $\mu$ l of protein A-Sepharose for another one hour. The immunoprecipitates were extracted with Laemmli sample buffer, boiled for 5 min, and separated by electrophoresis on a SDS-PAGE gel. After transfer to nitrocellulose membranes, [<sup>32</sup>P]G $\alpha_{12}$ , [<sup>32</sup>P]G $\alpha_{13}$ , or [<sup>32</sup>P]RhoA was visualized by autoradiography.

#### 7.2.11 Western blot analysis

Phosphorylation of MLC<sub>20</sub>, MYPT1, CPI-17, IKK2, and the p65 subunit of NF- $\kappa$ B was measured using phospho-specific antibodies and the degradation of I $\kappa$ B was measured using I $\kappa$ B antibody (1:1000) as described previously (112, 116). One milliliter of cells suspension (2 X 10<sup>6</sup> cell/ml) was treated with PAR1-AP (1  $\mu$ M) or PAR2-AP (1  $\mu$ M) and solubilized on ice for one hour in medium containing 20 mM Tris-HCl (pH 8.0), 1 mM DTT, 100 mM NaCl, 0.5% sodium dodecyl sulfate, 0.75% deoxycholate, 1 mM PMSF, 10  $\mu$ g/ml of leupeptin and 100  $\mu$ g/ml of aprotinin. The proteins were resolved using a SDS/PAGE gel and then electrophoretically transferred onto a nitrocellulose membranes. The membranes were incubated for 12 h with phospho-specific antibodies to MLC<sub>20</sub> (Ser<sup>19</sup>), MYPT1 (Thr<sup>696</sup>), CPI-17 (Thr<sup>38</sup>), IKK2 (Ser<sup>177/181</sup>), p65 subunit (Ser<sup>536</sup>) or antibody I $\kappa$ B $\alpha$ , the membrane were then incubated for 1 h with horse-radish peroxidase-conjugated secondary antibody (1:2000). The protein bands were identified



by an enhanced chemiluminescence reagent.

#### **7.2.12 Measurement of contraction in dispersed smooth muscle cells**

Contraction in freshly dispersed gastric circular smooth muscle cells was determined by scanning micrometry as previously described (51, 52, 120). Aliquots (0.4 ml) of cells containing approximately  $10^4$  cells/ml were treated with 100  $\mu$ l of medium containing various concentrations of PAR1-AP or PAR2-AP for different time periods (30 s to 10 min) and the reactions were terminated using 8% acrolein at a final concentration of 0.1%. Acrolein kills and fixes cells without affecting the cell length. The resting cell length was determined in control experiments in which muscle cells were incubated with 100  $\mu$ l of 0.1% bovine serum albumin without the agonists. Concentration-response curves for PAR1-AP and PAR2-AP were constructed for the peak contraction, which occurred at 30 s after addition of PAR1-AP or PAR2-AP. The mean lengths of 50 muscle cells treated with PAR1-AP or PAR2-AP agonists were measured by scanning micrometry and compared to the mean lengths of untreated cells. The contractile response was expressed as the percent decrease in mean cell length compared to control cell length.

## **Statistical Analysis**

The results were expressed as means  $\pm$  S.E. of  $n$  experiments and analyzed for statistical significance using Student's  $t$ -test for paired and unpaired values. Each experiment was performed on cells obtained from different animals. Differences among multiple groups were tested using ANOVA and checked for significance using Fisher's protected least significant difference test. A probability of  $P < 0.05$  was considered significant.

## Experimental Approach

1. We have used two approaches to determine the signaling pathways of PAR1 and PAR2. In the first approach, freshly dispersed muscle cells were used to examine the expression of PARs by Western blot analysis and their signaling by measuring of G protein activation, PI hydrolysis, adenylyl cyclase activity, Rho kinase activity and smooth muscle contraction. In the second approach, cultured muscle cells during the first passage were used for various molecular and biochemical studies. The purity of cultured muscle cells was determined using markers for smooth muscle, interstitial cells of Cajal, enteric neurons and endothelial cells. Use of cultured muscle cells was essential for expression of  $G\alpha$  minigenes and dominant negative mutants of various cDNAs.

2. PAR1 and PAR2 are activated separately and selectively by receptor-specific peptides. The amino acid sequences of these synthetic peptides correspond to the exposed sequences of the tethered ligand. The synthetic peptide, TFLLRN, was used as a surrogate activator of PAR1, whereas the synthetic peptide SLIGRL was used as a surrogate activator of PAR2. These peptides were used widely to selectively activate PAR1 and PAR2 in various studies (23, 28, 68, 71, 75).

3. The involvement of signaling intermediates in the signaling pathways mediated by PAR1 and PAR2 was examined using pharmacological inhibitors (Table 3) in freshly

**Table 3. Pharmacological inhibitors of signaling molecules.**

<b>Inhibitor</b>	<b>Target</b>	<b>Concentration used</b>
Bisindolylmaleimide	PKC	1 $\mu$ M
C3 exoenzyme	Rho A	2 $\mu$ g/ml
IKK IV	IKK2	10 $\mu$ M
MG-132	NF- $\kappa$ B	10 $\mu$ M
ML-9	MLCK	10 $\mu$ M
myristoylated PKI	PKA	1 $\mu$ M
PTx	G <sub>i</sub>	200 ng/ml
U73122	PLC	10 $\mu$ M
Y27632	Rho kinase	1 $\mu$ M

dispersed smooth muscle cells and by the overexpression of cDNA mutants (Table 2) in cultured muscle cells. The concentrations of inhibitors used in the present study was based on the previous studies performed on smooth muscle cells and have been shown to be maximally effective in eliciting an inhibitory response (48, 51, 106, 120-122, 170).

4. The involvement of PI hydrolysis, IP<sub>3</sub>-dependent Ca<sup>2+</sup> release and Ca<sup>2+</sup>/calmodulin-dependent activation of MLCK in contraction was examined using inhibitors of PI hydrolysis (U73122) and MLCK (ML-9).

5. The involvement of PKC in the signaling pathway was examined using selective inhibitor of PKC (bisindolylmaleimide).

6. The involvement of the Rho kinase pathway in the signaling pathway of contraction was examined using selective inhibitor of RhoA (*Clostridium botulinum* C3 exoenzyme) and Rho kinase (Y27632).

7. The involvement of the canonical NF- $\kappa$ B pathway in the signaling pathway of contraction was examined using inhibitors of IKK2 (IKK IV) and NF- $\kappa$ B (MG-132) in freshly dispersed muscle cells and by the expression of dominant negative IKK2(K44A) and I $\kappa$ B $\alpha$ (S32A/S36S) in cultured muscle cells.

8. The involvement of PKA in the feedback phosphorylation of RhoA and inhibition of Rho kinase activity was examined using the cell permeable selective PKA inhibitor (myristoylated PKI) in freshly dispersed muscle cells and by overexpression of PKA phosphorylation site-deficient RhoA (RhoA[S188A]) in cultured muscle cells.

## Results

### 10.1 Co-expression of PAR1 and PAR2 in Gastric Smooth Muscle

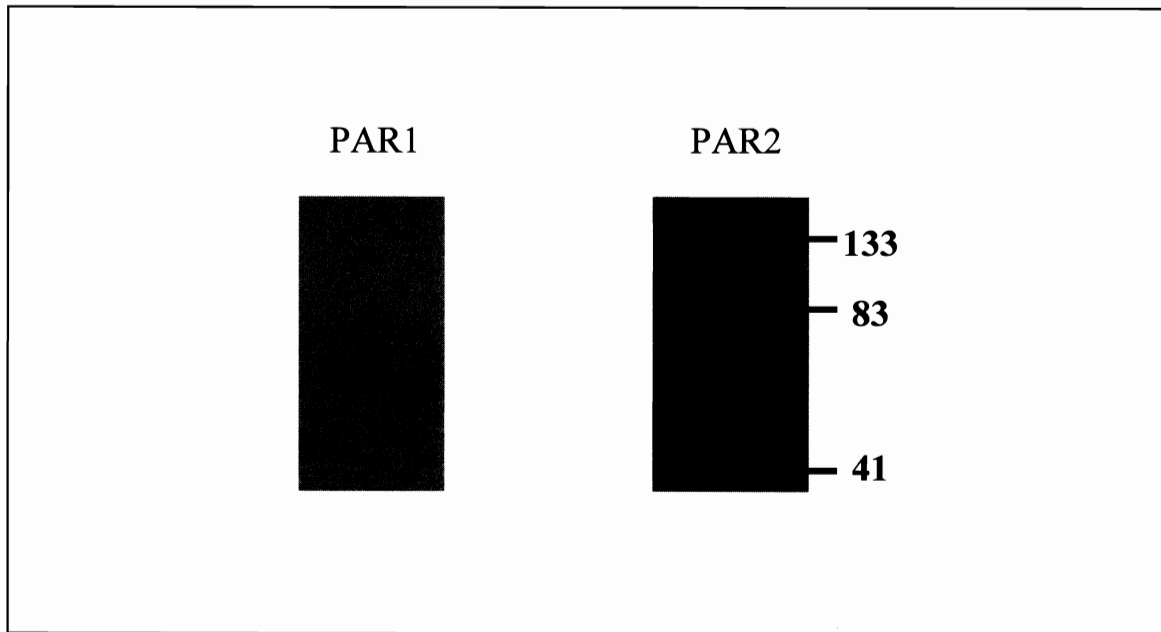
Western blot analysis of homogenates derived from dispersed rabbit gastric smooth muscle cells using antibodies to PAR1, PAR2, PAR3 and PAR4 disclosed the presence of PAR1 and PAR2, but not PAR3 and PAR4 (Fig. 3). The selective expression of PAR1 and PAR2 in smooth muscle conforms to the predominant expression of these isoforms in peripheral tissues.

### 10.2 Distinctive Patterns of G-protein Activation by PAR1 and PAR2 in Smooth Muscle

Studies in various tissues and cell lines suggest that PAR1 and PAR2 are coupled to both pertussis toxin (PTX)-sensitive ( $G_i$ ) and -insensitive ( $G_q$ ,  $G_{12}/G_{13}$ ) G proteins, but the specific  $G_i$  isoforms and  $G_{12}$  and  $G_{13}$  proteins coupled to each receptor have not been identified. We have used receptor-specific activating peptides to selectively activate PAR1 and PAR2 to identify the G proteins coupled to each receptor. Muscle cell membranes were incubated with [ $^{35}$ S]GTP $\gamma$ S (60 nM) with or without PAR activating peptides and added to wells precoated with different  $G\alpha$  antibodies; an increase in the binding of [ $^{35}$ S]GTP $\gamma$ S complexes to a specific  $G\alpha$  antibody reflected activation of the corresponding G protein. Addition of PAR1-activating peptide (PAR1-AP; TFLLRN)

**Figure 3. Selective expression of protease-activated receptor 1 (PAR1) and PAR2 in rabbit gastric smooth muscle cells.** Western blot analysis was performed on homogenates prepared from dispersed gastric smooth muscle cells. Proteins were resolved by SDS-polyacrylamide gel electrophoresis, electrophoretically transferred to nitrocellulose membrane, and probed with specific antibodies to PAR1, PAR2, PAR3, or PAR4 antibody. Immunoreactive bands for PAR1 and PAR2, but not PAR3 and PAR4 were detected.





caused a 2.0-, 2.8- and 1.8-fold ( $P<0.01$ - $P<0.001$ ) increase in the binding of [ $^{35}$ S]GTP $\gamma$ S to  $G\alpha_{i3}$ ,  $G\alpha_q$  and  $G\alpha_{i2}$ , respectively (Figs 4-6). PAR1-AP did not cause a significant increase in the binding to  $G\alpha_{i1}$ ,  $G\alpha_{i2}$ ,  $G\alpha_{i3}$ ,  $G\alpha_s$  and  $G\alpha_z$ . In contrast, addition of PAR2-AP (SLIGRL) caused a 2.2-, 2.0, 3.2, and 2.7-fold ( $P<0.01$ - $P<0.001$ ) increase in the binding of  $G\alpha_{i1}$ ,  $G\alpha_{i2}$ ,  $G\alpha_q$ , and  $G\alpha_{i3}$ , respectively (Figs 4-6). PAR2-AP did not cause a significant increase in the binding to  $G\alpha_{i3}$ ,  $G\alpha_{i2}$ ,  $G\alpha_s$ , and  $G\alpha_z$ . These results suggest that PAR1 is coupled to the activation of  $G_{i3}$ ,  $G_q$ , and  $G_{i2}$ , whereas PAR2 is coupled to  $G_{i1}$ ,  $G_{i2}$ ,  $G_q$  and  $G_{i3}$ . Only  $G_q$  activation is shared by both receptors (Figs. 4-6).

### **10.3 Signaling Pathways Activated by PAR1 and PAR2 in Smooth Muscle**

Previous studies in smooth muscle have shown that activation of  $G_q$  results in the stimulation of PLC- $\beta$ 1 and Rho kinase activities via  $G\alpha_q$ , whereas activation of  $G_i$  results in the stimulation of PLC- $\beta$ 3 via  $\beta\gamma$  subunits and inhibition of adenylyl cyclase via  $\alpha$  subunit (104, 105, 112, 122). Activation of  $G_{i2}$  or  $G_{i3}$  also results in the stimulation of Rho kinase activity. The effector enzymes stimulated by G proteins coupled to PAR1 and PAR2 were examined by measurements of PI hydrolysis (PLC- $\beta$  activity), Rho kinase activity and inhibition of adenylyl cyclase activity in response to PAR1-AP and PAR2-AP. Pertussis toxin was used to uncouple receptors from  $G_i$  proteins and minigene expression was used to identify the coupling specific G proteins to effector enzymes.

#### **10.3.1 Stimulation of phosphoinositide-specific PLC- $\beta$ activity (PI hydrolysis) by PAR1 and PAR2**

PAR1-AP stimulated PI hydrolysis in dispersed muscle cells in a concentration-

**Figure 4. Distinct pattern of pertussis toxin-sensitive G proteins activated by PAR1-AP and PAR2-AP in rabbit gastric smooth muscle cells.** Membranes isolated from freshly dispersed smooth muscle cells were incubated with <sup>35</sup>S-labeled guanosine 5-O-(3-thiotriphosphate) ([<sup>35</sup>S]GTP $\gamma$ S) in the presence or absence of PAR1-activating peptide (AP) (1  $\mu$ M) or PAR2-activating peptide (AP) (1  $\mu$ M) for 20 min. Aliquots were added to wells coated with G $\alpha_{i1}$ , G $\alpha_{i2}$  or G $\alpha_{i3}$  for 2 h and bound radioactivity was measured. Results are expressed as cpm/mg protein. PAR1-AP caused a significant increase in the binding of [<sup>35</sup>S]-GTP $\gamma$ S-G $\alpha$  complexes to wells coated with G $\alpha_{i3}$ , whereas PAR2-AP caused a significant increase in the [<sup>35</sup>S]-GTP $\gamma$ S-G $\alpha$  complexes to wells coated with G $\alpha_{i1}$  and G $\alpha_{i2}$ . Values are means  $\pm$  S.E. of four experiments. \*\* Significant increase in G protein activation (P<0.001).

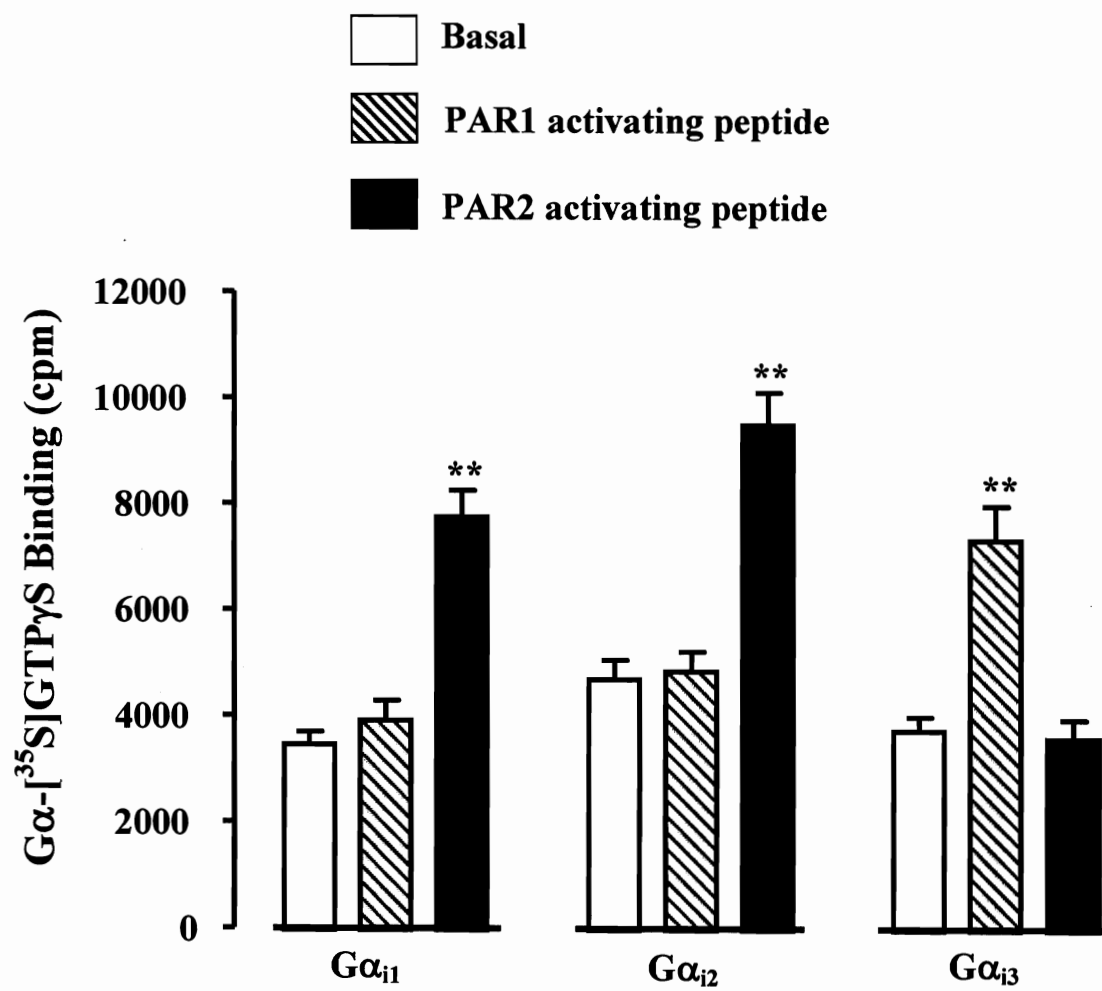


**Figure 5. Distinct pattern of pertussis toxin-insensitive G proteins activated by PAR1-AP and PAR2-AP in rabbit gastric smooth muscle cells.** Membranes isolated from freshly dispersed smooth muscle cells were incubated with  $^{35}\text{S}$ -labeled guanosine 5-O-(3-thiotriphosphate) ( $[^{35}\text{S}]\text{GTP}\gamma\text{S}$ ) in the presence or absence of PAR1-AP (1  $\mu\text{M}$ ) or PAR2-AP (1  $\mu\text{M}$ ) for 20 min. Aliquots were added to wells coated with  $\text{G}\alpha_q$ ,  $\text{G}\alpha_{12}$ , or  $\text{G}\alpha_{13}$  for 2 h and bound radioactivity was measured. Results are expressed as cpm/mg protein. PAR1-AP caused a significant increase in the binding of  $[^{35}\text{S}]\text{-GTP}\gamma\text{S-G}\alpha$  complexes to wells coated with  $\text{G}\alpha_q$  and  $\text{G}\alpha_{12}$ , whereas as PAR2-AP caused a significant increase in the  $[^{35}\text{S}]\text{-GTP}\gamma\text{S-G}\alpha$  complexes to wells coated with  $\text{G}\alpha_q$  and  $\text{G}\alpha_{13}$ . Values are means  $\pm$  S.E. of four experiments. \*\* Significant increase in G protein activation ( $P < 0.001$ ).

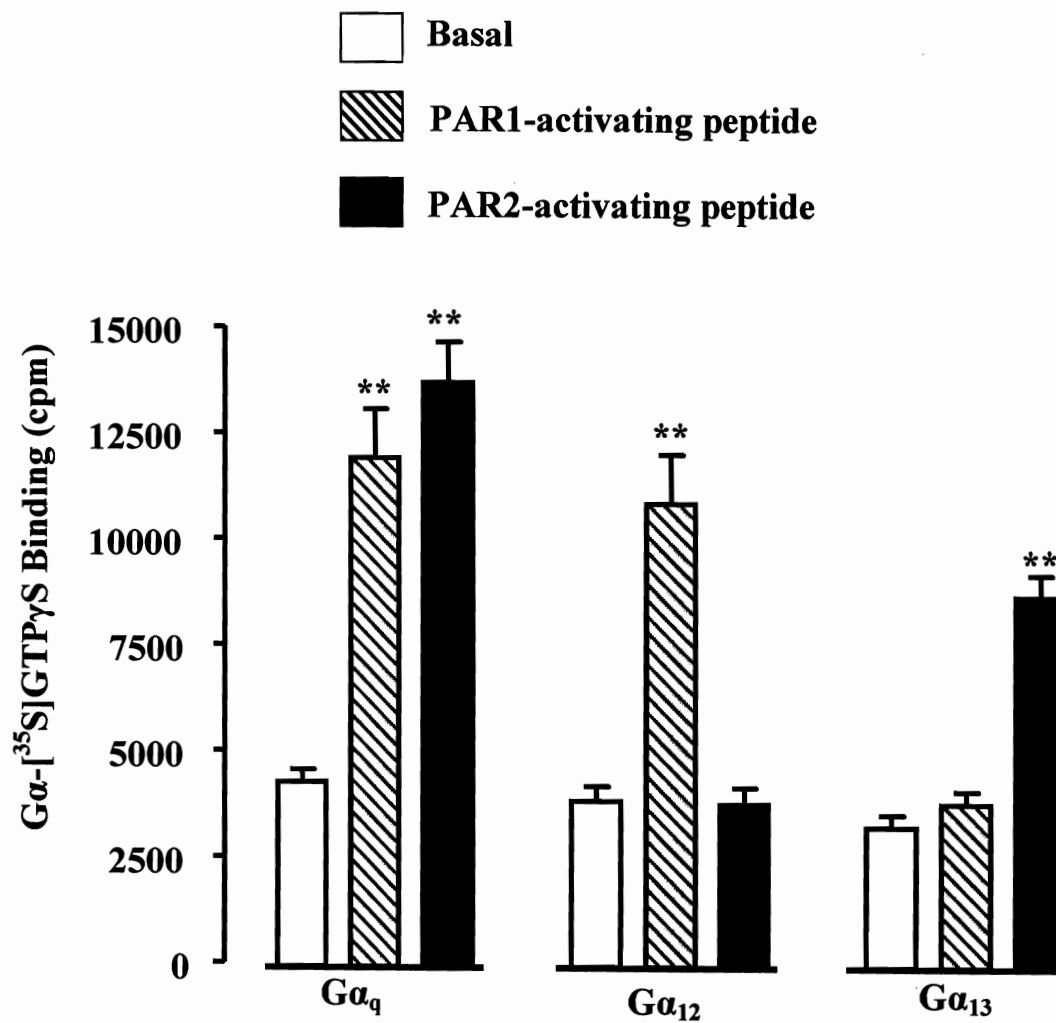
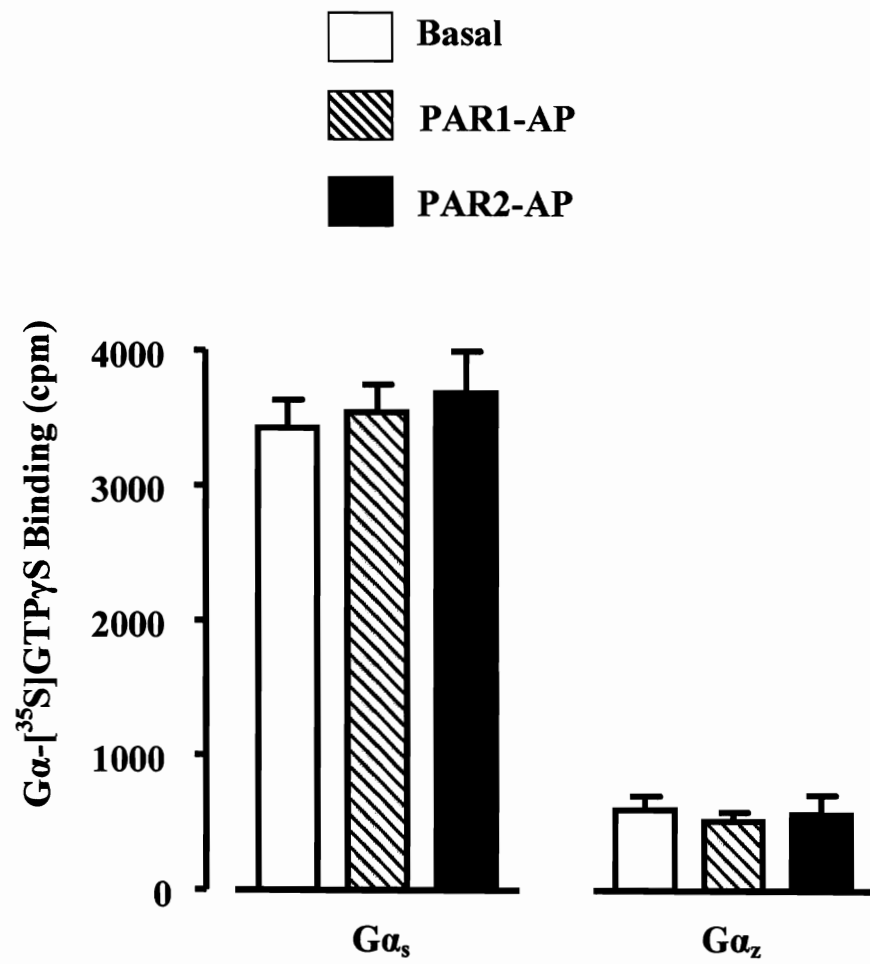


**Figure 6. PAR1-AP and PAR2-AP did not activate  $G\alpha_s$  and  $G\alpha_z$  in rabbit gastric smooth muscle cells.** Membranes isolated from freshly dispersed smooth muscle cells were incubated with [ $^{35}$ S]GTP $\gamma$ S in the presence or absence of PAR1-AP (1  $\mu$ M) or PAR2-AP (1  $\mu$ M) for 20 min. Aliquots were added to wells coated with  $G\alpha_s$  or  $G\alpha_z$  and bound radioactivity was measured. Results are expressed as cpm/mg protein. Neither PAR1-AP nor PAR2-AP caused a significant increase in the binding of [ $^{35}$ S]-GTP $\gamma$ S- $G\alpha$  complexes to wells coated with  $G\alpha_s$  or  $G\alpha_z$ . Values are means  $\pm$  S.E. of four experiments.





dependent fashion (Fig. 7) with an  $EC_{50}$  of 5 nM and maximal increase of  $460\pm 38\%$  ( $P<0.001$ ) above basal levels (basal activity  $520\pm 66$  cpm/mg protein). Similarly, PAR2-AP stimulated PI hydrolysis in a concentration-dependent fashion with an  $EC_{50}$  of 2 nM and maximal increase of  $503\pm 46\%$  ( $P<0.001$ ) above basal levels (basal activity  $520\pm 66$  cpm/mg protein). Treatment of cells with a selective inhibitor of PI hydrolysis abolished PI hydrolysis in response to both PAR1-AP and PAR2-AP (Fig. 8). Treatment of cells with PTx (200 ng/ml) for 1 h partially inhibited ( $33\pm 5\%$  inhibition,  $P<0.01$ ) PI hydrolysis in response to PAR2-AP, but had no effect on PI hydrolysis in response to PAR1-AP (Fig. 8). The results imply that PAR1 stimulated PI hydrolysis was mediated exclusively by pertussis toxin-insensitive  $G_q$  proteins. In contrast, PAR2 stimulated PI hydrolysis was mediated by both pertussis toxin-sensitive ( $G_i$ ) and -insensitive ( $G_q$ ) G proteins.

Further evidence for specific G protein coupling was obtained by expression of  $G\alpha$  minigenes in cultured smooth muscle cells. The synthetic peptide corresponding to the COOH terminus of  $G\alpha$  subunits selectively antagonized G protein activation by blocking receptor-G protein interaction. Minigene plasmid constructs that encode for the COOH-terminal peptide sequence of  $G\alpha_i$  and  $G\alpha_q$  were expressed to selectively block  $G_i$  and  $G_q$  activation, respectively. A minigene containing  $G\alpha$  in random order was expressed as a control. PAR1-AP (1  $\mu$ M) and PAR2-AP (1  $\mu$ M) induced PI hydrolysis (5-6 fold) in cultured smooth muscle cells that was closely similar to stimulated PI hydrolysis in freshly dispersed smooth muscle cells (~ 5 fold). Expression of  $G\alpha_q$

**Figure 7. Concentration-dependent stimulation of PI hydrolysis (PLC- $\beta$  activity) by PAR1-AP and PAR2-AP.** Freshly dispersed muscle cells labeled with myo-2- $^3\text{H}$ inositol were incubated with different concentrations of PAR1-AP and PAR2-AP for 60 s. Total  $^3\text{H}$ inositol phosphates were separated by ion-exchange chromatography. Results are expressed as total  $^3\text{H}$ inositol phosphate formation in cpm/mg protein above basal levels (basal levels:  $520 \pm 66$  cpm/mg protein). Values are means  $\pm$  S.E. of six experiments.

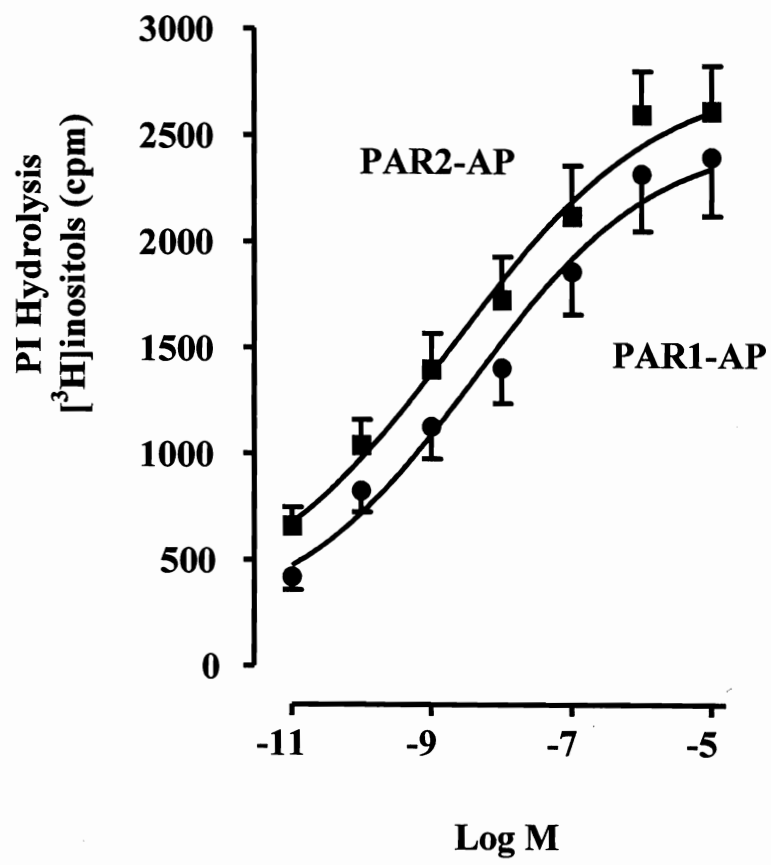
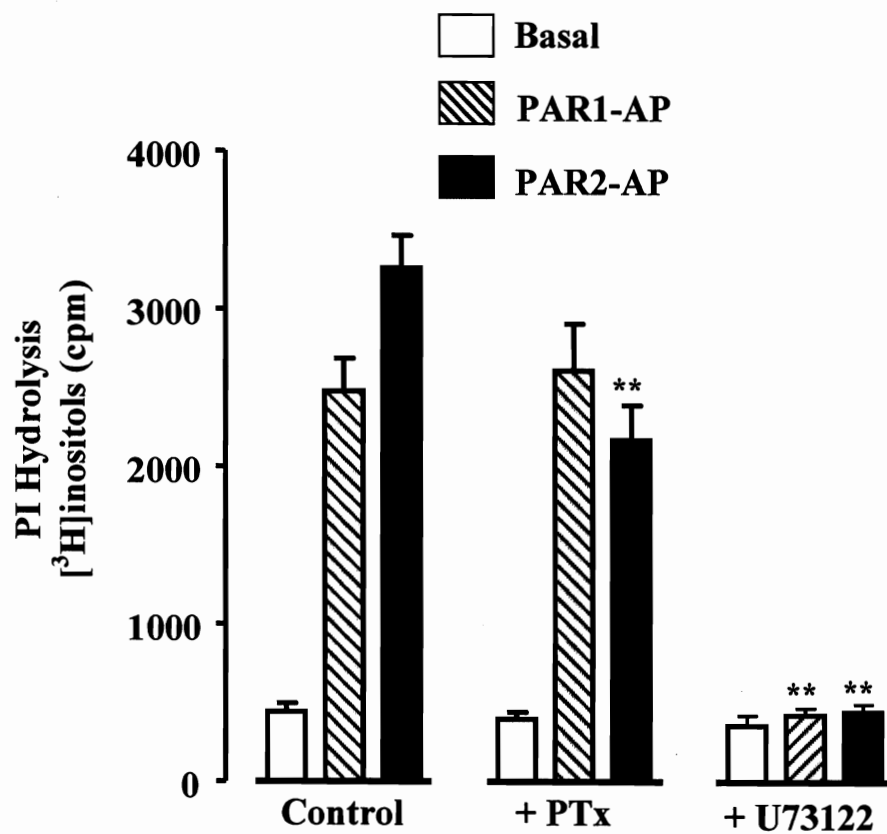


**Figure 8. Selective inhibition of PAR2-AP-stimulated PI hydrolysis by pertussis toxin.** Freshly dispersed muscle cells labeled with myo-2- $^3\text{H}$ inositol were incubated for 10 min with U73122 (10  $\mu\text{M}$ ) or with pertussis toxin (PTx, 200 ng/ml) for 60 min, and then treated with PAR1-AP (1  $\mu\text{M}$ ) or PAR2-AP (1  $\mu\text{M}$ ) for 60 s. Total  $^3\text{H}$ inositol phosphates were separated by ion-exchange chromatography. PI hydrolysis stimulated by both PAR1-AP and PAR2-AP was blocked by the PLC- $\beta$  inhibitor U73122. PI hydrolysis stimulated by PAR2-AP, but not PAR1-AP was partly inhibited by PTx. Results are expressed as total  $^3\text{H}$ inositol phosphate formation in cpm/mg protein. Values are means  $\pm$  S.E. of four experiments. \*\* Significant inhibition from control response ( $P < 0.01$ ).

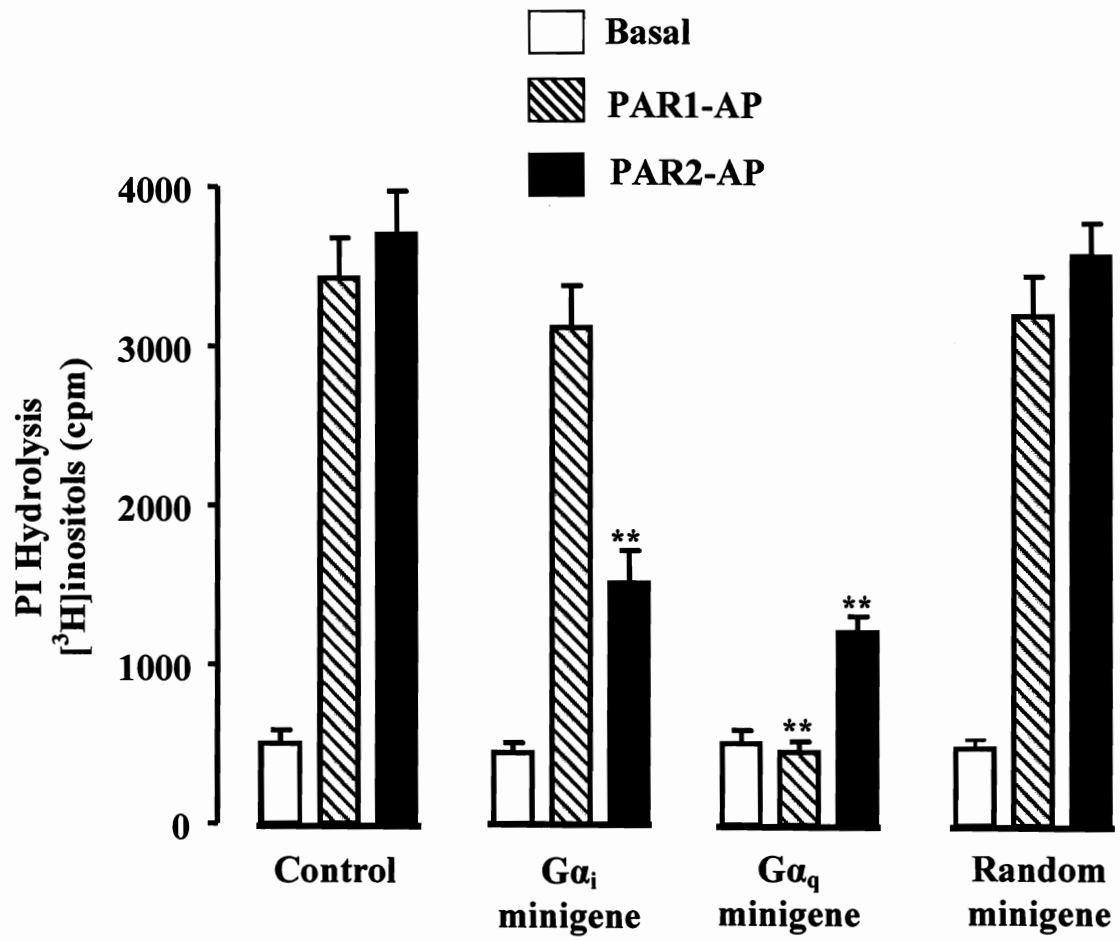


minigene abolished PI hydrolysis in response to PAR1-AP and partially inhibited ( $62\pm 5\%$  inhibition;  $P < 0.010$ ) PI hydrolysis in response to PAR2-AP (Fig. 9). In contrast, expression of  $G\alpha_i$  minigene had no effect on PI hydrolysis in response to PAR1-AP and partly inhibited ( $45\pm 4\%$  inhibition;  $P < 0.05$ ) PI hydrolysis in response to PAR2-AP (Fig. 9). It is worth noting that the inhibition of PAR2-AP-induced PI hydrolysis in cultured smooth muscle cells expressing  $G\alpha_i$  minigene was closely similar to inhibition of PI hydrolysis by PTx in freshly dispersed muscle cells. Expression of control minigene (random minigene) had no effect on PI hydrolysis in response to PAR1-AP or PAR2-AP (Fig. 9). The results corroborate that PI hydrolysis by PAR1 was solely mediated by  $G_q$ , whereas PI hydrolysis by PAR2 was mediated by both  $G_q$  and  $G_i$ .

### **10.3.2 Regulation of $G_q$ -coupled PI hydrolysis by PAR1 and PAR2 via RGS4 (Regulator of G protein Signaling)**

The strength and duration of  $G\alpha$ -GTP signaling are regulated by a family of GTPase-activating proteins known as regulators of G protein signaling (RGS). Smooth muscle cells of the gut express several RGS proteins (RGS3, RGS4, RGS6, RGS12 and RGS16). Previous studies have shown that activation of  $G_q$  by muscarinic m3 receptors and motilin receptors was regulated by RGS4 (52, 53). RGS4 accelerates  $G\alpha_q$ -GTPase activity and thus limits the activation of PLC- $\beta$ 1 by  $G\alpha_q$ . To examine whether the activation of  $G_q$  by PAR1 and PAR2 are regulated by RGS4, we overexpressed dominant negative RGS4(N88S) that lacks the ability to stimulate  $G\alpha$ -GTPase activity in cultured muscle cells and PI hydrolysis in response to PAR1-AP and PAR2-AP was measured.

**Figure 9. Inhibition of PAR1-AP- and PAR2-AP-stimulated PI hydrolysis by  $G\alpha_q$  minigene or  $G\alpha_i$  minigene.** Cultured gastric muscle cells labeled with myo-2- $[^3H]$ inositol and expressing  $G\alpha_q$  minigene,  $G\alpha_i$  minigene, random minigene or control vector were treated with PAR1-AP (1  $\mu$ M) or PAR2-AP (1  $\mu$ M) for 60 s. Total  $[^3H]$ inositol phosphates were separated by ion-exchange chromatography. PI hydrolysis stimulated by PAR1-AP was abolished in cells expressing  $G\alpha_q$  minigene, but was not affected in cells expressing  $G\alpha_i$  minigene. PI hydrolysis stimulated by PAR2-AP was partly inhibited in cells expressing  $G\alpha_q$  or  $G\alpha_i$  minigene. Results are expressed as total  $[^3H]$ inositol phosphate formation in cpm/mg protein. Values are means  $\pm$  S.E. of four experiments. \*\* Significant inhibition from control response ( $P < 0.01$ ).





PI hydrolysis in response to PAR1-AP and PAR2-AP was significantly augmented ( $71\pm 5\%$  and  $96\pm 7\%$ , respectively) in cells overexpressing RGS4(N88S) (Fig. 10). In contrast, PI hydrolysis in response to PAR1-AP and PAR2-AP was significantly attenuated ( $47\pm 6\%$  and  $42\pm 4\%$ , respectively) in cells overexpressing wild type RGS4 (Fig. 10). The pattern implied that PAR1- and PAR2-induced PI hydrolysis was mediated by  $G\alpha_q$ -dependent activation of PLC- $\beta 1$  and augmented by inactivation of RGS4.

### 10.3.3 Inhibition of adenylyl cyclase by PAR1 and PAR2

Freshly dispersed smooth muscle cells were used to examine the ability of  $G_i$ -coupled PAR1 and PAR2 to inhibit forskolin-stimulated cAMP formation. Treatment of muscle cells with forskolin ( $10\ \mu\text{M}$ ) for 10 min increased cAMP formation significantly ( $22.1\pm 1.86\ \text{pmol/mg}$  protein above basal level of  $2.4\pm 3\ \text{pmol/mg}$  protein) in the presence of  $100\ \mu\text{M}$  isobutyl methyl xanthine. At a concentration of  $1\ \mu\text{M}$ , PAR1-AP and PAR2-AP inhibited forskolin-stimulated cAMP formation by  $51\pm 5\%$  and  $61\pm 3\%$ , respectively (Fig. 11). Preincubation of muscle cells with PTx ( $200\ \text{ng/ml}$ ) for 1 h significantly attenuated the inhibitory effect of PAR1-AP and PAR2-AP ( $16\pm 3\%$  and  $17\pm 2\%$  inhibition of forskolin stimulated cAMP formation by PAR1-AP and PAR2-AP, respectively) (Fig. 11). The results are consistent with the activation of  $G_{i3}$  by PAR1-AP and  $G_{i2}$  and  $G_{i3}$  by PAR2-AP.

### 10.3.4 Activation of Rho kinase by PAR1 and PAR2

Previous studies in smooth muscles have shown that agonist coupled trimeric  $G_{i3}$  (ACh, motilin and S1P) and  $G_{i2}$  (lysophosphatidic acid) stimulate monomeric RhoA and

**Figure 10. PI hydrolysis stimulated by PAR1-AP and PAR2-AP was regulated by RGS4.** Cultured gastric muscle cells labeled with myo-2- $^3\text{H}$ inositol and overexpressing wild type RGS4, dominant negative RGS4 (RGS4[N88S]), or vector alone were treated with PAR1-AP (1  $\mu\text{M}$ ) or PAR2-AP (1  $\mu\text{M}$ ) for 60 s. Total  $^3\text{H}$ inositol phosphates were separated by ion-exchange chromatography. PI hydrolysis stimulated by PAR1-AP and PAR2-AP was inhibited in cells overexpressing wild type RGS4 and augmented in cells overexpressing RGS4(N88S). Results are expressed as total  $^3\text{H}$ inositol phosphate formation in cpm/mg protein. Values are means  $\pm$  S.E. of four experiments. \*\* Significant inhibition from control response ( $P < 0.01$ ); ## significant increase from control response ( $P < 0.01$ ).

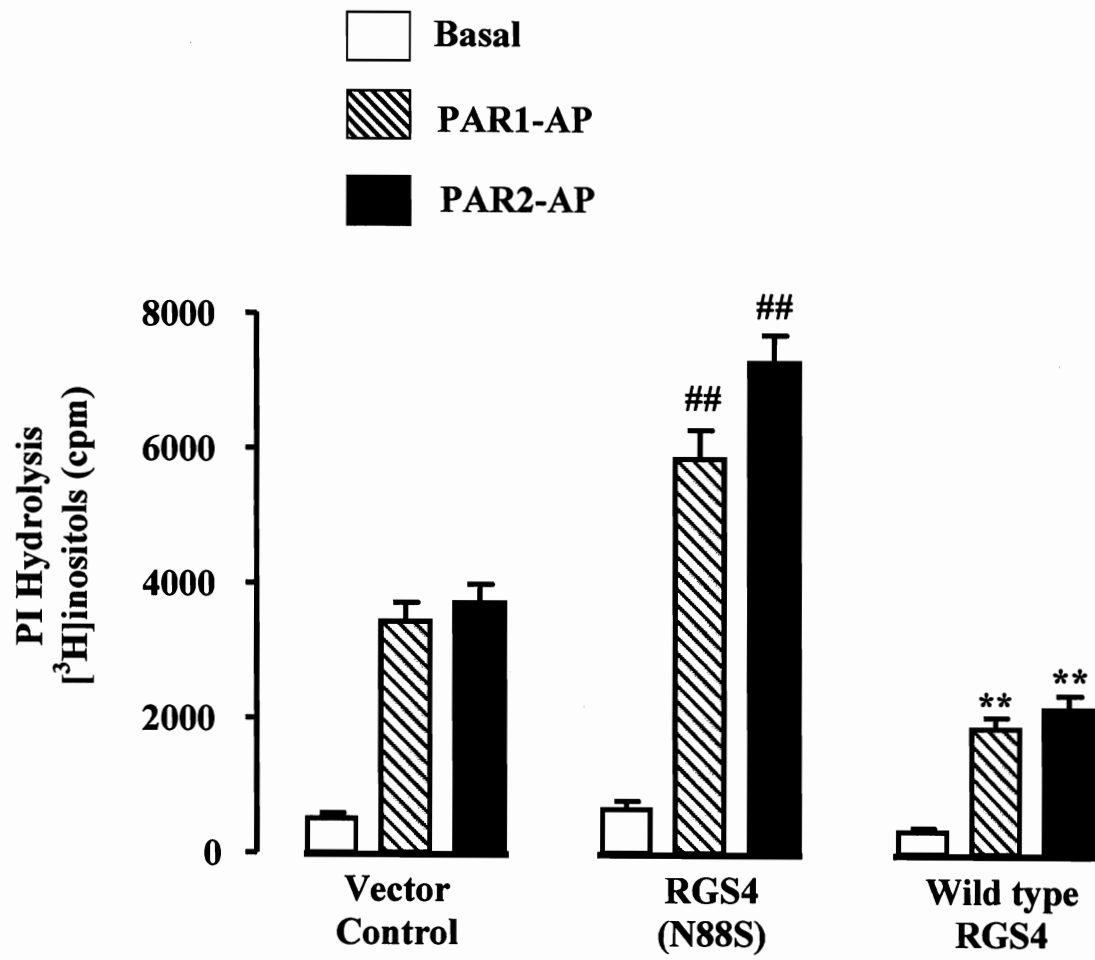
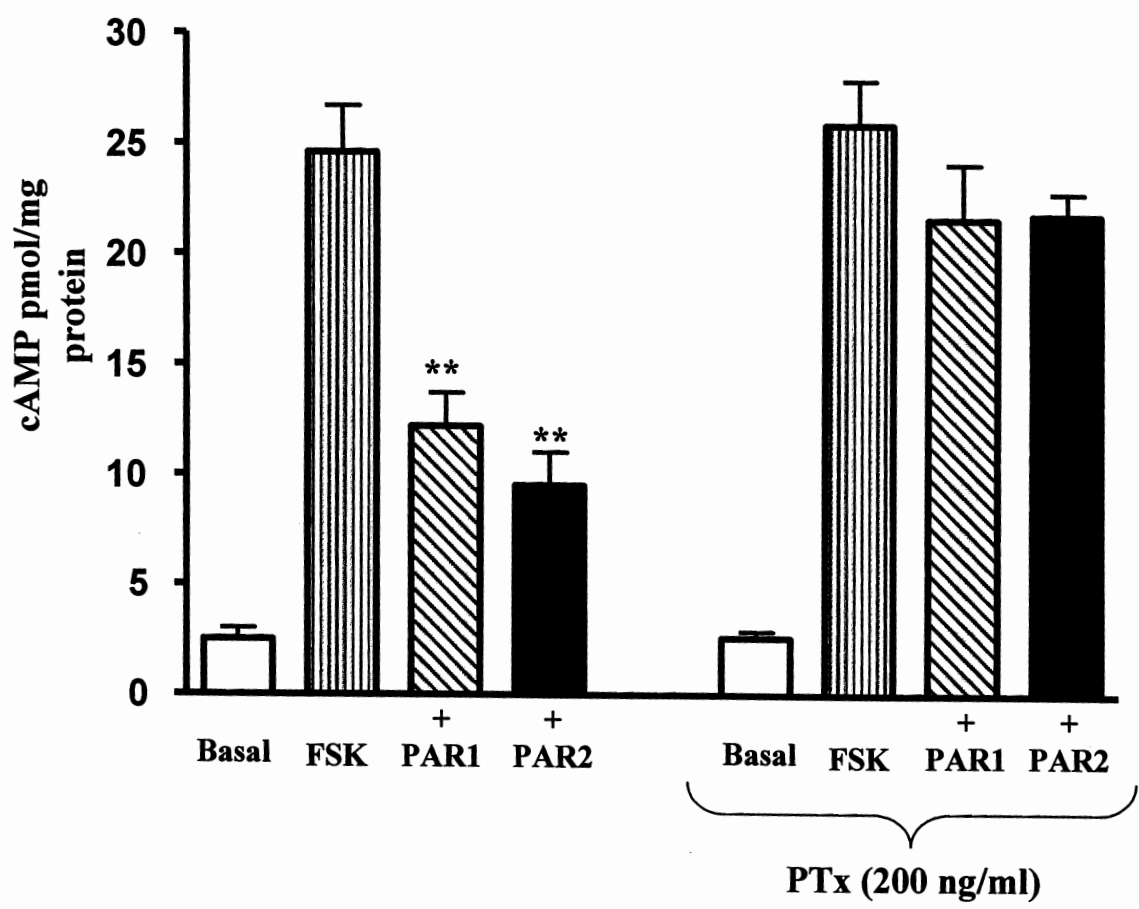


**Figure 11. Inhibition of forskolin-stimulated cAMP formation by PAR1-AP and PAR2-AP.** Cyclic AMP formation was measured in freshly dispersed muscle cells in the presence of 100  $\mu\text{M}$  isobutylmethylxanthine. Muscle cells were treated with forskolin (FSK, 10  $\mu\text{M}$ ) in the presence or absence of PAR1-AP (1  $\mu\text{M}$ ) or PAR2-AP (1  $\mu\text{M}$ ) for 60 s and cAMP was measured by radioimmunoassay. In some experiments cells were treated with pertussis toxin (200 ng/ml) for 60 min, and then treated with forskolin (10  $\mu\text{M}$ ) and PAR1-AP (1  $\mu\text{M}$ ) or PAR2-AP (1  $\mu\text{M}$ ) for 60 s. Results are expressed as pmol cAMP/mg protein. Values are means  $\pm$  S.E. of 4 experiments. \*\* Significant inhibition of forskolin-stimulated cAMP.



its downstream effector Rho kinase (52, 123, 171, 172). Activation of RhoA by G<sub>12</sub>-coupled PAR1 and G<sub>13</sub>-coupled PAR2 was examined as an increase in Rho kinase activity in response to PAR1-AP and PAR2-AP, respectively. In freshly dispersed smooth muscle cells both PAR1-AP and PAR2-AP stimulated Rho kinase activity by 155±19% and 216±24% above basal levels, respectively (basal levels: 3661±587 cpm/mg protein) (Fig. 12). Treatment of dispersed muscle cells with the selective inhibitor of Rho kinase (Y27632, 1 μM) abolished Rho kinase activity in response to PAR1-AP and PAR2-AP (Fig. 12).

Similarly, both PAR1-AP and PAR2-AP stimulated Rho kinase activity in cultured smooth muscle cells. PAR1-AP and PAR2-AP induced Rho kinase activity in cultured smooth muscle cells (146±7% and 218±16% increase, respectively) was not significantly different from PI hydrolysis in freshly dispersed smooth muscle cells. Overexpression of dominant negative RhoA (RhoA[T19N]) in cultured muscle cells significantly inhibited Rho kinase activity in response to PAR1-AP and PAR2-AP (Fig. 13). The results suggest that activation of Rho kinase is downstream of RhoA.

Evidence for the involvement of G<sub>12</sub> and G<sub>13</sub> in PAR1 and PAR2 mediated Rho kinase activity was obtained by expression of Gα minigenes in cultured smooth muscle cells. Minigene plasmid constructs that encode the COOH-terminal peptide sequence of Gα<sub>12</sub> and Gα<sub>13</sub> were expressed to selectively block G<sub>12</sub> and G<sub>13</sub> activation, respectively. Expression of the Gα<sub>12</sub> minigene abolished Rho kinase activation (94±3% inhibition; P<0.01) in response to PAR1-AP, whereas expression of the Gα<sub>13</sub> minigene had no effect on Rho kinase activity in response to PAR1-AP (Fig. 14). In contrast, the expression of

**Figure 12. Inhibition of PAR1-AP- and PAR2-AP-stimulated Rho kinase activity by the selective Rho kinase inhibitor Y27632.** Freshly dispersed muscle cells were incubated with PAR1-AP (1  $\mu$ M) or PAR2-AP (1  $\mu$ M) for 10 min in the presence or absence of selective Rho kinase inhibitor Y27632 (1  $\mu$ M). Rho kinase activity was measured using [ $^{32}$ P]ATP by immunokinase assay. Rho kinase activity stimulated by PAR1-AP and PAR2-AP was blocked by Y27632. Results are expressed as cpm/mg protein. Values are means  $\pm$  S.E. of four experiments. \*\* Significant inhibition from control response ( $P < 0.01$ ).

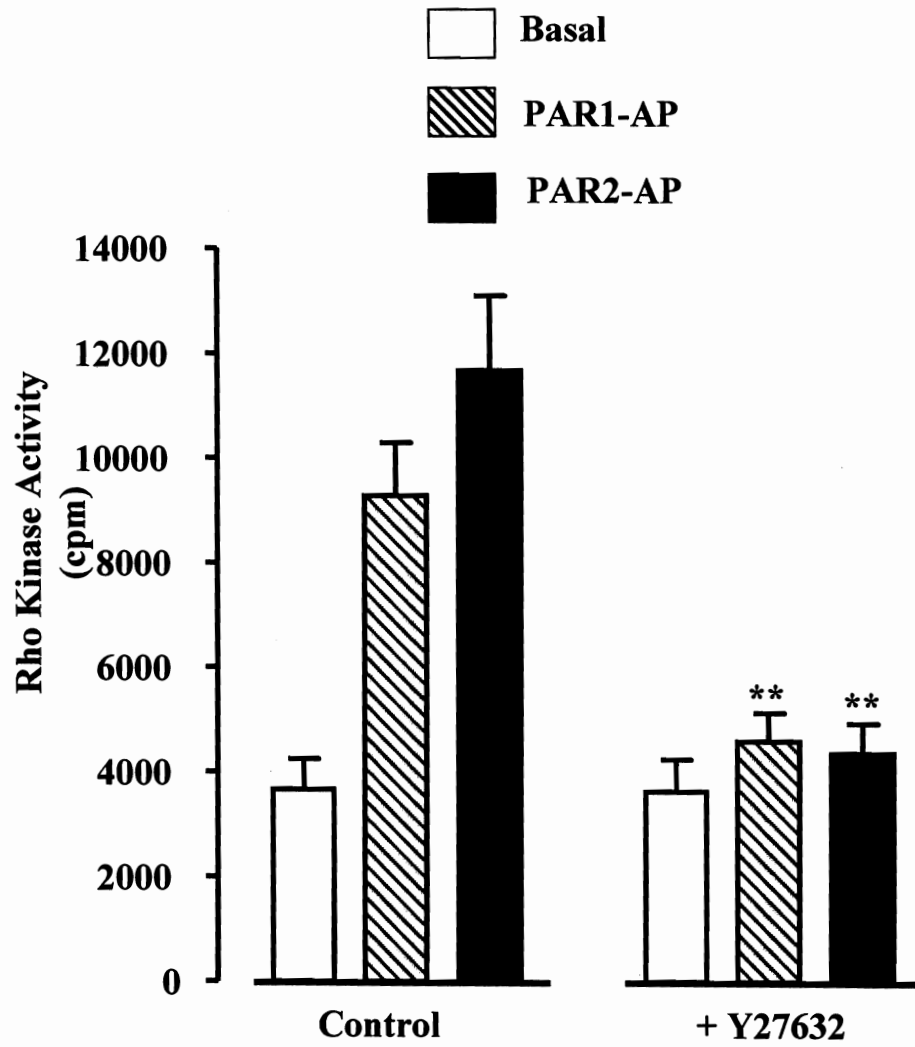




**Figure 13. Inhibition of PAR1-AP- and PAR2-AP-stimulated Rho kinase activity in muscle cell expressing dominant negative RhoA.** Cultured smooth muscle cells expressing dominant negative RhoA (RhoA[T19N]) or vector alone were incubated with PAR1-AP (1  $\mu$ M) or PAR2-AP (1  $\mu$ M) for 10 min. Rho kinase activity was measured using [ $^{32}$ P]ATP by immunokinase assay. Rho kinase activity stimulated by PAR1-AP and PAR2-AP was blocked in cells expressing RhoA(T19N). In muscle cells transfected with vector only, basal and PAR-stimulated Rho kinase activities were similar to those in freshly dispersed muscle cells. Results are expressed as cpm/mg protein. Values are means  $\pm$  S.E. of four experiments. \*\* Significant inhibition from control response (P<0.01).

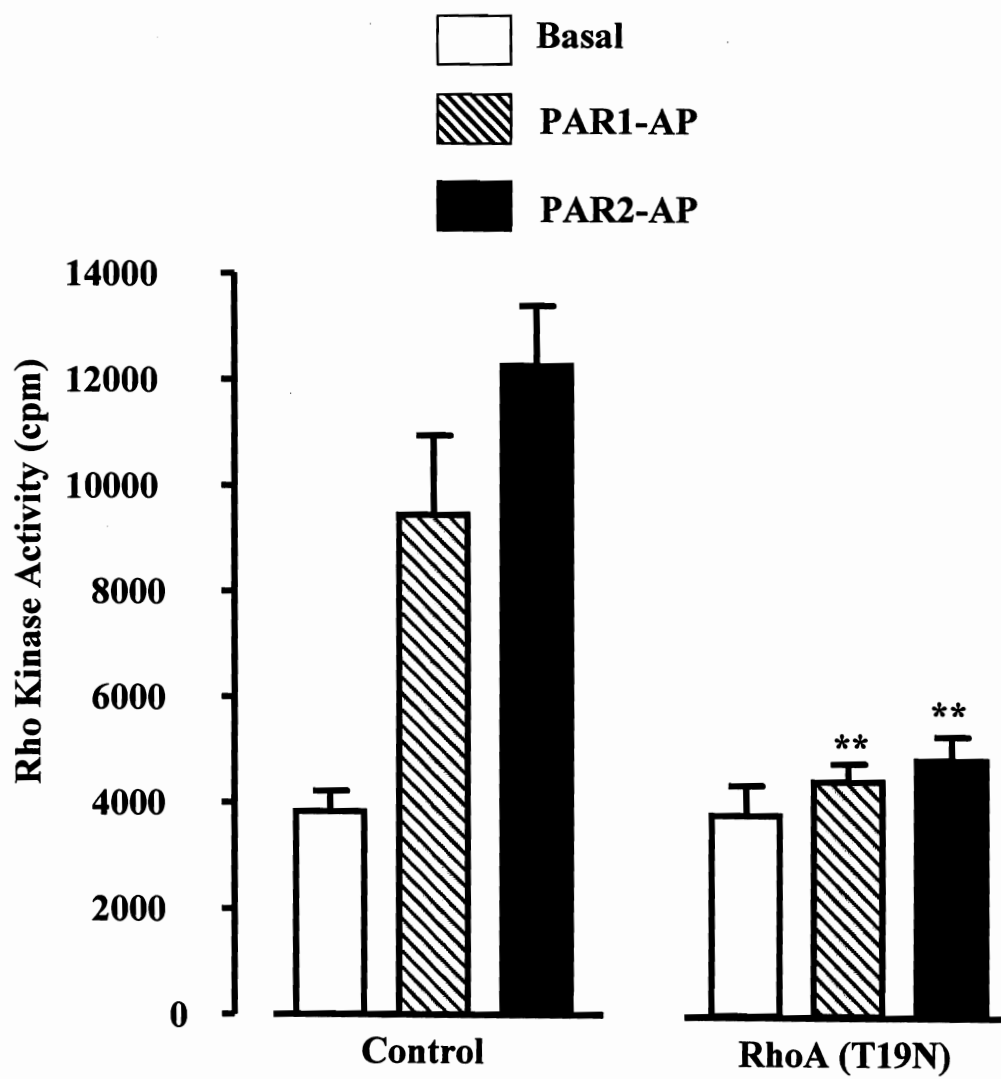
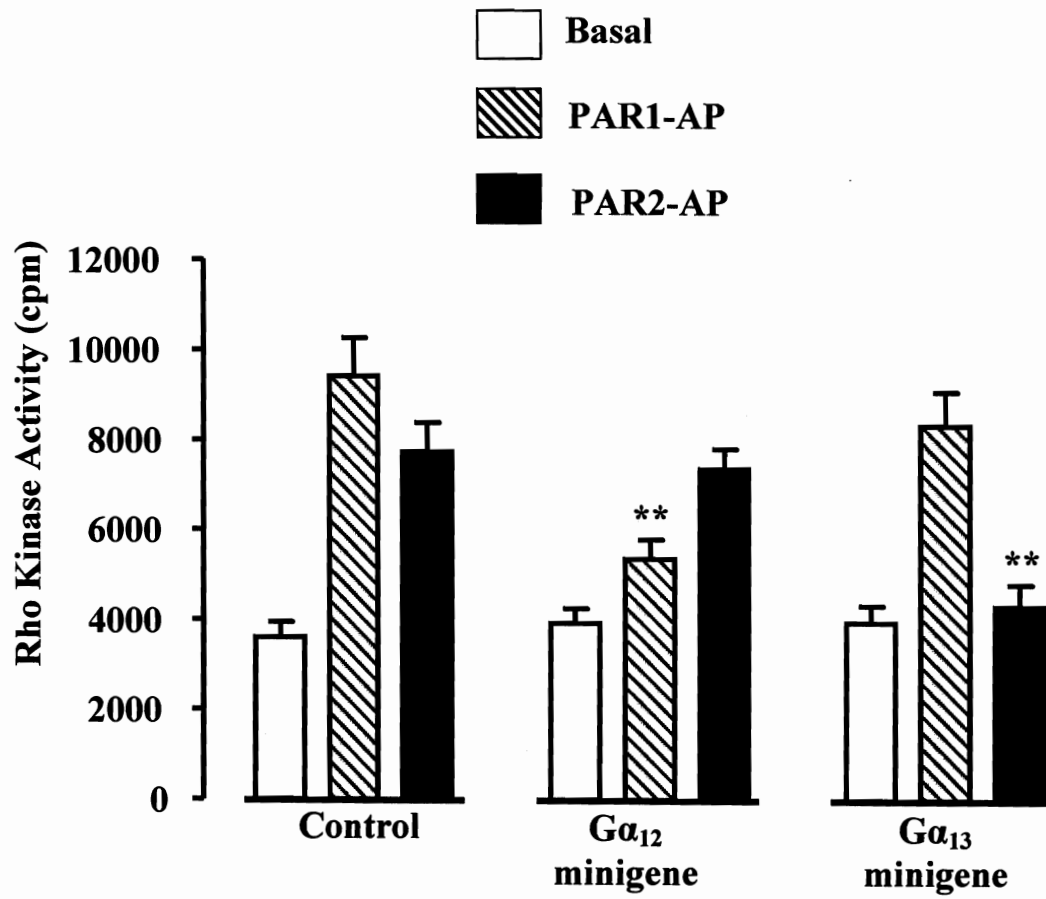


**Figure 14. Inhibition of PAR1-AP- and PAR2-AP-stimulated Rho kinase activity by  $G\alpha_{12}$  minigene or  $G\alpha_{13}$  minigene, respectively.** Cultured gastric muscle cells expressing  $G\alpha_{12}$  or  $G\alpha_{13}$  minigene, or control vector were treated with PAR1-AP (1  $\mu$ M) or PAR2-AP (1  $\mu$ M) for 10 min. Rho kinase activity was measured using [ $^{32}$ P]ATP by immunokinase assay. Rho kinase activity stimulated by PAR1-AP was selectively blocked in cells expressing  $G\alpha_{12}$  minigene, whereas Rho kinase activity stimulated by PAR2-AP was selectively blocked in cells expressing  $G\alpha_{13}$  minigene. Results are expressed as cpm/mg protein. Values are means  $\pm$  S.E. of four experiments. \*\* Significant inhibition from control response ( $P < 0.01$ ).



the  $G\alpha_{13}$  minigene abolished Rho kinase activation ( $96\pm 3\%$  inhibition;  $P < 0.01$ ) in response to PAR2-AP, whereas expression of the  $G\alpha_{12}$  minigene had no effect on Rho kinase activity in response to PAR2-AP (Fig. 14). These results provide the evidence that PAR1 stimulates Rho kinase activity via  $G_{12}$  whereas PAR2 stimulates Rho kinase activity via  $G_{13}$ . The results are also consistent with the selective activation of  $G_{12}$  by PAR1-AP and  $G_{13}$  by PAR2-AP.

### 10.3.5 Contraction induced by PAR1 and PAR2 in smooth muscle

The ability of PAR1 and PAR2 to induce smooth muscle contraction was examined in dispersed muscle cells. Contraction was measured by scanning micrometry and expressed as percent decrease in muscle cell length compared to control cell length (mean control cell length:  $105 \pm 3 \mu\text{m}$ ). Consistent with their ability to stimulate PLC- $\beta$ 1 and Rho kinase activity, PAR1-AP and PAR2-AP caused contraction of dispersed gastric smooth muscle cells. As with other agonists that activated PLC- $\beta$ 1 and Rho kinase (e.g., acetylcholine, motilin, S1P), PAR1-AP and PAR2-AP induced contraction was characterized by an initial transient phase followed by a sustained phase (Fig. 15). Contraction induced by PAR1-AP and PAR2-AP was concentration-dependent with an  $EC_{50}$  of 1 nM (Fig. 16). Maximal contraction induced by PAR1-AP ( $30\pm 2\%$  decrease in cell length) and PAR2-AP ( $32\pm 3\%$  decrease in cell length) was similar to that elicited by other contractile agonists, such as ACh ( $31\pm 5\%$ ), S1P ( $29\pm 3\%$ ), cholecystokinin ( $32\pm 2\%$ ) or 5-hydroxytryptamine ( $29\pm 4\%$ ).

MLC<sub>20</sub> phosphorylation by PAR1-AP and PAR2-AP which measured using phospho-specific substrate (MLC<sub>20</sub> Ser<sup>19</sup>), was rapid (within 30 s) and sustained (10 min)

**Figure 15. Time course of PAR1-AP- and PAR2-AP-induced contraction in dispersed gastric smooth muscle cells.** PAR1-AP (1  $\mu$ M) or PAR2-AP (1  $\mu$ M) was added to freshly isolated muscle cells for different periods of time ranging from 30 s to 10 min. Contraction attained a peak within 30 s, and sustained for 10 min. Muscle contraction was measured by scanning micrometry, and the results are expressed as percent decrease in cell length from control cell length ( $105 \pm 3 \mu$ m). Values are means  $\pm$  S.E. of six experiments.

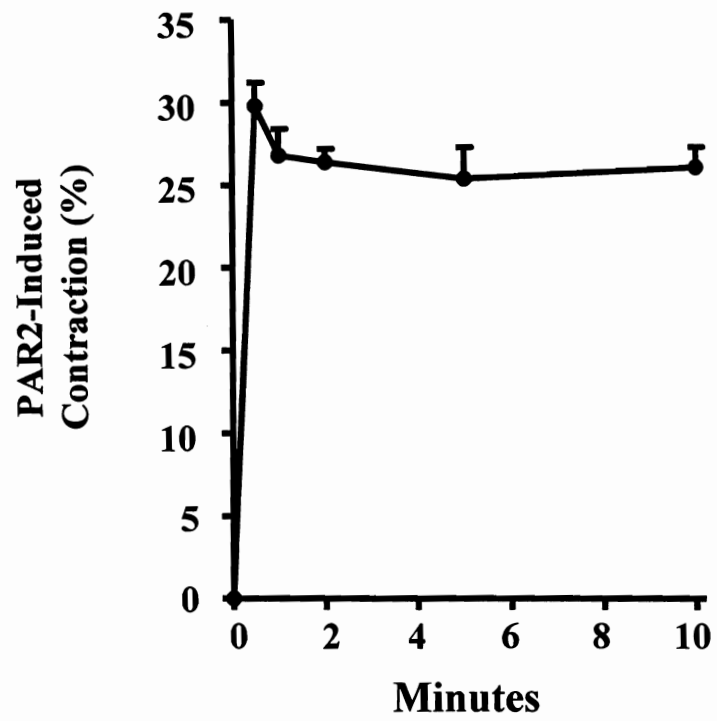
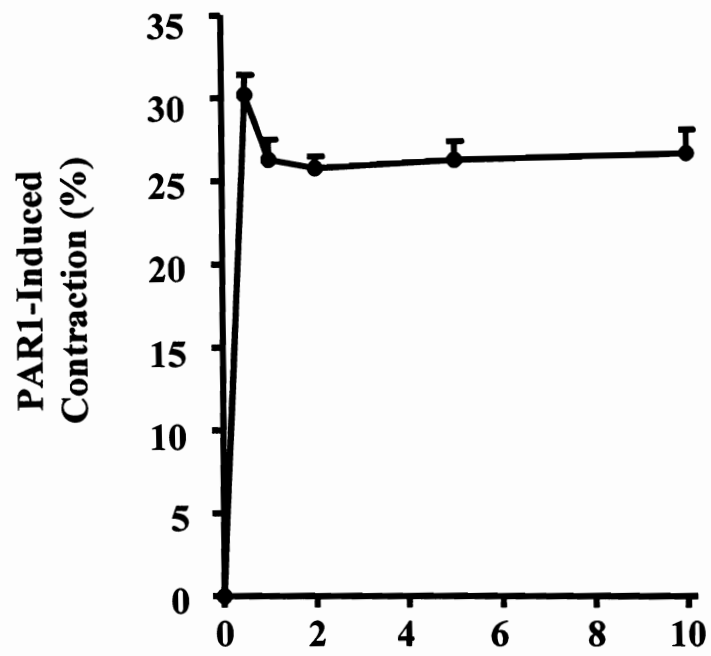
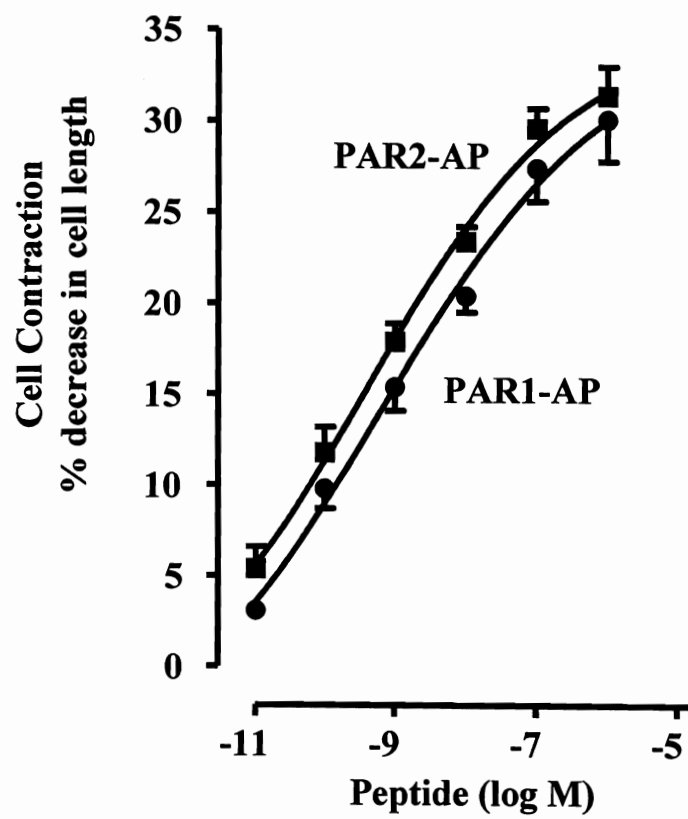


**Figure 16. Concentration-response curves for the contractile effect of PAR1-AP and PAR2-AP in dispersed gastric smooth muscle cells.** PAR1-AP or PAR2-AP was added to freshly isolated muscle cells at a concentration ranging from 10 pM to 1  $\mu$ M, and peak contraction was measured at 30 s. Contraction was measured by scanning micrometry, and the results are expressed as percent decrease in cell length from control cell length ( $105 \pm 3 \mu\text{m}$ ). Values are means  $\pm$  S.E. of six experiments.





closely paralleling the biphasic nature of contraction (Fig. 17).

### **10.3.6 Pathways mediating initial contraction induced by PAR1 and PAR2**

Previous studies have shown that agonist-induced initial contraction is  $\text{Ca}^{2+}$ -dependent and reflects the sequential activation of PLC- $\beta$ ,  $\text{IP}_3$  formation,  $\text{IP}_3$ -dependent  $\text{Ca}^{2+}$  release,  $\text{Ca}^{2+}$ /calmodulin-dependent activation of MLC kinase and phosphorylation of Ser<sup>19</sup> on MLC<sub>20</sub>, leading to interaction of actin and myosin and muscle contraction (52, 104, 120, 172). Consistent with this pathway, the initial (30 s) contraction by PAR1-AP and PAR2-AP was abolished by the PLC- $\beta$  inhibitor U73122 (10  $\mu\text{M}$ ) and the MLC kinase inhibitor ML-9 (10  $\mu\text{M}$ ) (Figs. 18 and 19). Pretreatment of muscle cells with PTx (200 ng/ml) for 1 h partly inhibited contraction induced by PAR2-AP, but had no effect on contraction induced by PAR1-AP (Figs. 18 and 19). The partial inhibition of contraction by PTx implied participation of both  $G_q$  and  $G_{i1}$  in the stimulation of PI hydrolysis. These results are consistent with PAR2-induced activation of PLC- $\beta$  by both  $G_q$  and  $G_i$  proteins and selective inhibition of PI hydrolysis by PTx. Initial contraction induced by PAR1-AP and PAR2-AP was not affected by the PKC inhibitor bisindolylmaleimide (1  $\mu\text{M}$ ) or the Rho kinase inhibitor Y27632 (1  $\mu\text{M}$ ) (Figs 18 and 19).

### **10.3.7 Pathways mediating sustained contraction induced by PAR1 and PAR2**

Unlike initial contraction, agonist-stimulated contraction and MLC<sub>20</sub> phosphorylation are  $\text{Ca}^{2+}$ -independent but are dependent on inhibition of MLC phosphatase. Inhibition of MLC phosphatase is mediated by RhoA-dependent cascades

**Figure 17. Phosphorylation of MYPT1, CPI-17, and MLC<sub>20</sub> by PAR1-AP and PAR2-AP in dispersed muscle cells.** Freshly dispersed muscle cells were treated with PAR1-AP (1  $\mu$ M) or PAR2-AP for 30 s and 10 min. MLC<sub>20</sub> phosphorylation was measured using phospho-specific-Ser<sup>19</sup> MLC<sub>20</sub> antibody. MYPT1 phosphorylation was measured using phospho-specific-Thr<sup>696</sup> MYPT1 antibody. CPI-17 phosphorylation was measured using phospho-specific-Thr<sup>38</sup> antibody. Equal amounts of total protein (50  $\mu$ g) were loaded and confirmed by Western blotting using  $\beta$ -actin antibody.

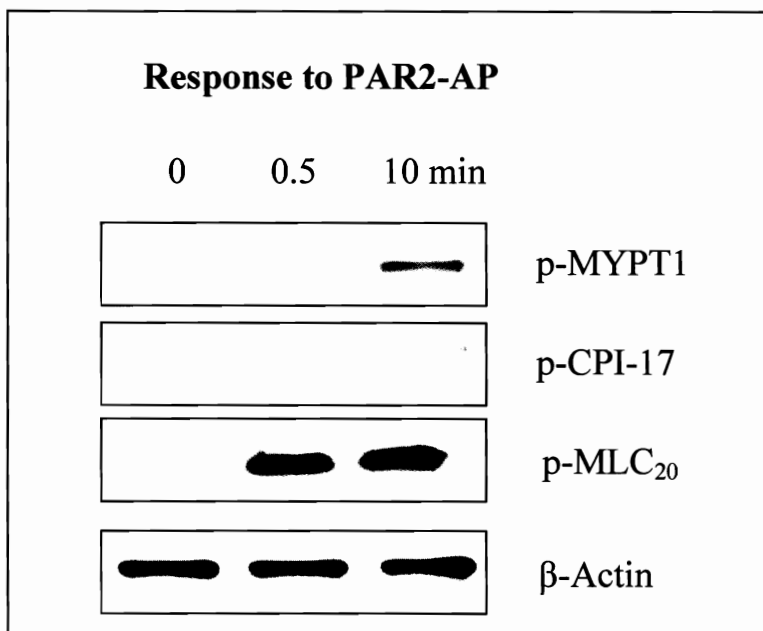
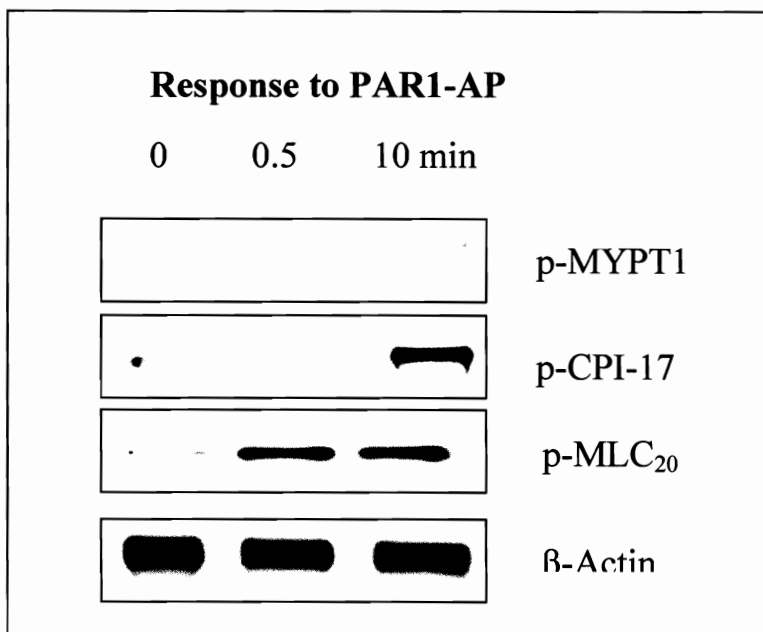


**Figure 18. Blockade of PAR1-AP-induced initial contraction by inhibitors of phospholipase C and MLC kinase.** Freshly dispersed muscle cells were treated separately with the PLC inhibitor U73122 (10  $\mu$ M), MLC kinase inhibitor ML-9 (10  $\mu$ M), PKC inhibitor bisindolylmaleimide (1  $\mu$ M), Rho kinase inhibitor Y27632 (1  $\mu$ M) for 10 min, or pertussis toxin (200 ng/ml) for 60 min, and then treated with PAR1-AP (1  $\mu$ M) for 30 s. Muscle contraction was measured by scanning micrometry, and the results are expressed as percent decrease in cell length from control cell length ( $105 \pm 3 \mu\text{m}$ ). Values are means  $\pm$  S.E. of six experiments. \*\* Significant inhibition from control response ( $P < 0.01$ ).

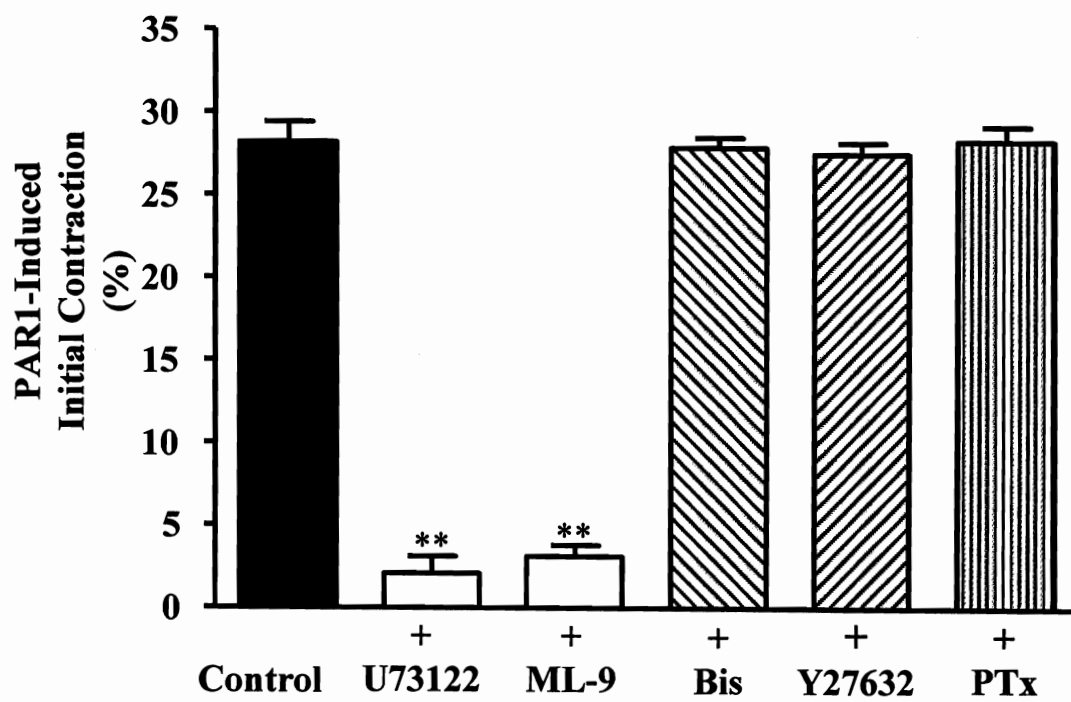
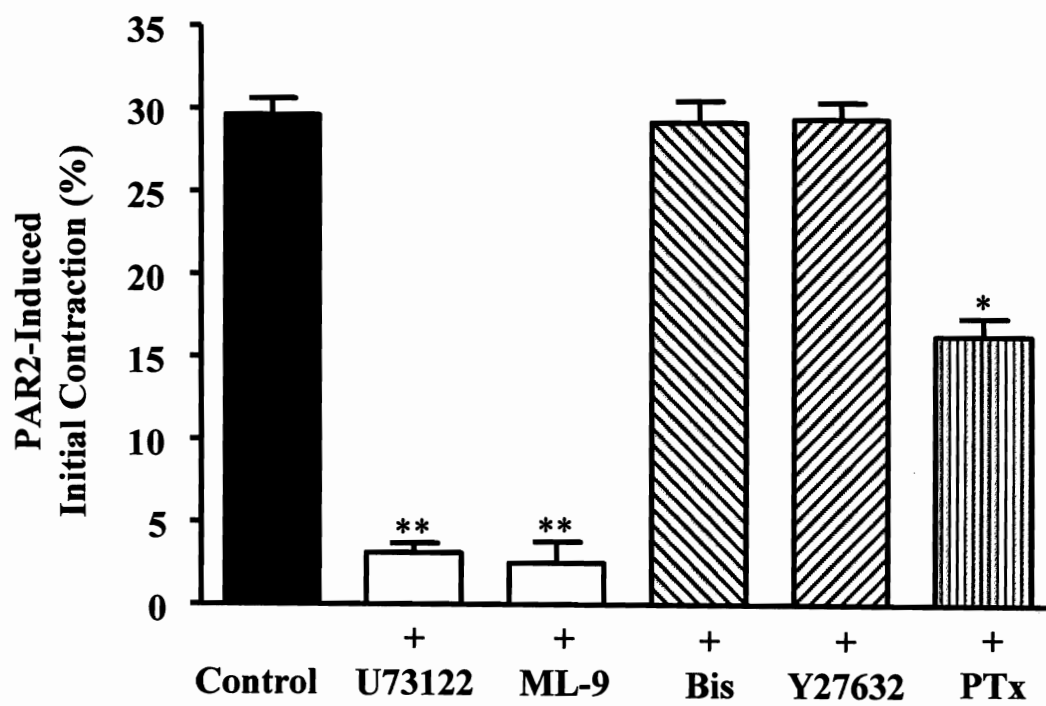


**Figure 19. Blockade of PAR2-AP-induced initial contraction by inhibitors of phospholipase C, MLC kinase, and pertussis toxin.** Freshly dispersed muscle cells were treated separately with the PLC inhibitor U73122 (10  $\mu$ M), MLC kinase inhibitor ML-9 (10  $\mu$ M), PKC inhibitor bisindolylmaleimide (1  $\mu$ M), Rho kinase inhibitor Y27632 (1  $\mu$ M) for 10 min, or pertussis toxin (200 ng/ml) for 60 min, and then treated with PAR2-AP (1  $\mu$ M) for 30 s. Muscle contraction was measured by scanning micrometry, and the results are expressed as percent decrease in cell length from control cell length (105  $\pm$  3  $\mu$ m). Values are means  $\pm$  S.E. of six experiments. \*\* Significant inhibition from control response (P<0.01); \* Significant inhibition from control response (P<0.05).





involving phosphorylation of MYPT1 (at Thr<sup>696</sup>), the regulatory subunit of MLC phosphatase, by Rho kinase and CPI-17 (at Thr<sup>38</sup>), an endogenous inhibitor of MLC phosphatase, by PKC Activation of RhoA results in the stimulation of phospholipase D (PLD), which yields phosphatidic acid as its primary product. Dephosphorylation of phosphatidic acid to diacylglycerol results in sustained activation of PKC. The involvement of Rho kinase and PKC are receptor specific. Both Rho kinase (MYPT1) and PKC (CPI-17) participate in the responses to muscarinic m3, S1P<sub>2</sub>, and motilin receptors. Only Rho kinase participates in the response to endothelin ETA receptors, whereas only PKC participates in response to lysophosphatidic acid LPA3 receptors.

The sustained (10 min) contraction by PAR1-AP was preferentially blocked by the PKC inhibitor bisindolylmaleimide (1  $\mu$ M), whereas sustained contraction by the PAR2-AP was preferentially blocked by the Rho kinase inhibitor Y27632 (1  $\mu$ M) (Figs. 20 and 21). Sustained contraction by both agonists was not affected by the PLC inhibitor U73122 and the MLC kinase inhibitor ML-9, suggesting that contraction was Ca<sup>2+</sup>-independent (Figs. 20 and 21).

The results with the inhibitors are corroborated by measurements of MYPT1 and CPI-17 phosphorylation in response to PAR1-AP and PAR2-AP. MYPT1 phosphorylation by Rho kinase and CPI-17 phosphorylation by PKC was measured using antibody phospho-specific substrates MYPT1-Thr<sup>696</sup> and CPI-17-Thr<sup>38</sup> respectively. Although both PAR1-AP and PAR2-AP induced sustained MLC<sub>20</sub> phosphorylation, only PAR1-AP induced CPI-17 phosphorylation whereas PAR2-AP induced MYPT1 phosphorylation (Fig. 17). The pattern implied that Rho kinase (MYPT1) did not

**Figure 20. Blockade of PAR1-AP-induced sustained contraction by the inhibitor of PKC.** Freshly dispersed muscle cells were treated separately with U73122 (10  $\mu$ M), ML-9 (10  $\mu$ M), bisindolylmaleimide (1  $\mu$ M), or Y27632 (1  $\mu$ M) for 10 min, or pertussis toxin (200 ng/ml) for 60 min, and then treated with PAR1-AP (1  $\mu$ M) for 10 min. Sustained contraction was greatly inhibited by the PKC inhibitor bisindolylmaleimide. Muscle contraction was measured by scanning micrometry, and the results are expressed as percent decrease in cell length from control cell length ( $105 \pm 3 \mu\text{m}$ ). Values are means  $\pm$  S.E. of six experiments. \*\* Significant inhibition from control response ( $P < 0.01$ ); \* Significant inhibition from control response ( $P < 0.05$ ).

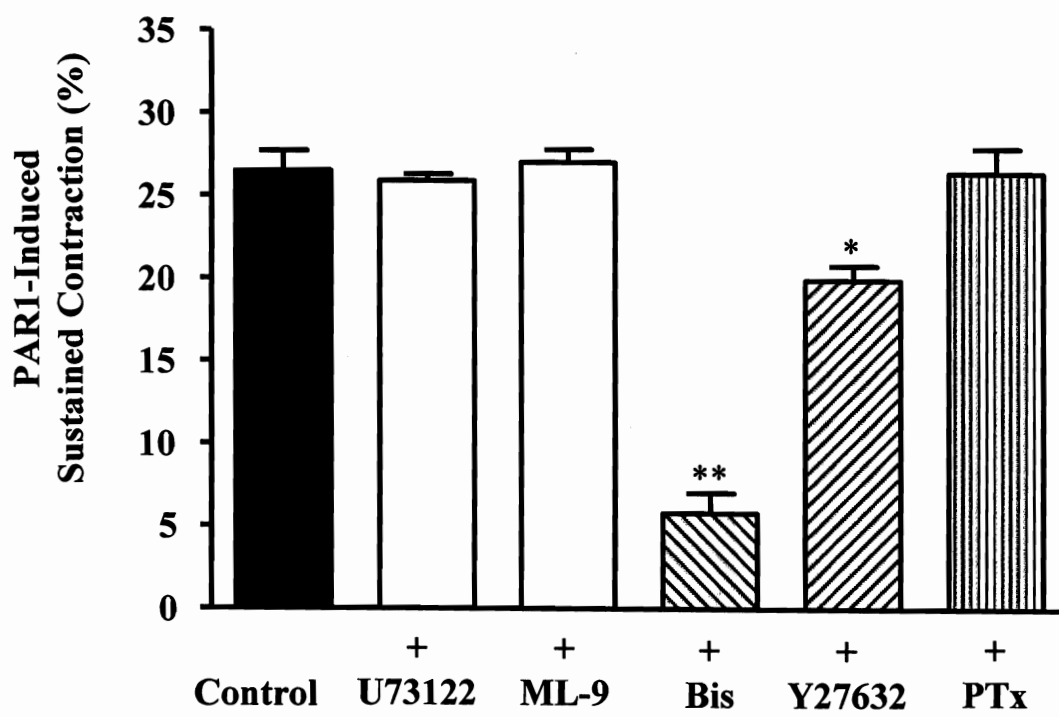
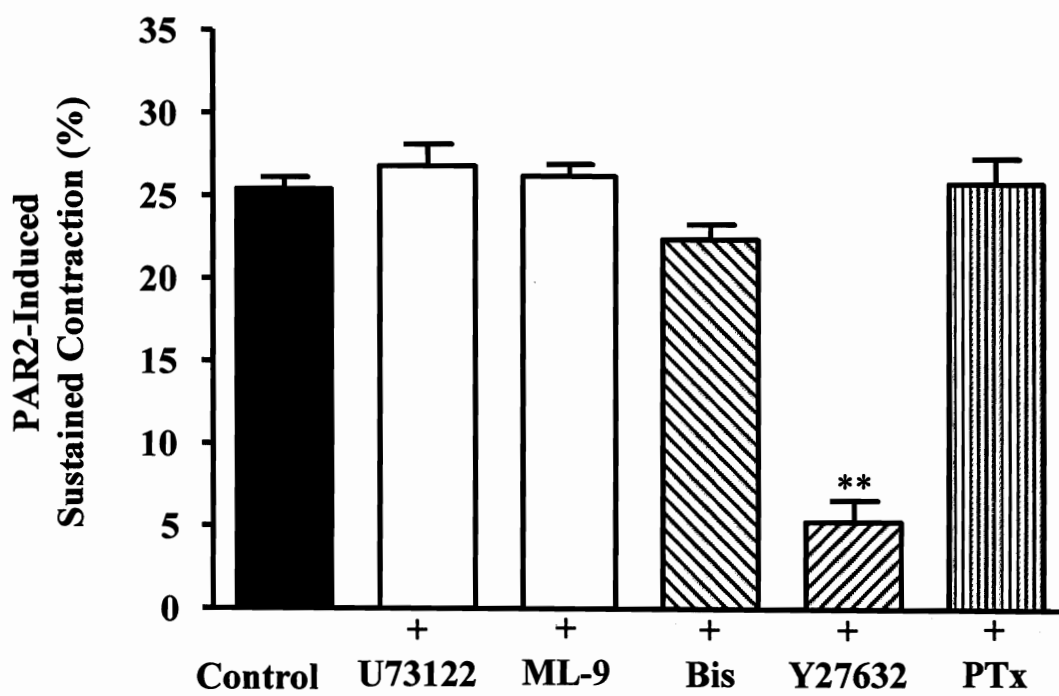


**Figure 21. Blockade of PAR2-AP-induced sustained contraction by the inhibitor of Rho kinase.** Freshly dispersed muscle cells were treated separately with U73122 (10  $\mu$ M), ML-9 (10  $\mu$ M), bisindolylmaleimide (1  $\mu$ M), or Y27632 (1  $\mu$ M) for 10 min, or pertussis toxin (200 ng/ml) for 60 min, and then treated with PAR2-AP (1  $\mu$ M) for 10 min. Sustained contraction was selectively blocked by the Rho kinase inhibitor Y27632. Muscle contraction was measured by scanning micrometry, and the results are expressed as percent decrease in cell length from control cell length ( $105 \pm 3 \mu\text{m}$ ). Values are means  $\pm$  S.E. of 5-6 experiments. \*\* Significant inhibition from control response ( $P < 0.01$ ).



participate in the inhibition of MLC phosphatase leading to the phosphorylation of MLC<sub>20</sub> with PAR1 activation and PKC (CIP-17) did not participate with PAR2 activation.

### **10.3.8 Activation of nuclear factor NF- $\kappa$ B pathway by PAR1 and PAR2**

NF- $\kappa$ B is activated by a variety of stimuli, cytokines (e.g., IL-1 $\beta$ ) and G protein-coupled receptor agonists (e.g. lipopolysacchride). In the basal state, NF- $\kappa$ B is in the cytoplasm and its activity is masked by binding to NF- $\kappa$ B inhibitor I $\kappa$ B $\alpha$ . The canonical pathway for activation of NF- $\kappa$ B involves phosphorylation of I $\kappa$ B $\alpha$  by I $\kappa$ B $\alpha$  kinase (IKK2), degradation of I $\kappa$ B $\alpha$  via the proteasomal pathway, and translocation of NF- $\kappa$ B dimer to the nucleus. We have examined whether PAR1 and PAR2 are coupled to the activation of NF- $\kappa$ B in smooth muscle cells. Activation of IKK2 was measured by phosphorylation of IKK2 using phospho-specific substrate (Ser<sup>176/180</sup>). I $\kappa$ B $\alpha$  degradation was measured by Western blot and NF- $\kappa$ B activation was measured by phosphorylation of the p65 subunit using an antibody to phospho-specific substrate (Ser<sup>536</sup>).

Both PAR1-AP (1  $\mu$ M) and PAR2-AP (1  $\mu$ M) induced activation of IKK2, degradation of I $\kappa$ B $\alpha$ , and activation of NF- $\kappa$ B in cultured muscle cells. The effect of PAR1-AP and PAR2-AP was abolished by treatment of cells with the RhoA inhibitor (C3 exoenzyme (2  $\mu$ g/ml)) suggesting that activation of NF- $\kappa$ B was downstream of RhoA (Figs. 22 and 23).

### **10.3.9 Feedback inhibition of RhoA by G<sub>12</sub>-coupled PAR1**

Rho kinase activity stimulated by PAR1-AP was augmented (106 $\pm$ 7% increase)

**Figure 22. Sequential activation of RhoA and NF- $\kappa$ B pathways by PAR1-AP.**

Gastric muscle cells were incubated for 2 h with the RhoA inhibitor *Clostridium botulinum* C3 exoenzyme (2  $\mu$ g/ml) and then treated with PAR1-AP for 10 min. Cells were homogenized in lysis buffer and proteins were separated on SDS-PAGE. Phosphorylation (i.e., activation) of IKK2 was measured by Western blot using phospho-specific (Ser<sup>177/181</sup>) antibody and phosphorylation of p65 subunit (activation of NF- $\kappa$ B) was measured using phospho-specific (Ser<sup>536</sup>) antibody. Degradation of I $\kappa$ B $\alpha$  was measured using antibody to I $\kappa$ B $\alpha$ . Western blot of the  $\beta$ -actin protein is shown for control loading. PAR1-AP induced phosphorylation of IKK2 and NF- $\kappa$ B (p-p65), and degradation of I $\kappa$ B $\alpha$  in smooth muscle cells. The effect of PAR1-AP was reversed upon blockade of RhoA activity by C3 exoenzyme (C3 Exo), implying that NF- $\kappa$ B is activated downstream of RhoA.

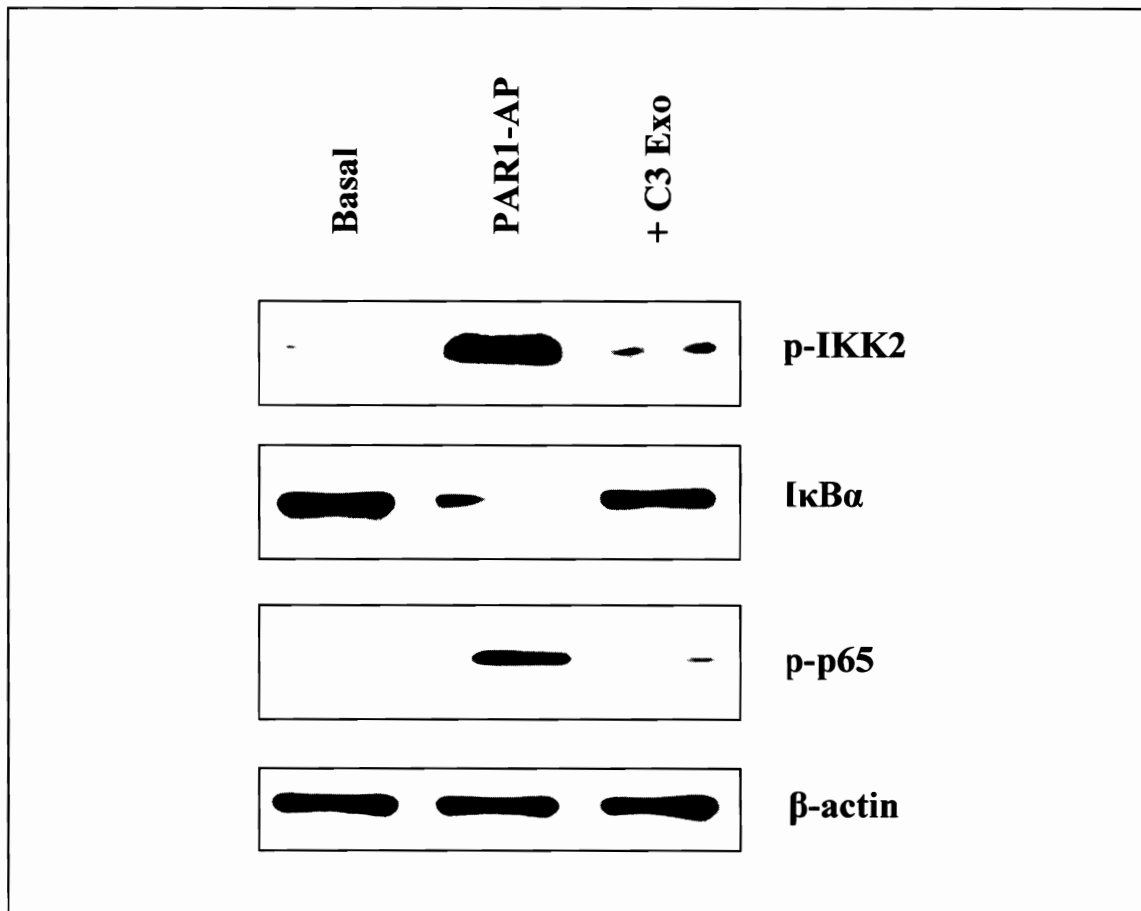
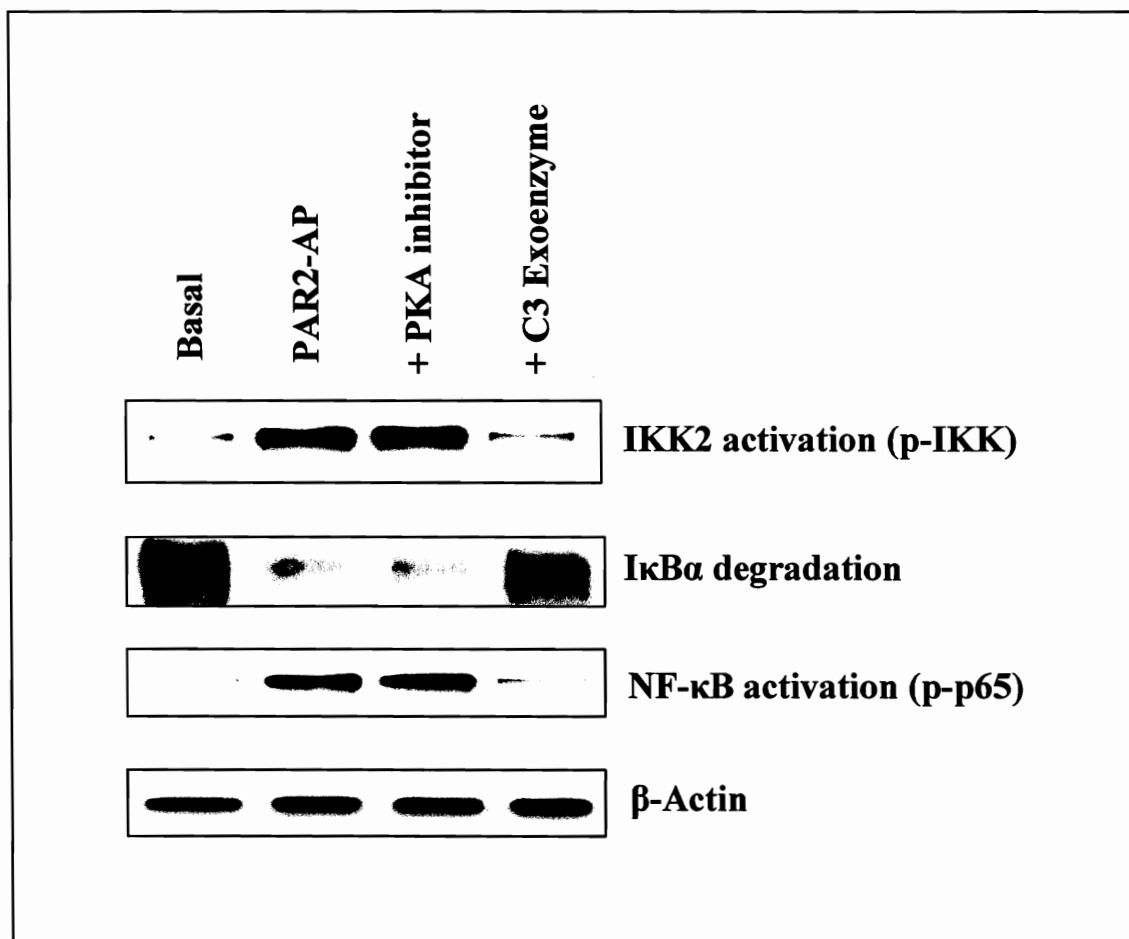




**Figure 23. Sequential activation of RhoA and NF- $\kappa$ B pathways by PAR2-AP and PKA-mediated phosphorylation of RhoA.** Gastric muscle cells were incubated with myristoylated PKI for 10 min or with the RhoA inhibitor *Clostridium botulinum* C3 exoenzyme (2  $\mu$ g/ml) for 2 h, and then treated with PAR2-AP for 10 min. Cells were homogenized in lysis buffer and proteins were separated on SDS-PAGE. Phosphorylation (i.e., activation) of IKK2 was measured by Western blot phospho-specific (Ser<sup>177/181</sup>) antibody and phosphorylation of p65 subunit (activation of NF- $\kappa$ B) was measured using phospho-specific (Ser<sup>536</sup>) antibody. Degradation of I $\kappa$ B $\alpha$  was measured using antibody to I $\kappa$ B $\alpha$ . Western blot of the  $\beta$ -actin protein is shown for a control loading. PAR2-AP induced phosphorylation of IKK2 and NF- $\kappa$ B (p-p65), and degradation of I $\kappa$ B $\alpha$  in smooth muscle cells. The effect of PAR2-AP was reversed upon blockade of RhoA activity by C3 exoenzyme (C3 Exo), implying that NF- $\kappa$ B is activated downstream of RhoA.



by the PKC inhibitor, bisindolylmaleimide, implying that PKC inhibited RhoA activity stimulated by PAR1 (Fig. 24). The inhibitors of IKK2 (IKK IV), NF- $\kappa$ B (MG-132) or PKA (myristoylated PKI) had no significant effect on PAR1-AP-stimulated Rho kinase activity in the absence of bisindolylmaleimide. In the presence of bisindolylmaleimide, however, IKK IV, MG-132 or myristoylated PKI further augmented PAR1-AP stimulated Rho kinase activity (Fig. 25). The results imply that feedback inhibition of Rho kinase is mediated by both PKC and PKA. The results also imply that PKA was derived from activation of the canonical NF- $\kappa$ B pathway. The lack of effect of IKK IV, MG-132 or myristoylated PKI in the absence of bisindolylmaleimide suggests that the target of PKA could be distal to the target of PKC.

In vitro studies in cell lines have shown that PKC phosphorylates and thus inhibits  $G\alpha_{12}$ . Studies in smooth muscle have shown that PKA phosphorylates RhoA at Ser<sup>188</sup> and thus inhibits RhoA activity. Based on these findings, we hypothesized that the effect of PKC could be exerted at the level of  $G\alpha_{12}$  and the effect of PKA could be exerted at the level of RhoA. This notion was examined by measurements of  $G\alpha_{12}$  phosphorylation and Rho kinase activity in cells expressing PKA phosphorylation-site deficient RhoA (S188A) blocking phosphorylation of RhoA by PKA and in cells expressing dominant negative mutants of IKK2 and I $\kappa$ B $\alpha$  to block activation of PKA.

Treatment of cells with PAR1-AP caused  $G\alpha_{12}$  phosphorylation, measured in cells metabolically labeled with <sup>32</sup>P, and the effect of PAR1-AP was blocked by bisindolylmaleimide (Fig. 26). The results imply that  $G\alpha_{12}$  was phosphorylated by PAR1 in a feedback mechanism via PKC. Treatment of cells with PAR1-AP also caused RhoA

**Figure 24. Feedback inhibition of PAR1-AP-stimulated Rho kinase activity by PKC.** Freshly dispersed gastric smooth muscle cells were treated with PAR1-AP (1  $\mu$ M) for 10 min in the presence or absence of inhibitor for PKC (bisindolylmaleimide, 1  $\mu$ M). Rho kinase activity was measured using [ $^{32}$ P]ATP by immunokinase assay. Rho kinase activity stimulated by PAR1-AP was augmented by bisindolylmaleimide. Results are expressed as cpm/mg protein. Values are means  $\pm$  S.E. of four experiments. \*\* Significant increase from control response ( $P < 0.01$ ).

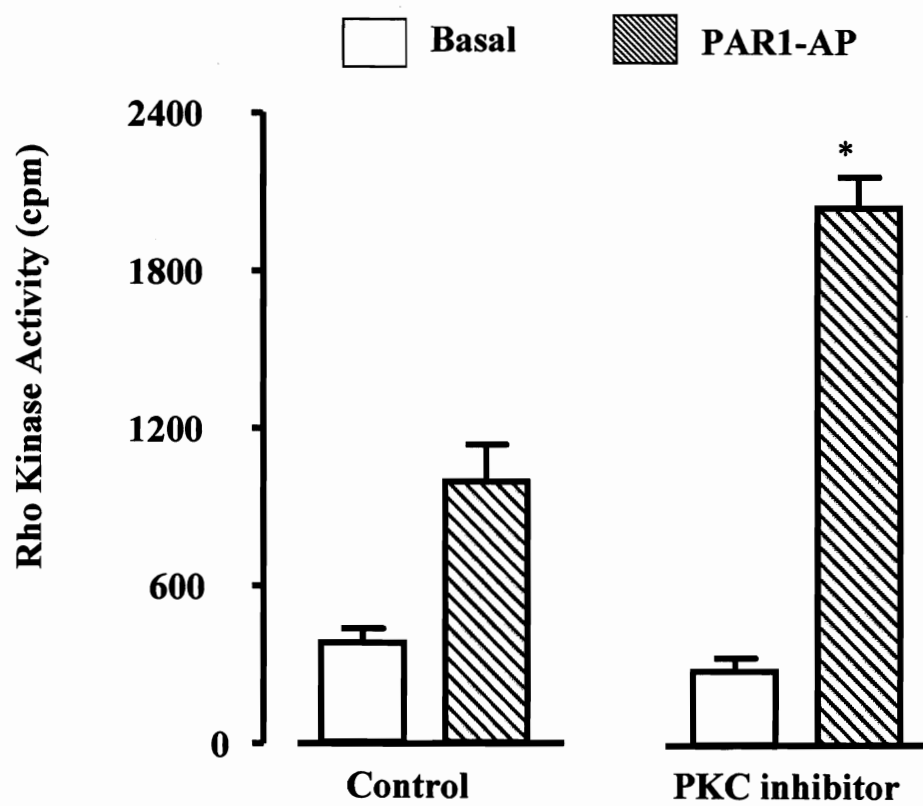


**Figure 25. Feedback inhibition of PAR1-AP-stimulated Rho kinase activity by PKA derived from NF- $\kappa$ B pathway and by PKC.** Freshly dispersed gastric smooth muscle cells were treated with PAR1-AP (1  $\mu$ M) plus bisindolylmaleimide in the presence or absence of IKK IV (10  $\mu$ M), MG-132 (10  $\mu$ M) or myristoylated PKI (1  $\mu$ M). Rho kinase activity was measured using [ $^{32}$ P]ATP by immunokinase assay. Rho kinase activity stimulated by PAR1-AP in the presence of bisindolylmaleimide was augmented by IKK2, NF- $\kappa$ B and PKA. The results imply that the feedback inhibition of Rho kinase activity is mediated by PKA derived from activation of NF- $\kappa$ B pathway, and by PKC, a downstream effector of RhoA. Results are expressed as cpm/mg protein. Values are means  $\pm$  S.E. of four experiments. \*\* Significant increase from control response and from response in the presence of bisindolylmaleimide (P<0.01).

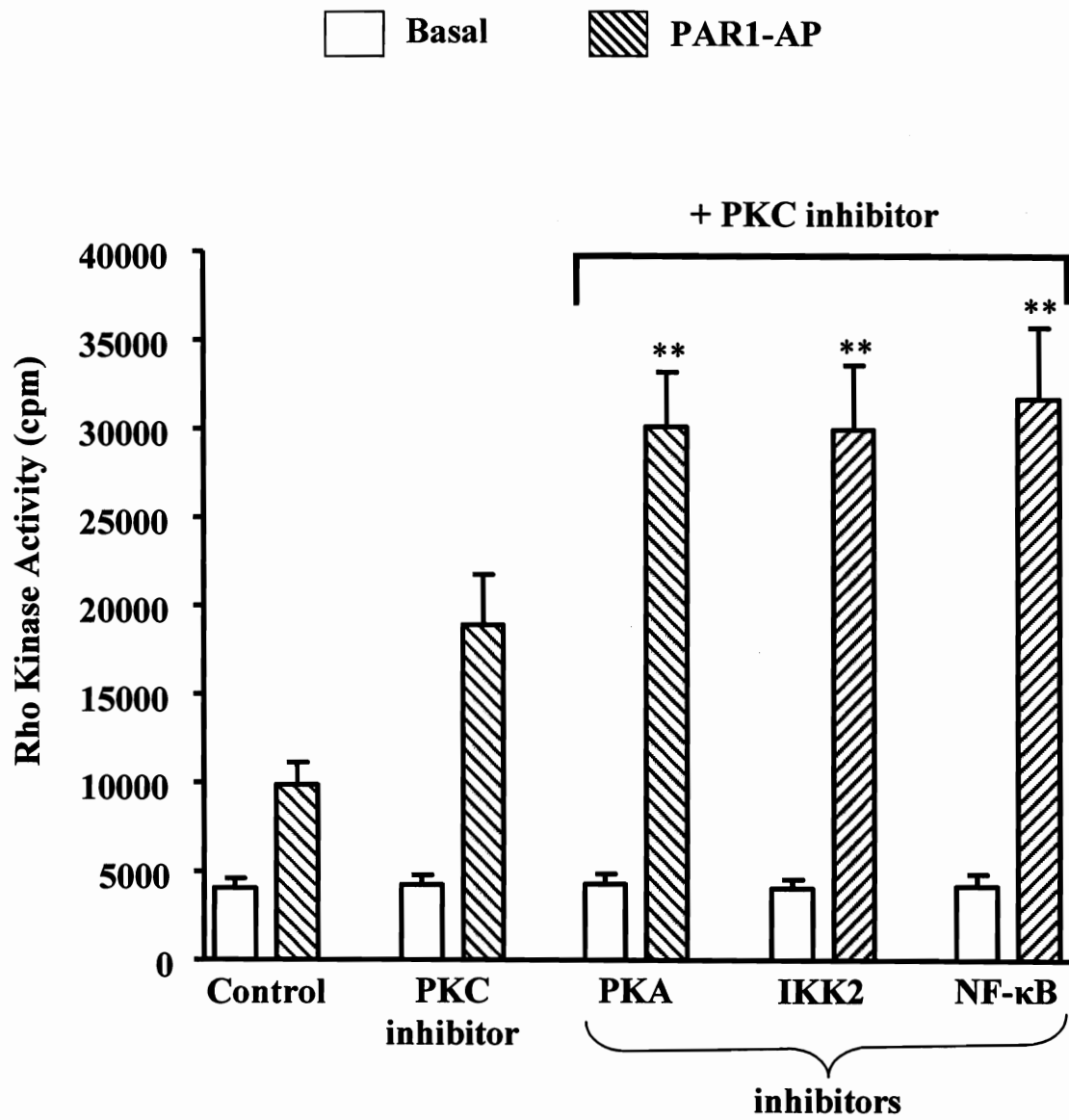
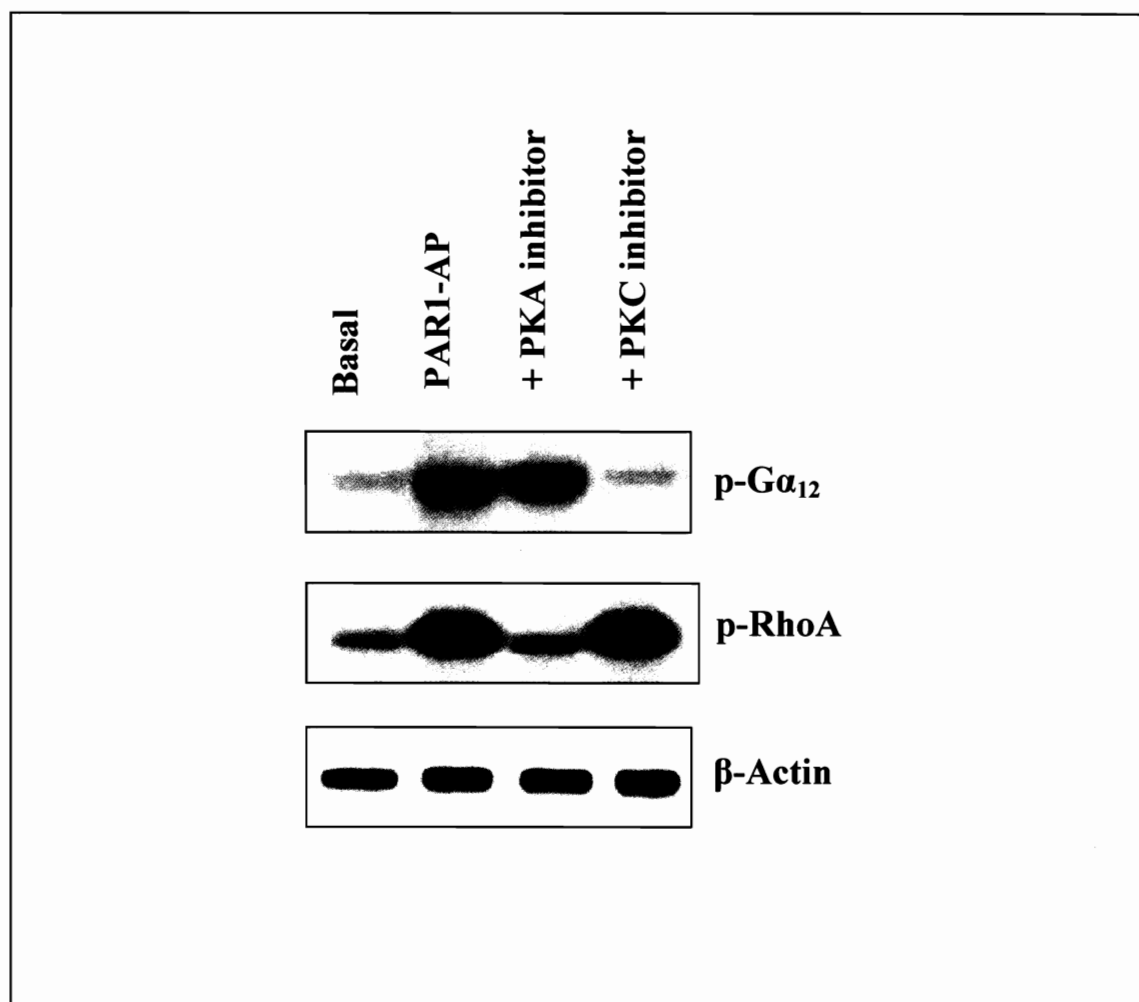


**Figure 26. PKC-mediated phosphorylation of  $G\alpha_{12}$  and PKA-mediated phosphorylation of RhoA by PAR1-AP in freshly dispersed muscle cells.** Gastric smooth muscle cells labeled with  $^{32}\text{P}$  were incubated with PAR1-AP (1  $\mu\text{M}$ ) for 10 min in the presence or absence of bisindolylmaleimide (1  $\mu\text{M}$ ) or the cell permeable PKA inhibitor myristoylated PKI (1  $\mu\text{M}$ ). Cells were homogenized in lysis buffer and immunoprecipitates derived using antibody to  $G\alpha_{12}$  or RhoA were separated on SDS-PAGE. [ $^{32}\text{P}$ ] $G\alpha_{12}$  or [ $^{32}\text{P}$ ]RhoA was identified by autoradiography. Western blot of the  $\beta$ -actin protein is shown for control loading. Phosphorylation of  $G\alpha_{12}$  induced by PAR1-AP was selectively inhibited by bisindolylmaleimide, whereas phosphorylation of RhoA was selectively inhibited by the myristoylated PKI.





phosphorylation, measured in cells metabolically labeled with  $^{32}\text{P}$ , and the effect of PAR1-AP was blocked by PKA inhibitor (Fig. 26). The results imply that RhoA was phosphorylated by PAR1 in a feedback mechanism via PKA.

Rho kinase activity stimulated by PAR1-AP was increased by the PKC inhibitor suggesting feedback inhibition of Rho kinase by PKC, probably via phosphorylation of  $\text{G}\alpha_{12}$ . The effect of bisindolylmaleimide was further augmented in cells expressing RhoA(S188A), IKK2(K44A), and  $\text{I}\kappa\text{B}\alpha$ (S32A/S36A) ( Fig. 27). In the absence of bisindolylmaleimide, however, expression of RhoA(S188A), IKK2(K44A) and  $\text{I}\kappa\text{B}\alpha$ (S32A/S36A) had no significant effect on PAR1-AP-induced Rho kinase activity (data not shown). The results imply the existence of distinct pathways for feedback inhibition of RhoA mediated by the downstream effectors, PKC and PKA. The latter is released upon degradation of  $\text{I}\kappa\text{B}\alpha$ .

#### **10.3.10 Feedback inhibition of RhoA by $\text{G}_{13}$ -coupled PAR2**

In contrast to its effect on Rho kinase activity stimulated by PAR1-AP, bisindolylmaleimide had no effect on Rho kinase activity stimulated by PAR2-AP. PAR2-AP-induced Rho kinase activity, however, was significantly augmented by IKK IV, MG-132 or myristoylated PKI ( $102\pm 7\%$ ,  $109\pm 9\%$   $103\pm 6\%$  respectively) (Fig. 28). The combination of bisindolylmaleimide with IKK IV, MG-132 or myristoylated PKI had no affect on augmentation (data not shown). The results imply that feedback inhibition of PAR2-induced Rho kinase is mediated by PKA and not by PKC. The results also imply that PKA derived from the activation of the canonical NF- $\kappa$ B pathway inhibits RhoA.

**Figure 27. Feedback inhibition of PAR1-AP-stimulated Rho kinase activity by PKA via phosphorylation of RhoA at Ser<sup>188</sup>.** Cultured smooth muscle cells expressing dominant negative mutants of IKK2 (K44A) or I $\kappa$ B $\alpha$  (S32A/S36A) or the PKA phosphorylation site-deficient RhoA(S188A) were treated with PAR1-AP (1  $\mu$ M) and bisindolylmaleimide (1  $\mu$ M). Rho kinase activity was measured using [<sup>32</sup>P]ATP by immunokinase assay. Rho kinase activity stimulated by PAR1-AP in the presence of bisindolylmaleimide was augmented in cells expressing IKK2 (K44A), I $\kappa$ B $\alpha$  (S32A/S36A) or RhoA(S188A). The results imply that the feedback inhibition of Rho kinase activity is mediated by PKA, derived from the activation of the NF- $\kappa$ B pathway, via phosphorylation of RhoA at Ser<sup>188</sup>, and also by PKC, possibly via phosphorylation of G $\alpha_{12}$ . Results are expressed as cpm/mg protein. Values are means  $\pm$  S.E. of four experiments. \*\* Significant increase from control response (P<0.01).

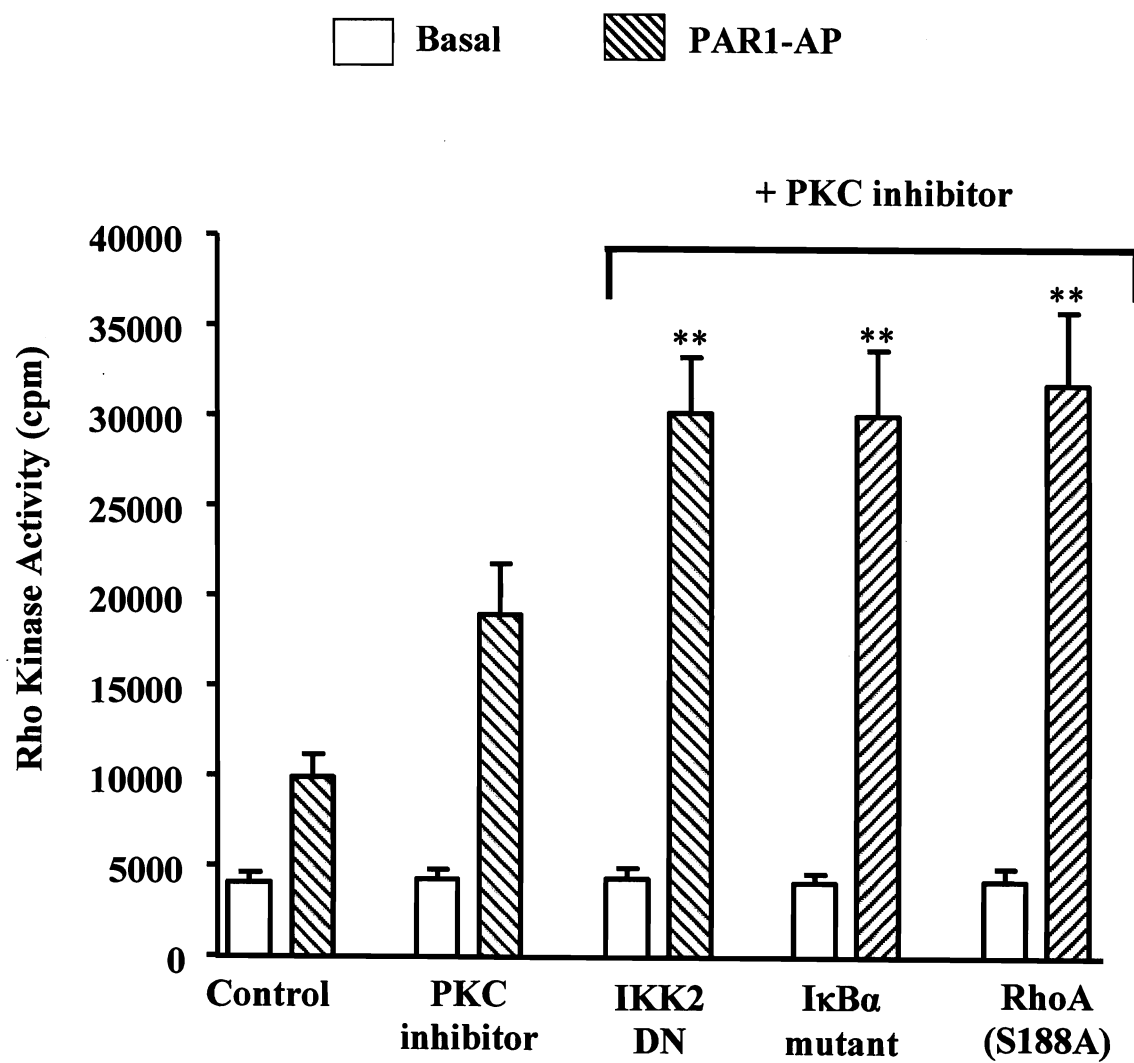
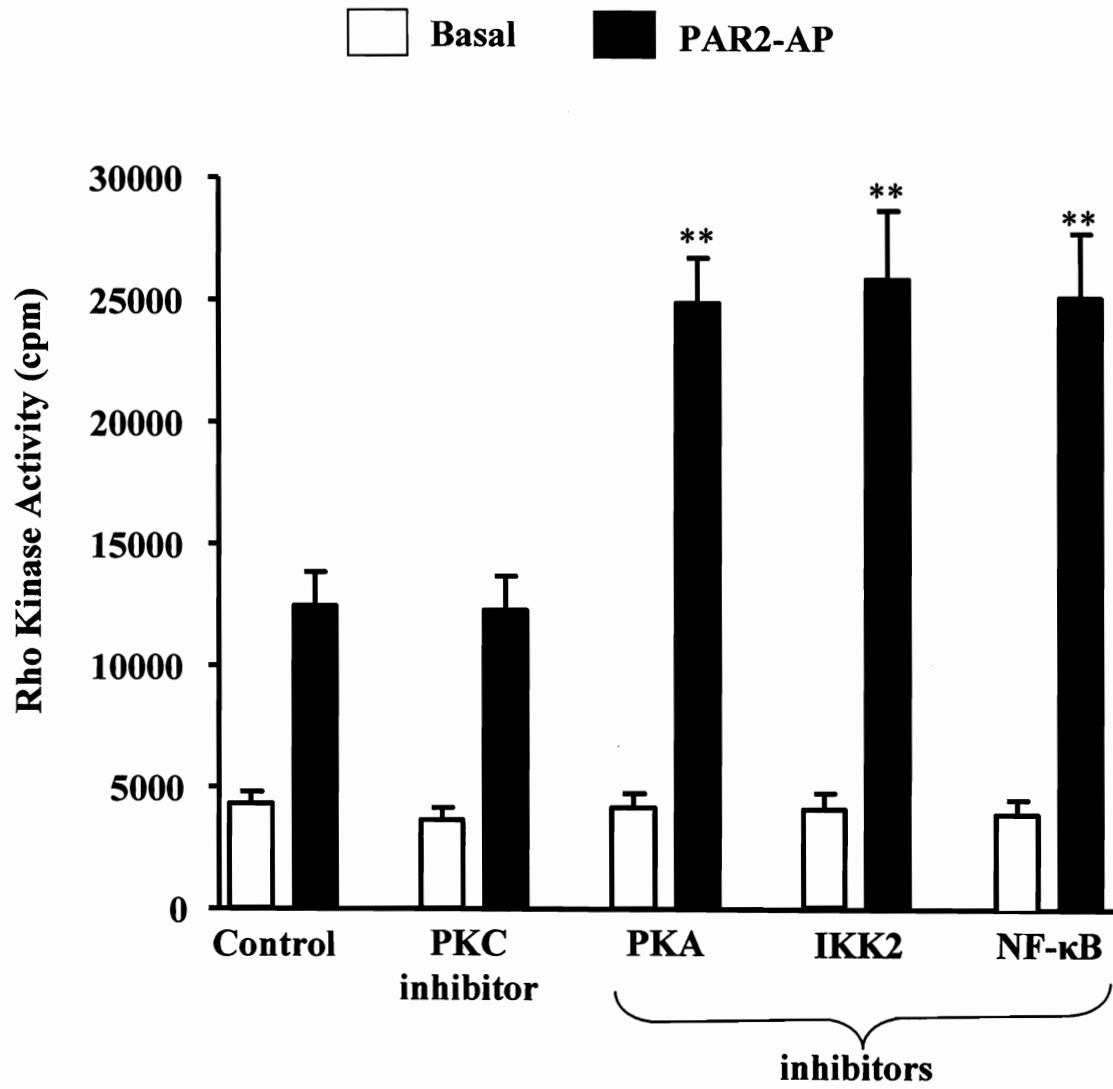


**Figure 28. Feedback inhibition of PAR2-AP-stimulated Rho kinase activity by PKA derived from NF- $\kappa$ B pathway and by PKC.** Freshly dispersed gastric smooth muscle cells were treated with PAR2-AP (1  $\mu$ M) in the presence or absence of IKK IV (10  $\mu$ M), MG-132 (10  $\mu$ M), myristoylated PKI (1  $\mu$ M) or bisindolylmaleimide (1  $\mu$ M). Rho kinase activity was measured using [ $^{32}$ P]ATP by immunokinase assay. Rho kinase activity stimulated by PAR2-AP was augmented by inhibitors of IKK2, NF- $\kappa$ B and PKA, but not by the inhibitor of PKC. The results imply that the feedback inhibition of Rho kinase activity is mediated by PKA derived from activation of the NF- $\kappa$ B pathway. Results are expressed as cpm/mg protein. Values are means  $\pm$  S.E. of four experiments.

**\*\* Significant increase from control response (P<0.01).**



This notion was examined by measuring Rho kinase activity in cells expressing PKA phosphorylation-site deficient RhoA (S188A) blocking phosphorylation of RhoA by PKA and in cells expressing dominant negative mutants of IKK2 and I $\kappa$ B $\alpha$  to block activation of PKA.

Rho kinase activity stimulated by PAR2-AP was augmented in cells expressing RhoA(S188A), IKK2(K44A),and I $\kappa$ B $\alpha$ (S32A/S36A) (Fig. 29). The results imply that PAR2-induced Rho kinase activity was inhibited in a feedback mechanism via phosphorylation of RhoA at Ser<sup>188</sup> by PKA and the PKA was derived from the activation of the NF- $\kappa$ B pathway. In support to this, treatment of cells with PAR2-AP also induced RhoA phosphorylation, measured in cells metabolically labeled with <sup>32</sup>P. The effect of PAR2-AP was blocked by PKA inhibitor (Fig. 30). The results imply that RhoA was phosphorylated by PAR2 in a feedback mechanism via PKA derived from NF- $\kappa$ B activation.

In addition, consistent with the lack of involvement of PKC in the feedback inhibition of PAR2-induced Rho kinase activity, there was no detectable phosphorylation of G $\alpha$ <sub>13</sub>. This is in contrast to G $\alpha$ <sub>12</sub> phosphorylation and PKC-mediated inhibition of Rho kinase activity by G $\alpha$ <sub>12</sub>-coupled PAR1.

***In summary,***

1. PAR1 and PAR2, but not PAR3 and PAR4 are expressed in gastric smooth muscle cells.
2. PAR1 and PAR2 are differentially coupled G proteins: PAR1 is coupled to G $\alpha$ <sub>13</sub>, G $\alpha$ <sub>q</sub> and G $\alpha$ <sub>12</sub>, whereas PAR2 is coupled to G $\alpha$ <sub>11</sub>, G $\alpha$ <sub>12</sub>, G $\alpha$ <sub>q</sub> and G $\alpha$ <sub>13</sub>.

**Figure 29. Feedback inhibition of PAR2-AP-stimulated Rho kinase activity by PKA via phosphorylation of RhoA at Ser<sup>188</sup>.** Cultured smooth muscle cells expressing dominant negative mutants of IKK2 (K44A) or I $\kappa$ B $\alpha$  (S32A/S36A) or the PKA phosphorylation site-deficient RhoA (S188A) were treated with PAR2-AP (1  $\mu$ M). Rho kinase activity was measured using [<sup>32</sup>P]ATP by immunokinase assay. Rho kinase activity stimulated by PAR2-AP was augmented in cells expressing IKK2 (K44A), I $\kappa$ B $\alpha$  (S32A/S36A) or RhoA(S188A). The results imply that the feedback inhibition of Rho kinase activity is mediated by PKA, derived from the activation of the NF- $\kappa$ B pathway, via phosphorylation of RhoA at Ser<sup>188</sup>. Results are expressed as cpm/mg protein. Values are means  $\pm$  S.E. of four experiments. \*\* Significant increase from control response (P<0.01).



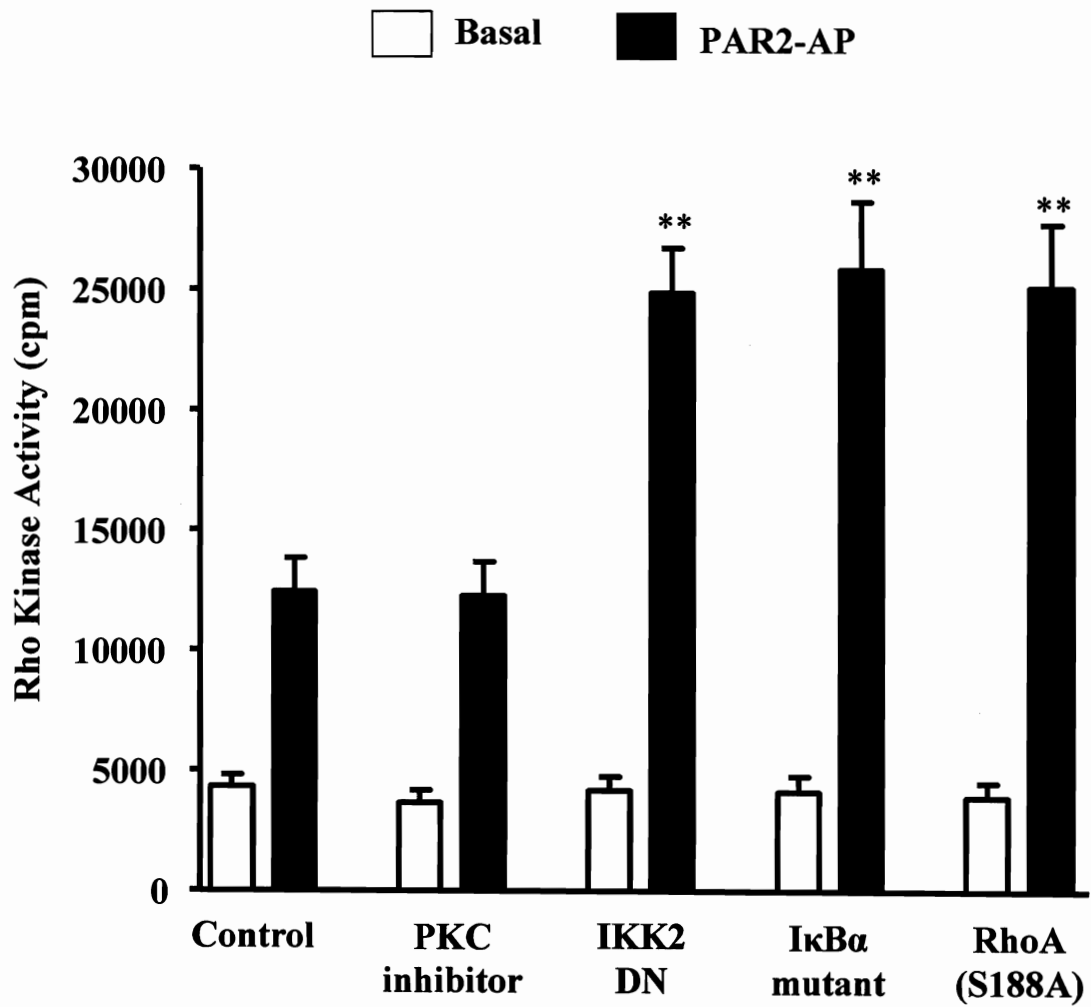
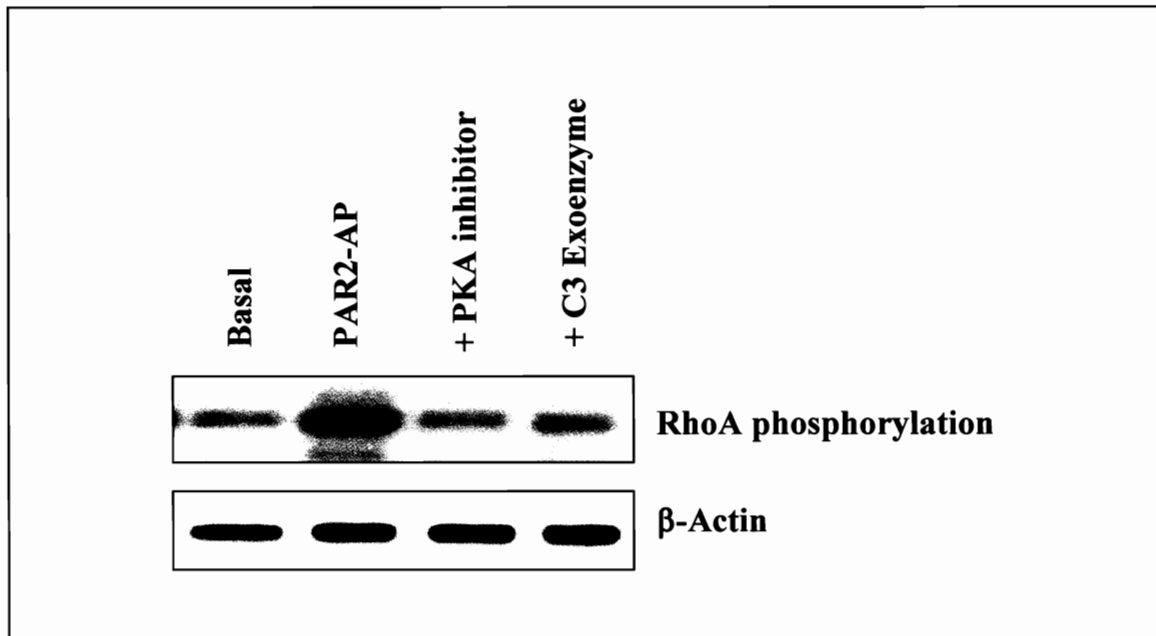


**Figure 30. PKA-mediated phosphorylation of RhoA by PAR2-AP.** Gastric muscle cells were incubated with myristoylated PKI for 10 min or with the RhoA inhibitor *Clostridium botulinum* C3 exoenzyme (2  $\mu\text{g/ml}$ ) for 2 h, and then treated with PAR2-AP for 10 min. RhoA phosphorylation was measured in cells labeled with  $^{32}\text{P}$ . Cells were homogenized in lysis buffer and proteins were separated on SDS-PAGE. Western blot of the  $\beta$ -actin protein is shown for a control loading. PAR2-AP induced phosphorylation of RhoA was blocked by C3 exoenzyme and PKI, implying activation of PKA was downstream of RhoA, probably via activation of NF- $\kappa$ B pathway.



3. PAR1 stimulates PI hydrolysis via the PTx-insensitive  $G_q$ , whereas PAR2 is stimulated via PTx-insensitive  $G_q$  and PTx-sensitive  $G_{i1}$  and  $G_{i2}$ .

4.  $G_q$ -coupled stimulation of PI hydrolysis by PAR1 and PAR2 was regulated by RGS4

5. PAR1 and PAR2 are coupled to RhoA via distinct G proteins: PAR1 via  $G_{12}$  and PAR2 via  $G_{13}$ .

6. PAR1 and PAR2 are coupled to the inhibition of adenylyl cyclase consistent with the activation of  $G_i$  proteins.

7. PAR1 and PAR2 mediate muscle contraction, which is biphasic.

8. Initial (30 s) contraction by PAR1 and PAR2 was mediated by sequential activation of PI hydrolysis,  $IP_3$ -dependent  $Ca^{2+}$  release, activation of  $Ca^{2+}$ /calmodulin-dependent MLC kinase and phosphorylation of  $MLC_{20}$

9. Sustained contraction by PAR1 and PAR2 was mediated by inhibition of MLC phosphatase and sustained  $MLC_{20}$  phosphorylation via distinct mechanisms: inhibition of MLC phosphatase by PAR1 was mediated via PKC-dependent phosphorylation of CPI-17, whereas by PAR2 was mediated via Rho kinase-dependent phosphorylation of MYPT1.

10. Activation of Rho kinase by PAR1 was regulated by a feedback inhibitory mechanism involving PKC-mediated phosphorylation of  $G_{\alpha_{12}}$  and PKA-mediated phosphorylation of RhoA at Ser<sup>188</sup>.

11. Activation of Rho kinase by PAR2 was regulated by a feedback inhibitory mechanism involving PKA-mediated phosphorylation of RhoA at Ser<sup>188</sup>.

12. Although both PAR1 and PAR2 are coupled to inhibition of adenylyl cyclase activity and cAMP formation, both activate cAMP-independent PKA. PAR1 and PAR2 activate the canonical NF- $\kappa$ B pathway by the activation of the IKK2/I $\kappa$ B $\alpha$  pathway resulting in the release of PKA catalytic subunits and activation of cAMP-independent PKA.

## Discussion

The present study characterized the signaling pathways mediated by PAR1 and PAR2 in gastric smooth muscle cells using biochemical, molecular and functional methods. The results demonstrate the co-expression of PAR1 and PAR2 in gastric smooth muscle cells and their ability to induce  $\text{Ca}^{2+}$ -dependent and  $\text{Ca}^{2+}$ -independent smooth muscle contraction and MLC<sub>20</sub> phosphorylation. The initial contraction by PAR1 reflected activation of PLC- $\beta$  via PTX-insensitive G protein, G<sub>q</sub>, whereas contraction by PAR2 reflected activation of PLC- $\beta$  via PTX-sensitive, G<sub>i1</sub> and G<sub>i2</sub>, and PTX-insensitive G<sub>q</sub>. The sustained contraction by PAR1 reflected activation of monomeric G protein RhoA via G<sub>12</sub> and inhibition of MLC phosphatase via PKC-mediated phosphorylation of endogenous MLC phosphatase inhibitor, CPI-17 at Thr<sup>38</sup>. In contrast, the sustained contraction by PAR2 reflected activation of RhoA via G<sub>13</sub> and inhibition of MLC phosphatase via Rho kinase-mediated phosphorylation of the MLC phosphatase regulatory subunit MYPT1 at Thr<sup>696</sup>.

Activation of RhoA by PAR1 and PAR2 also results in the stimulation of the canonical NF- $\kappa$ B pathway and activation of cAMP-independent PKA, which, in turn, phosphorylates RhoA at Ser<sup>188</sup> and causes feedback inhibition of RhoA activity. In addition, PAR1-induced RhoA activity was regulated by feedback inhibition involving

phosphorylation of  $G\alpha_{12}$  via PKC.

### **11.1 Co-expression of PAR1 and PAR2 in Gastric Smooth Muscle**

Co-expression of PAR1 and PAR2 was demonstrated in freshly dispersed rabbit gastric muscle cells. Western blot analysis using a type-specific antibody detected PAR1 and PAR2 in dispersed rabbit gastric smooth muscle cells. PAR3 and PAR4 could not be detected by Western blot analysis, raising the possibility that the expression of these proteins is either absent or not abundant in these cells.

The selective expression of PAR1 and PAR2 in smooth muscle cells of the gut is consistent with their expression in other cells types of the gut. PAR1 and PAR2 are co-expressed in enteric neurons (41), myenteric glia (42), epithelial cell of intestine and colon (30, 87), and endothelial cells and vascular smooth muscle cells of the gut (31, 64). Expression of PAR1 mRNA in the gut is relatively high compared with other tissues, both in mice and humans.

### **11.2 Distinctive Pattern of G protein-dependent Signaling by PAR1 and PAR2 in Smooth Muscle**

Studies in various cell lines suggest that PARs are coupled to both PTx-sensitive and PTx-insensitive G proteins, but the specific G protein isoforms coupled to each receptor type have not been characterized. The coupling of PARs to G proteins likely depends on the cell type and the relative abundance of G protein subtypes. In this study small synthetic peptides, TFLLRN and SLIGRL, corresponding to tethered ligand sequences were used to selectively activate PAR1 and PAR2 respectively and to identify the signaling pathways activated by each receptor. We have demonstrated that in gastric

smooth muscle cells, PAR1 and PAR2 are differentially coupled to G proteins. PAR1 is coupled to  $G_{i3}$ ,  $G_q$  and  $G_{12}$ , whereas PAR2 is coupled to  $G_{i1}$ ,  $G_{i2}$ ,  $G_q$  and  $G_{13}$ .

Receptor-specific coupling to G proteins is not unique to PARs. Previous studies in smooth muscle cells have shown similar receptor-specific coupling to distinct G proteins with endothelin  $ET_A$  ( $G_q$  and  $G_{13}$ ) receptors,  $ET_B$  ( $G_q$  and  $G_{i3}$ ) receptors (48), muscarinic m3 ( $G_q$  and  $G_{13}$ ) receptors, muscarinic m2 ( $G_{i3}$  only) receptors (113, 121),  $S1P_1$  ( $G_i$ ) receptors,  $S1P_2$  ( $G_i$ ,  $G_q$  and  $G_{13}$ ) receptors (172),  $NPY_1$  ( $G_{i2}$ ) receptors,  $NPY_2$  ( $G_q$  and  $G_{i2}$ ) receptors (99), adenosine A1 ( $G_{i3}$ ) receptors and adenosine A2b ( $G_s$ ) receptors (110, 119).

Interaction of PAR1 and PAR2 with  $G_i$ ,  $G_q$  and  $G_{12/13}$  suggests activation of PI hydrolysis via  $G_q/G_i$ , inhibition of adenylyl cyclase via  $G_i$  and activation of RhoA/Rho kinase via  $G_{12/13}$ .

### 11.3 Stimulation of PI Hydrolysis by PAR1 and PAR2

Receptors coupled to both  $G_q$  and  $G_i$  proteins stimulate PI hydrolysis via distinct PLC- $\beta$  isoforms.  $G_q$  coupled receptors such as muscarinic m3,  $S1P_2$ , endothelin  $ET_A$ , purinergic P2Y2, and  $NPY_2$  are coupled to the stimulation of PI hydrolysis via  $G\alpha_q$ -dependent PLC- $\beta_1$  isozyme, whereas  $G_{i3}$ -coupled m2, P2Y2, and adenosine A1 receptors,  $G_{i1}$ -coupled somatostatin sst3 receptors,  $G_{i2}$ -coupled opioid,  $\mu$ ,  $\kappa$ ,  $\delta$  receptors, and  $G_{i1/2}$ -coupled  $S1P_2$  receptors are coupled to the stimulation of PI hydrolysis via  $G\beta\gamma_i$ -dependent PLC- $\beta_3$ . Thus, P2Y2 and  $S1P_2$  receptors are coupled to the stimulation of PI hydrolysis via  $G\alpha_q$ -dependent PLC- $\beta_1$  isozyme and  $G\beta\gamma_i$ -dependent PLC- $\beta_3$  isozyme.

Although all four PLC- $\beta$  isozymes are expressed in the smooth muscle of the gut,



neither PLC- $\beta$ 2 nor PLC- $\beta$ 4 is activated. PLC- $\beta$ 1 is activated via binding of its COOH-terminal tail, a characteristic feature of PLC- $\beta$  isozymes, to  $G\alpha_q$ , whereas PLC- $\beta$ 3 is activated via binding to its NH<sub>2</sub>-terminal pleckstrin homology (PH) domain to  $G\beta\gamma_i$ . Phosphatidylinositol 4,5-bisphosphate (PIP<sub>2</sub>) is the predominant phosphoinositide substrate hydrolyzed by both PLC- $\beta$ 1 and PLC- $\beta$ 3 isozyme, resulting in the generation of diacylglycerol, an activator of PKC and inositol 1,4,5-trisphosphate, a diffusible Ca<sup>2+</sup>-mobilizing messenger.

The specific G proteins activated by PAR1 and PAR2 involved in the stimulation of PI hydrolysis were examined using both pharmacological and molecular approaches. Although PAR1 and PAR2 are coupled to both  $G_i$  and  $G_q$  proteins, blockade of  $G_i$  activation with PTx inhibited PI hydrolysis by PAR2 and had no effect on PI hydrolysis by PAR1. The results imply that PAR1 stimulates PI hydrolysis by activating PLC- $\beta$ 1 via  $G\alpha_q$ , whereas PAR2 stimulates PI hydrolysis by activating PLC- $\beta$ 1 and PLC- $\beta$ 3 via  $G\alpha_q$  and  $G\beta\gamma_i$ , respectively. This notion was further confirmed using the minigene approach. Previous studies have shown that the COOH-terminus of G protein  $\alpha$  subunits is critical in mediating receptor-G protein interaction and that peptides corresponding to the COOH-terminus serve as competitive inhibitors of receptor-G protein interaction (78, 172). The minigene plasmid vectors were designed to express the COOH-terminal peptide sequences of various  $G\alpha$  subunits after transfection into cells.

In gastric muscle cells transfection of minigene plasmid constructs that encode oligonucleotide sequences corresponding to  $G\alpha_i$  and  $G\alpha_q$  completely blocked  $G_i$  and  $G_q$  activation. The results provide evidence that the minigene approach is a powerful tool

for identifying G protein-specific biochemical or physiological function. PI hydrolysis stimulated by PAR1 was inhibited by  $G\alpha_q$  minigene only, whereas PI hydrolysis stimulated by PAR2 was inhibited by both  $G\alpha_q$  and  $G\alpha_i$  minigene.

It is worth noting that coupling of PAR1  $G_{i3}$  did not lead to activation of PLC- $\beta$ . The inability of  $G_{i3}$ -coupled PAR1 to stimulate PLC- $\beta$  via  $G\beta\gamma_i$  in smooth muscle contrasts with muscarinic m2 and adenosine A1 receptors in smooth muscle cells where ACh or A1 selective agonists (cyclopentyl adenosine) that activate  $G_{i3}$  leading to the activation of PLC- $\beta_3$  via  $G\beta\gamma_{i3}$ . Instead PAR1 stimulation pattern is similar to the stimulation pattern obtained with  $G_i$ -coupled S1P $_1$ , NPY $_1$ , and cannabinoid CB $_1$  receptors where activation of  $G_i$  by S1P, NPY $_1$  selective agonist (Leu, Pro NPY), and CB $_1$  agonist (anandamide) had no effect on PI hydrolysis.

#### **11.4 Inhibition of Adenylyl Cyclase by PAR1 and PAR2**

The cAMP response to G protein-coupled receptor activation depends on the isozymes of adenylyl cyclase expressed in a given cell type. Gastric smooth muscle was shown to selectively express adenylyl cyclase V/VI. Types V and VI are inhibited by various isoforms of  $G_i$  and by submicromolar concentrations of cytosolic  $Ca^{2+}$  elicited by capacitative  $Ca^{2+}$  influx and not by  $Ca^{2+}$  release from sarcoplasmic stores. In contrast, adenylyl cyclase types II and IV are not susceptible to inhibition by  $G_i$  or  $Ca^{2+}$ . Consistent with the expression of adenylyl cyclase V/VI and activation of  $G_i$ , PAR1 and PAR2 receptors are coupled to the inhibition of cAMP formation in gastric smooth muscle cells. The physiological significance of cAMP formation in muscle cells should be viewed as a functional antagonism of on-going muscle relaxation mediated by cAMP-

dependent pathways to facilitate contraction via  $G_q$  and  $G_{12/13}$ -dependent pathways. Inhibition of adenylyl cyclase in smooth muscle by various isoforms of  $G_i$  appears to be receptor-specific. Inhibition by somatostatin (sst3) is mediated via  $G_{i1}$ , inhibition by  $\mu$ ,  $\kappa$ , and  $\delta$  is mediated via  $G_{i2}$ , and inhibition by A1 is mediated via  $G_{i3}$ . Muscarinic m2 receptors are coupled to the inhibition of adenylyl cyclase formation via the  $\alpha$  subunit of  $G_{i3}$ , whereas m3 receptors are coupled to the activation of the enzyme via the  $\beta\gamma$  subunit of  $G_q$ . The cAMP response to muscarinic agonists reflects the predominant inhibitory influence of m2 receptors. Although PAR1 and PAR2 are coupled to the inhibition of cAMP formation, activation of PAR1 and PAR2 results in the stimulation of cAMP-independent protein kinase A (PKA) activity via RhoA-dependent mechanisms involving the activation of canonical NF- $\kappa$ B pathways as discussed below.

### 11.5 Activation of RhoA-dependent Pathways by PAR1 and PAR2

Agonists that activate  $G_q$  also activate  $G_{12}$  or  $G_{13}$ : all these G proteins are capable of activating the monomeric G protein RhoA. The inactive form of RhoA (RhoA.GDP) is present in the cytosol bound to a guanine dissociation inhibitor (GDI). Activation of RhoA by  $G_{\alpha_q}$ ,  $G_{\alpha_{12}}$ , or  $G_{\alpha_{13}}$  is mediated by various Rho-specific guanine nucleotide exchange factors (RhoGEFs) that promote the exchange of GDP for GTP. The RhoGEF family of proteins includes p115RhoGEF, PDZ-RhoGEF, and LARG (leukemia-associated RhoGEF). RhoGEF shares common motifs responsible for binding to activated  $G_{\alpha}$  subunits and for the exchange of GDP for GTP on RhoA. Thus RhoGEFs are thought to serve as effectors for activated  $G_{\alpha}$  subunits and as a molecular link between heterotrimeric G proteins and monomeric G proteins. The involvement of

different RhoGEFs in the activation of RhoA is receptor-specific. For example, in cell lines PAR1-induced activation of RhoA is mediated by LARG, whereas LPA1-induced activation of RhoA is mediated by PDZ-RhoGEF. RhoA and not other RhoA family G proteins, such as Cdc42 and Rac1, are inactivated via ADP ribosylation by *Clostridium botulinum* C3 exoenzyme.

In the GTP-bound conformation, RhoA interacts with and stimulates the activity of downstream effectors including Rho kinase and phospholipase D (PLD). Hydrolysis of phosphatidylcholine by PLD yields phosphatidic acid, which is dephosphorylated to DAG, leading to sustained activation of various PKC isozymes. PKC and Rho kinase act to inhibit MLC phosphatase via distinct yet cooperative mechanisms. PKC phosphorylates CPI-17, a 17-kDa endogenous inhibitor of MLC phosphatase, greatly augmenting its ability to inhibit MLC phosphatase. Rho kinase phosphorylates MYPT1, a 130-kDa myosin phosphatase targeting subunit that inhibits the MLC phosphatase activity.

The Rho kinases, ROCK I and ROCK II, which are predominantly expressed in smooth muscle, are serine/threonine kinases of ~160 kDa that are involved in many cellular functions including smooth muscle contraction. Rho kinases possess a NH<sub>2</sub>-terminal catalytic domain, a central coiled-coil domain that includes a RhoA binding region, and a COOH-terminal pleckstrin homology (PH) domain. In the inactive form, the PH and Rho-binding domains of Rho kinase bind to the catalytic NH<sub>2</sub>-terminal region, forming an auto-inhibitory loop. The interaction of activated GTP-bound RhoA with the Rho-binding domain causes the enzyme to unfold and release its catalytic

activity.

The involvement of G proteins in the activation of Rho kinase in smooth muscle of the gut is receptor-specific. Muscarinic m3 and CCK-A receptors activate RhoA via  $G\alpha_{13}$  only, whereas  $S1P_2$  and motilin receptors activate RhoA via both  $G\alpha_q$  and  $G\alpha_{13}$ . Studies in cell lines have demonstrated that RhoA activation via  $G_q$  occurs with lower potency than RhoA activation via  $G_{12}/G_{13}$ . The involvement of G proteins with the activation of Rho kinase by PAR1 and PAR2 are receptor-specific. Consistent with the activation of  $G_{12}$  by PAR1, Rho kinase activity by PAR1 was blocked in cells expressing  $G\alpha_{12}$  minigene, and consistent with the activation of  $G_{13}$  by PAR2, Rho kinase activity stimulated by PAR2 was blocked in cells expressing  $G\alpha_{13}$  minigene. It remains to be determined whether  $G_{12}$ -coupled PAR1 and  $G_{13}$ -coupled PAR2 stimulate RhoA via distinct RhoGEFs in smooth muscle cells.

#### **11.6 PAR1 and PAR2 Mediated Contraction in Gastric Smooth Muscle**

Signaling by the effector enzymes activated by PAR1 and PAR2 has been implicated in a variety of biological processes, such as cell growth and differentiation, cell survival, cell migration and contraction.

Considerable information has been accumulated on the biological effects of PAR activation in the gastrointestinal system. The effects of PAR1 and PAR2 on gut motility are diverse, which include relaxation, contraction, or biphasic response of relaxation followed by contraction. Activation of PAR2 in the isolated rat colon smooth muscle strips inhibited spontaneous contractile activity. The inhibitory effect is resistant to tetrodotoxin and independent of nitric oxide and prostaglandin formation (102).

Activation of PAR2 in guinea pig gastric longitudinal smooth muscle strips, however, induced contraction that is partially dependent on prostaglandins and the activation of tyrosine kinase (144). Activation of PAR1 in rat duodenal longitudinal smooth muscle strips elicited dual responses consisting of relaxation followed by contraction, whereas activation of PAR2 elicited only a contraction response (68, 72). Thus, in muscle strips, it is clear that there is wide variation in response to PAR activation depending on species and the region of the gut examined.

A variety of mechanisms have been proposed to explain contraction and relaxation in response to PAR activation in muscle strips. These include activation of L-type  $\text{Ca}^{2+}$  channels, PKC and tyrosine kinases to mediate contraction and activation of apamin-sensitive  $\text{K}^{+}$  channels to mediate relaxation. The major problem with muscle strips or whole segments of gut in the characterization of the cellular mechanism responsible for muscle contraction or relaxation has been cellular heterogeneity. These preparations retain all or some components of the enteric nervous system. The effect of PAR agonists could include direct activation of PARs on the smooth muscle or PARs on myenteric neurons leading to transmitter release. In the present study, we have used dispersed muscle cells devoid of neural elements to examine the direct effect of PAR agonists on the response of the muscle. This preparation also makes it possible to characterize the distinct signaling pathways activated by PAR1 and PAR2.

In gastric smooth muscle both PAR1 and PAR2 induce contraction and  $\text{MLC}_{20}$  phosphorylation. The response consisted of two phases, a transient  $\text{Ca}^{2+}$ -dependent phase and a sustained  $\text{Ca}^{2+}$ -independent phase, mediated by distinct G proteins and signaling

pathways. Similar biphasic response has been obtained with activation of  $G_q/G_{13}$ -coupled (m3, S1P<sub>2</sub>, ET<sub>A</sub>, motilin) and  $G_i$ -coupled (somatostatin sst3, opioid  $\mu$ ,  $\kappa$ , and  $\delta$ , and adenosine A1) receptors in gastric smooth muscle cells.

### **11.6.1 Signaling pathways mediating the initial muscle contraction by PAR1 and PAR2 in smooth muscle**

The initial, transient phase of contraction mediated by PAR1 and PAR2 was initiated by the stimulation of PLC- $\beta$  activity, generation of IP<sub>3</sub>, IP<sub>3</sub>-dependent Ca<sup>2+</sup> release, Ca<sup>2+</sup>/calmodulin-dependent activation of MLC kinase and phosphorylation of MLC<sub>20</sub> at Ser<sup>19</sup>, where MLC<sub>20</sub> phosphorylation is a prerequisite for initiating the interaction of actin and myosin. Consistent with this model, blockade of IP<sub>3</sub> generation by the PLC- $\beta$  inhibitor, U73122 or MLC kinase activity by ML-9 inhibited initial contraction by PAR1 and PAR2.

In smooth muscle of the gut, G protein-coupled receptor agonists initiate contraction by increasing cytosolic Ca<sup>2+</sup> via IP<sub>3</sub>-dependent Ca<sup>2+</sup> release from sarcoplasmic Ca<sup>2+</sup> stores. The sarcoplasmic Ca<sup>2+</sup> stores contain high-affinity IP<sub>3</sub> receptors and release Ca<sup>2+</sup> in response to an increase in cytosolic IP<sub>3</sub> levels. Three types of IP<sub>3</sub> receptors, IP<sub>3</sub> R-I, IP<sub>3</sub> R-II and IP<sub>3</sub> R-III, have been cloned. Although smooth muscle of the gut expresses both IP<sub>3</sub> R-I and IP<sub>3</sub> R-II, only IP<sub>3</sub> R-I is involved in Ca<sup>2+</sup>-release in response to receptor activation. The transient increase in cytosolic Ca<sup>2+</sup> is rapidly dissipated by the reuptake of Ca<sup>2+</sup> into sarcoplasmic Ca<sup>2+</sup> stores via Ca<sup>2+</sup>-ATPase and by efflux from the cell. Coincidentally, MLC kinase activity decreases as the cytosolic Ca<sup>2+</sup> decreases and is also inactivated by Ca<sup>2+</sup>-calmodulin-dependent phosphorylation.

Previous studies have shown that agonist-stimulated increases in the cytosolic  $\text{Ca}^{2+}$  and contraction are abolished by inhibitors of PI hydrolysis (U73122 or neomycin) (7, 91, 172) and upon depletion of  $\text{Ca}^{2+}$  stores by thapsigargin in intact muscle cells as well as by treatment of permeabilized muscle cells with  $\text{G}\alpha_q$  ( $\text{G}_q$ -coupled receptors) or  $\text{G}\beta$  antibody ( $\text{G}_i$ -coupled receptors), PLC- $\beta$ 1 or PLC- $\beta$ 3 antibodies, or  $\text{IP}_3$  receptors inhibitors (heparin) (84, 107, 109, 111, 112, 172).

In addition, initial contractions are also inhibited by the blockade of MLC kinase either by calmodulin antagonist (calmidazolium) or kinase inhibitors (ML-9) (106). Initial contractions induced by  $\text{G}_q$ -coupled receptors ( $\text{m}3$ ,  $\text{S1P}_2$ ,  $\text{ET}_A$ , motilin, 5-HT $_2$ , 5-HT $_{1p}$ ) (48, 52, 85, 121, 172) and  $\text{G}_i$ -coupled receptors (somatostin sst3, opioid  $\mu$ ,  $\kappa$ , and  $\delta$ , adenosine A1) (105, 110, 116) follow a similar  $\text{Ca}^{2+}$ /calmodulin dependent pathway except for the fact that the PLC- $\beta$  isozymes and the G proteins subunits are distinct. PLC $\beta$ 1 is activated by  $\text{G}\alpha_q$ , whereas PLC- $\beta$ 3 is activated by  $\text{G}\beta\gamma_i$ . It is important to note that the blockade of PI hydrolysis or MLC kinase activity had no effect on agonist-induced sustained contraction, implying that the sustained contraction is  $\text{Ca}^{2+}$ - and MLC kinase-independent.

### **11.6.2 Signaling pathways mediating the sustained muscle contraction by PAR1 and PAR2 in smooth muscle**

Although the increase in cytosolic  $\text{Ca}^{2+}$  and MLC kinase activity is transient, MLC $_{20}$  phosphorylation and contraction are maintained. This pattern led to a search for alternative mechanisms responsible for sustained MLC $_{20}$  phosphorylation and contraction. The degree of MLC $_{20}$  phosphorylation is determined by the balance of the



activity between phosphorylation by MLC kinase and dephosphorylation by MLC phosphatase. Either activation of MLC kinase or inhibition of MLC phosphatase leads to an increase in MLC<sub>20</sub> phosphorylation.

For several years it was thought that MLC phosphatase was an unregulated enzyme, but recent studies suggest the contrary. These studies include: a) cloning and identification of MLC phosphatase subunits consisting of a 130-kDa regulatory subunit (MYPT1), a 36-kDa catalytic subunit and a 20-kDa subunit with an undefined function; b) cloning and identification of CPI-17, a 17-kDa endogenous MLC phosphatase inhibitor; and c) regulation of MLC phosphatase activity by Rho kinase and PKC. Phosphorylation of MYPT1 at Thr<sup>696</sup> by Rho kinase fosters dissociation from the catalytic subunit (PP1c $\delta$ ) and inhibits the activity of the MLC phosphatase subunit, whereas phosphorylation of CPI-17 by PKC at Thr<sup>38</sup> greatly augments (~ 1000-fold) the ability of CPI-17 to cause inhibition of MLC phosphatase activity. CPI-17 is abundantly expressed in both vascular and visceral smooth muscle.

Inhibition of MLC phosphate activity by G protein-coupled agonists is considered to play a critical role in the maintenance of MLC<sub>20</sub> phosphorylation and contraction after a decline in the cytosolic Ca<sup>2+</sup> and MLC kinase activity. Sustained contraction induced by agonists in intact smooth muscles or by experimentally fixed Ca<sup>2+</sup> concentrations in permeabilized cells involves a) G protein activation, b) regulated inhibition of MLC phosphates, and c) probably, MLC<sub>20</sub> phosphorylation via a Ca<sup>2+</sup>-independent MLC kinase (e.g., Zipper interacting protein kinase or integrin-linked kinase).

Receptors coupled to G<sub>q</sub> are also coupled to G<sub>12</sub> and/or G<sub>13</sub>, and they initiate the

pathways that inhibit MLC phosphatase via RhoA. Activated RhoA is translocated to the plasma membrane where it stimulates Rho kinase and PLD, leading to sustained activation of PKC. Rho kinase and PKC, either singly or co-operatively, are involved in the inhibition of MLC phosphatase. The requirement for inhibition of MLC phosphatase by Rho kinase/MYPT1 and/or CPI-17/PKC is receptor-specific.

Both RhoA-dependent pathways participate in the response to muscarinic (m3), motilin, and sphingosine-1-phosphate (S1P<sub>2</sub>) receptors. While only Rho kinase/MYPT1 participates in the response to endothelin (ET<sub>A</sub>) receptors, the phosphorylation of CPI-17 is suppressed via concurrent activation of ET<sub>B</sub> receptors. Activation of ET<sub>B</sub> receptors initiates an inhibitory pathway involving p38 MAP kinase-dependent activation of protein phosphatase 2A (PP2A) that causes dephosphorylation of CPI-17.

Previous studies (52, 106, 121, 124) have shown that sustained MLC<sub>20</sub> phosphorylation and contraction by G<sub>α13</sub>-coupled receptors are blocked by the expression of G<sub>α13</sub> minigenes, by *Clostridium Botulinum* C3 exoenzyme, which inactivates RhoA, by the expression of dominant negative RhoA (RhoA [T19N]), and by the inhibitor of Rho kinase (Y27632) and PKC (bisindolylmaleimide), but not by the inhibitors of PI hydrolysis, calmodulin or MLC kinase. Thus in smooth muscle cells of the gut, initial and sustained phases of MLC<sub>20</sub> phosphorylation and contraction can be distinguished clearly.

In gastric smooth muscle both PAR1-AP and PAR2-AP induce sustained MLC<sub>20</sub> phosphorylation and contraction, but the participation of MYPT1/Rho kinase and/or CPI-17/PKC in the inhibition of MLC phosphatase and stimulation of MLC<sub>20</sub> phosphorylation

is receptor-specific. Sustained contraction by PAR1 was mediated via a pathway involving the sequential activation of  $G\alpha_{12}$ , RhoA and PKC, resulting in the phosphorylation of CPI-17 and the inhibition of MLC phosphatase. Although Rho kinase was activated, MYPT1 was not phosphorylated at the Rho kinase specific site Thr<sup>696</sup>, and thus did not contribute to the inhibition of MLC phosphatase. In contrast, sustained contraction by PAR2 was mediated via a pathway involving the sequential activation of  $G\alpha_{13}$ , RhoA and Rho kinase, resulting in the phosphorylation of MYPT1 at Thr<sup>696</sup> and the inhibition of MLC phosphatase. Although RhoA, and presumably PLD and PKC, were activated, CPI-17 was not phosphorylated and thus did not contribute to the inhibition of MLC phosphatase. The pathways that lead to inhibition of MYPT1 phosphorylation by PAR1 and inhibition of CPI-17 phosphorylation by PAR2 were not examined.

Models depicting the pathways involved in initial and sustained contraction by PAR1 and PAR2 are shown in Figs. 31 and 32.

### **11.7 Feedback Inhibition of RhoA by $G_{12}$ -coupled PAR1 and $G_{13}$ -coupled PAR2 in Smooth Muscle**

The present studies identified a novel pathway for feedback inhibition of PAR1- and PAR2-stimulated RhoA. The pathway involves activation of the canonical NF- $\kappa$ B pathway by PAR1 and PAR2 leading to the release of the catalytic subunit of PKA from its binding to I $\kappa$ B $\alpha$  and causing inhibitory phosphorylation of RhoA at Ser<sup>188</sup>. This study also identified a separate pathway for the inhibition of PAR1-stimulated RhoA involving phosphorylation of  $G\alpha_{12}$  by PKC. Models depicting the pathways involved in feedback

**Figure 31. Pathways mediating initial and sustained contraction by PAR1.** Initial contraction induced by PAR1-AP involves  $G_q$ -dependent PLC- $\beta$  activation,  $IP_3$  generation, and  $Ca^{2+}$  release and  $Ca^{2+}$ /calmodulin-dependent activation of MLC kinase. Sustained contraction involves sequential activation of  $G_{12}$ , RhoA, and PKC, and phosphorylation of CPI-17 and inhibition of MLC phosphatase.

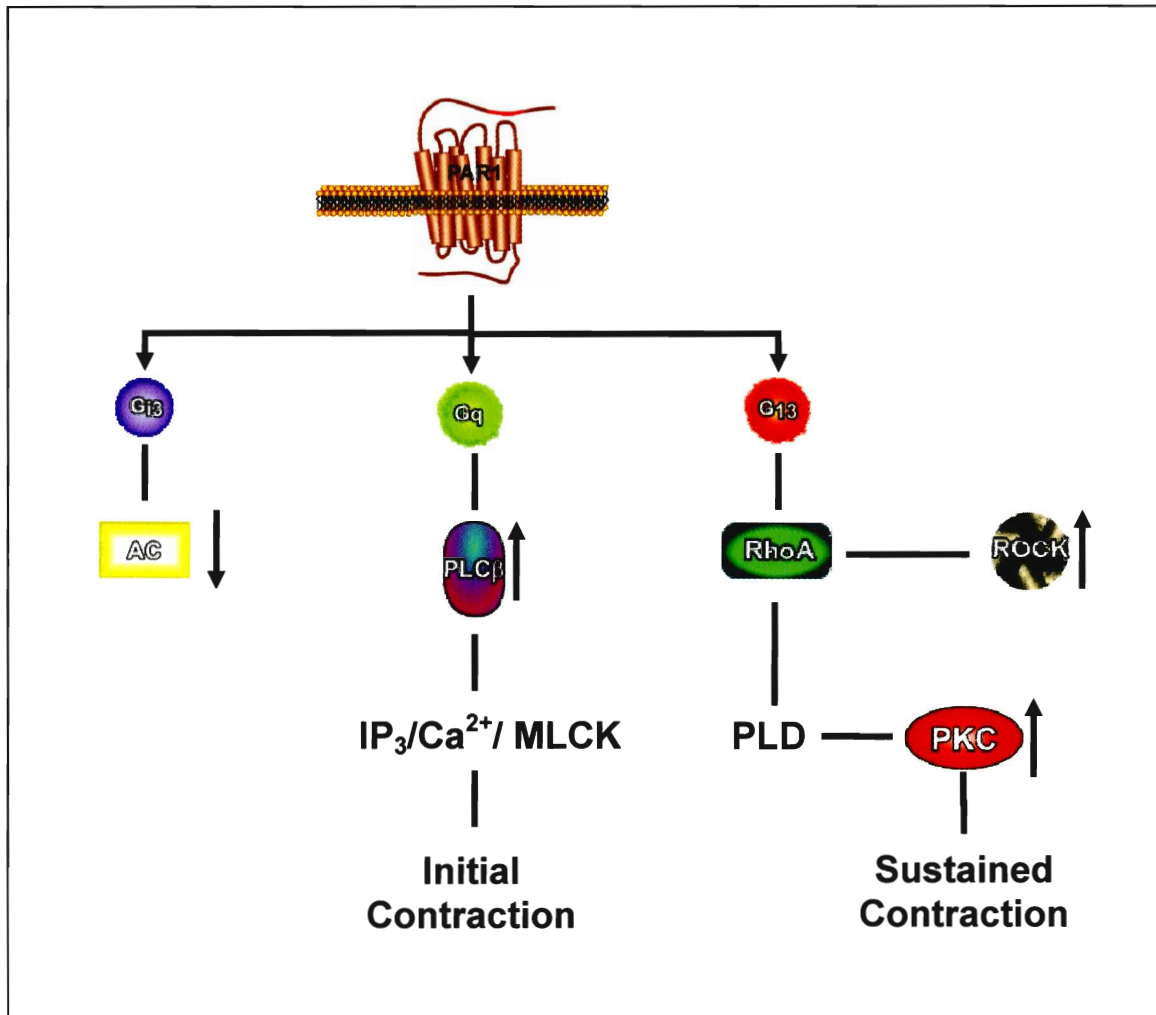
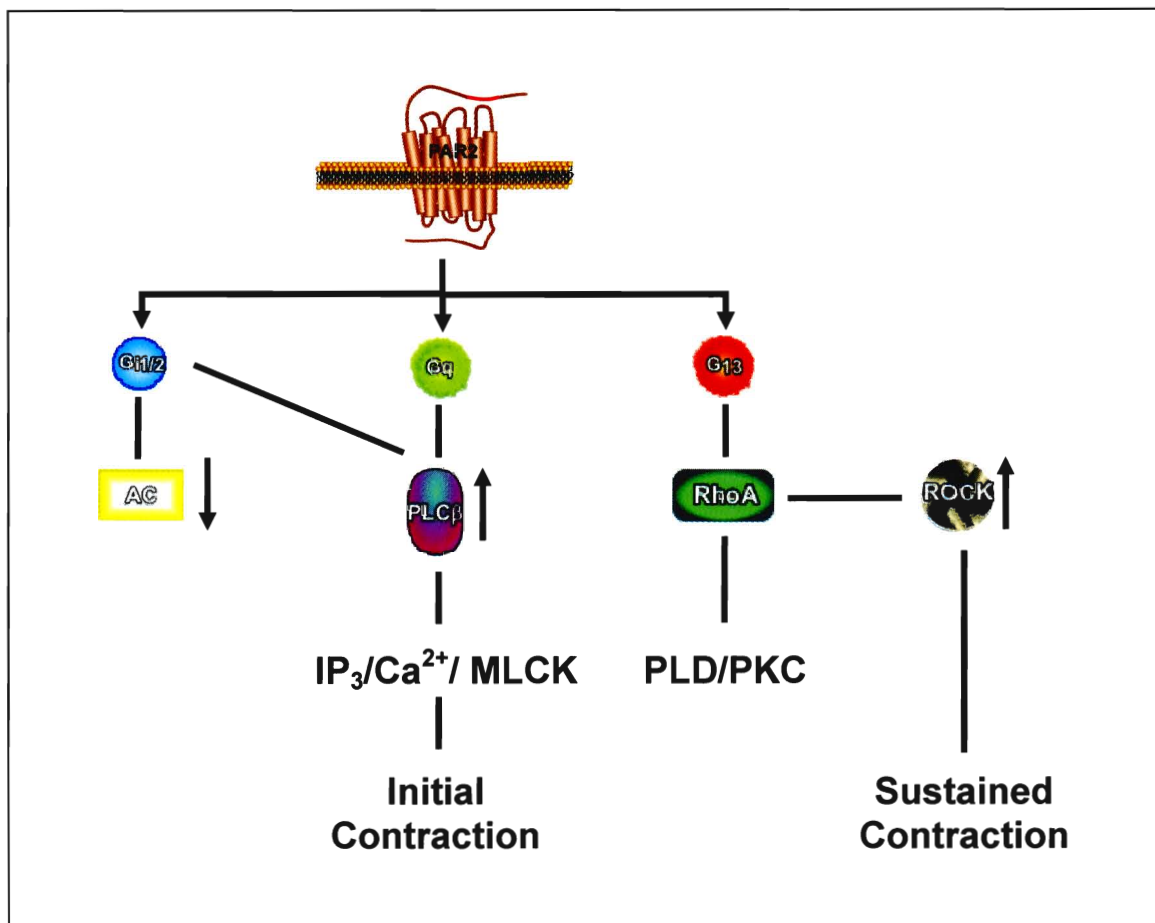


**Figure 32. Pathways mediating initial and sustained contraction by PAR2.** Initial contraction induced by PAR2-AP involves  $G_q$  and  $G_{i1/2}$ -dependent PLC- $\beta$  activation,  $IP_3$  generation, and  $Ca^{2+}$  release and  $Ca^{2+}$ /calmodulin-dependent activation of MLC kinase. Sustained contraction involves sequential activation of  $G_{13}$ , RhoA, and Rho kinase, and phosphorylation of MYPT1 and inhibition of MLC phosphatase.



inhibition of RhoA by PAR1 and PAR2 are shown in Figs. 33 and 34.

PAR1-stimulated RhoA was inhibited via two mechanisms, one mechanism involves PKA-induced phosphorylation of RhoA at Ser<sup>188</sup>, and the other involves phosphorylation of G $\alpha_{12}$  upstream of RhoA. Blockade of G $\alpha_{12}$  phosphorylation by bisindolylmaleimide, suggests that phosphorylation is mediated PKC. The role of PKC-dependent phosphorylation in feedback inhibition was demonstrated by the measurements of Rho kinase activity stimulated by PAR1 in the presence of bisindolylmaleimide. Rho kinase activity stimulated by G $_{12}$ -coupled PAR1, but not G $_{13}$ -coupled PAR2, was augmented by bisindolylmaleimide, implying that PKC-induced G $\alpha_{12}$  phosphorylation inhibited RhoA activity stimulated by PAR1. Phosphorylation of G $\alpha_{12}$  appears to decrease the affinity of G $\alpha$  for G $\beta\gamma$ , impeding re-association of the subunits and decreasing the availability of the heterotrimeric G proteins in the plasma membrane. The primary site of G $\alpha_{12}$  phosphorylation (Ser<sup>38</sup>) is located in the NH<sub>2</sub>-terminal domain of the G $\alpha_{12}$  subunit that determines the binding of  $\alpha$ - and  $\beta\gamma$ -subunits.

The effect of PKA derived from I $\kappa$ B degradation on RhoA phosphorylation downstream of G $\alpha_{12}$  was masked in the presence of PKC activation and G $\alpha_{12}$  phosphorylation. PAR1-stimulated Rho kinase activity in the presence of bisindolylmaleimide, however, was further augmented in the presence of inhibitors of IKK (IKK IV), proteasome degradation (MG-132) or PKA (PKI) suggesting that the effect of PKA on RhoA was unmasked in the presence of bisindolylmaleimide. These studies provide the evidence that PAR1-stimulated RhoA leads to the activation of PKC, which in turn phosphorylates G $\alpha_{12}$  to limit the activation of RhoA. Activation of RhoA



**Figure 33. Feedback inhibition of PAR1-stimulated RhoA by cAMP-independent PKA derived from activation of canonical NF- $\kappa$ B pathway and by PKC.** Two novel pathways for feedback inhibition of Rho kinase activity stimulated by PAR1 were identified. The pathway involves two downstream effectors of RhoA: PKC, which phosphorylates and thus inactivates  $G\alpha_{12}$ , and PKA, derived from the activation of the NF- $\kappa$ B pathway via degradation of  $I\kappa B\alpha$  and release of the catalytic subunit of PKA. PKA, in turn, phosphorylates RhoA at Ser<sup>188</sup> and thus, inactivates RhoA.

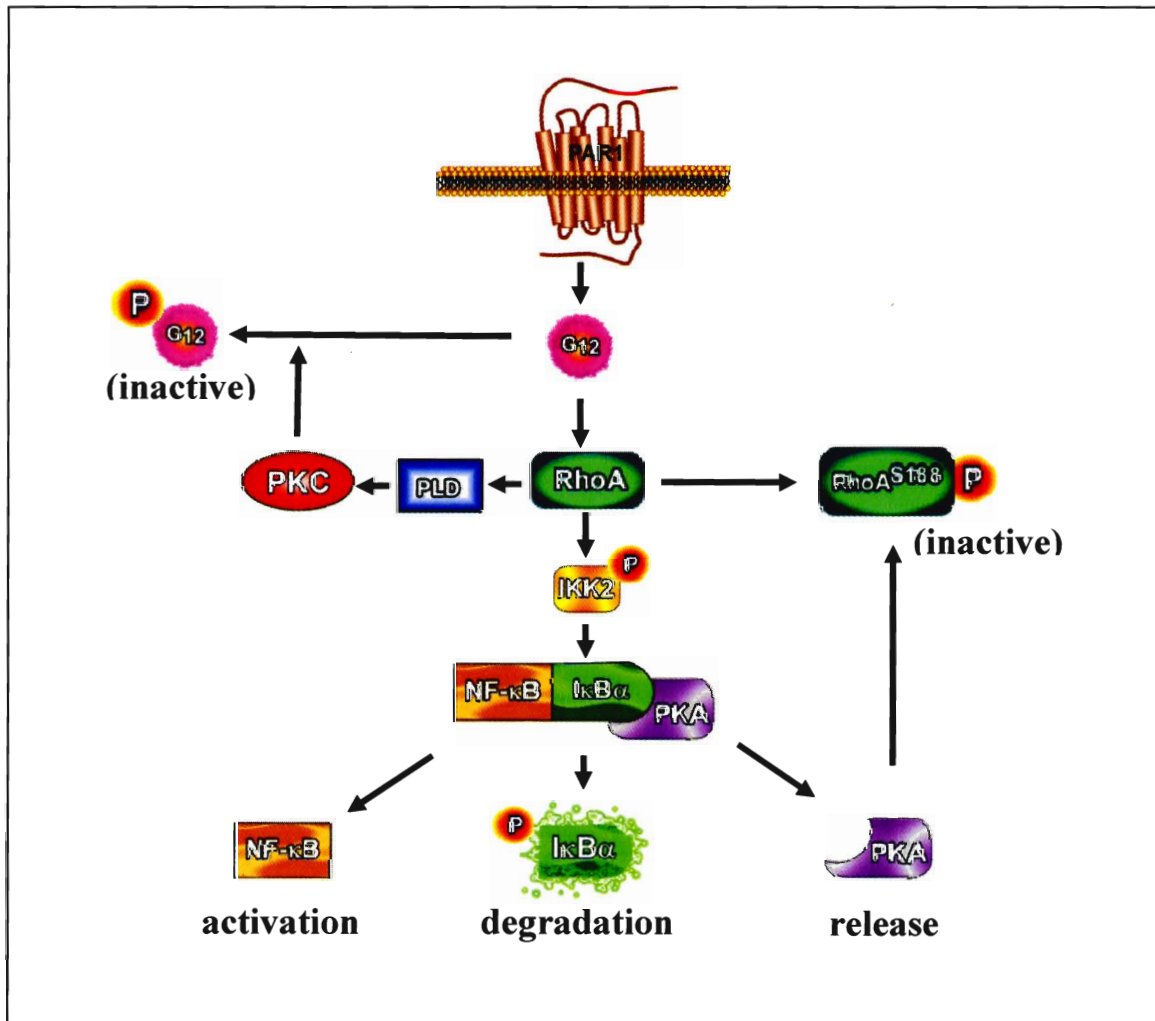
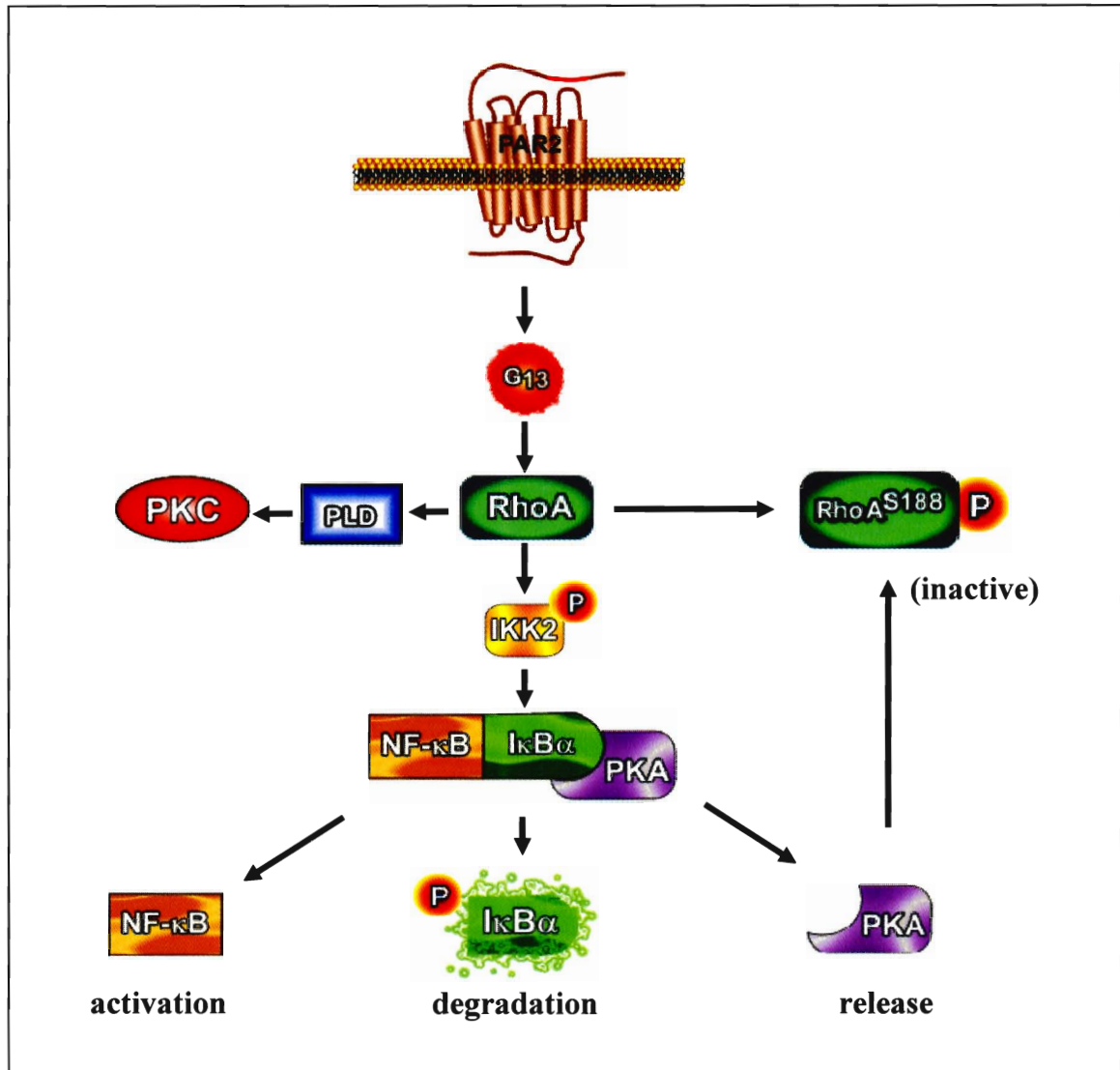


**Figure 34. Feedback inhibition of PAR2-stimulated RhoA by cAMP-independent PKA derived from activation of canonical NF- $\kappa$ B pathway.** A novel pathway for feedback inhibition of Rho kinase activity stimulated by PAR2 was identified. The pathway involves the sequential activation of RhoA and NF- $\kappa$ B by PAR2 leading to the release of the catalytic subunit of PKA from its binding to I $\kappa$ B $\alpha$  and resulting in feedback phosphorylation of RhoA by PKA on Ser<sup>188</sup> and inhibition of RhoA activity.



also results in the stimulation of PKA, which in turn phosphorylates RhoA at Ser<sup>188</sup> to limit further activation of RhoA. The former pathway is specific for PAR1 activation, whereas the latter pathway is shared by both PAR1 and PAR2 activation.

The notion that PKA derived from the degradation of I $\kappa$ B results in the phosphorylation of RhoA at Ser<sup>188</sup> and the inhibition of Rho kinase activity was corroborated using six different complimentary approaches. We first measured the activation of the canonical NF- $\kappa$ B pathway by PAR1 and PAR2. In the second approach we used IKK2 inhibitor to block I $\kappa$ B phosphorylation and subsequent degradation. In the third approach we used a proteasomal inhibitor, MG-132, to prevent degradation of I $\kappa$ B and thus prevent release of PKA catalytic subunits. In the fourth approach we used the membrane-permeable specific PKA inhibitory peptide, myristoylated PKI 14-22 amide. PKI contains a PKA pseudosubstrate sequence and specifically inhibits PKA catalytic subunits by binding to the substrate-binding sites. In the fifth approach we used a dominant negative mutant IKK2 that lacks the ability to phosphorylate I $\kappa$ B, a prerequisite for degradation. In the final approach we used a mutant RhoA(S188A) that lacks the PKA phosphorylation site.

We concluded that PAR1 and PAR2-stimulated RhoA were inhibited in a feedback mechanism via cAMP-independent PKA derived from RhoA-dependent activation of the canonical NF- $\kappa$ B pathway based on the following evidence: i) PAR1-AP and PAR2-AP induced phosphorylation (i.e activation) of IKK2, degradation of I $\kappa$ B, and phosphorylation of the p65 subunit of NF- $\kappa$ B (activation of NF $\kappa$ B); ii) PAR1-AP and PAR2-AP-induced IKK2 activation, I $\kappa$ B degradation and NF- $\kappa$ B activation were

abolished by a RhoA inhibitor, C3 exoenzyme; and iii) PAR1-AP- and PAR2-AP-stimulated Rho kinase activity was significantly augmented by PKI, IKK IV or MG132 in freshly dispersed muscle cells and in cells expressing IKK(K44A), I $\kappa$ B $\alpha$ (S32A/S36A) or RhoA(S188A).

Although PAR1 and PAR2 are coupled to G<sub>i</sub> and inhibit cAMP, they stimulate PKA. The PKA holoenzyme is a heterotetramer consisting of two catalytic subunits bound to two regulatory subunits. Classically, the mechanism of PKA activation in response to cAMP elevating agents (G<sub>s</sub>-coupled receptor agonist or forskolin) involves release of the catalytic subunits upon binding of two cAMP molecules to each of the regulatory subunits. Apparently, a certain pool of PKA catalytic subunits is found to be associated with the NF- $\kappa$ B inhibitor protein, I $\kappa$ B. Recent studies have identified a novel cAMP-independent mechanism for activation of PKA by various G protein-coupled receptor agonists. The mechanism involves release of PKA catalytic subunits from the I $\kappa$ B complex upon phosphorylation and degradation of I $\kappa$ B. In the basal state, a pool of PKA catalytic subunits is maintained in an inactive state through association with the inhibitor of NF- $\kappa$ B (I $\kappa$ B) in an NF- $\kappa$ B/I $\kappa$ B/PKA (catalytic subunits) complex, and this pool of PKA is not sensitive to changes in intracellular cAMP levels. I $\kappa$ B retains the catalytic subunits of PKA in the inactive state, presumably by masking its ATP binding site, and the signals that lead to phosphorylation and degradation of I $\kappa$ B, a prerequisite for NF- $\kappa$ B activation, resulting in the release and activation of PKA catalytic subunits.

In the present study, employing a variety of complimentary approaches, we describe a novel mechanism of PKA activation by PAR1 and PAR2 in smooth muscle

cells. These findings raise an interesting possibility for the regulation of signaling molecules involved in the contractile pathway by PKA. It is well established that the activation of PKA in gastric smooth muscle cells inhibits muscle contraction, resulting from a decrease in  $[Ca^{2+}]_i$  and  $MLC_{20}$  phosphorylation. These effects of PKA are a consequence of the inhibitory action of PKA on multiple components of  $G\alpha_q/G\alpha_{13}$  signaling culminating in muscle relaxation.

## Conclusion

In conclusion, PAR1 and PAR2 are expressed in gastric smooth muscle cells. PAR1 and PAR2 are differentially coupled to G proteins. PAR1 is coupled to the activation of  $G_q$ ,  $G_{12}$ , and  $G_{i3}$ , but not  $G_{i1}$ ,  $G_{i2}$ ,  $G_{13}$ ,  $G_s$  or  $G_z$ , whereas PAR2 is coupled to the activation of  $G_q$ ,  $G_{13}$ ,  $G_{i1}$ , and  $G_{i2}$ , but not  $G_{i3}$ ,  $G_{12}$ ,  $G_s$  or  $G_z$ . Both PAR1 and PAR2 are coupled to the stimulation of PI hydrolysis and inhibition of cAMP formation. Although, PAR1 is coupled to the activation of  $G_{i3}$ , stimulation of PI hydrolysis by PAR1 was exclusively mediated via  $G\alpha_q$ , whereas stimulation of PI hydrolysis by PAR2 was mediated by both  $G\alpha_q$  and  $G\beta\gamma_i$ . Both PAR1 and PAR2 are coupled to the activation of RhoA and RhoA-dependent canonical NF- $\kappa$ B pathway. Stimulation of RhoA/Rho kinase activity by PAR1 was mediated via  $G\alpha_{12}$ , whereas stimulation of Rho kinase activity by PAR2 was mediated via  $G\alpha_{13}$ . Activation of the NF- $\kappa$ B pathway induced release of the catalytic subunit of PKA from its binding to I $\kappa$ B and PKA-dependent phosphorylation of RhoA at Ser<sup>188</sup> leading to feedback inhibition of RhoA. In addition, phosphorylation of  $G\alpha_{12}$  by PKC derived from RhoA activation induced feedback inhibition of RhoA activity stimulated by PAR1 receptors only.

Activation of PAR1 and PAR2 induced an initial  $Ca^{2+}$ -dependent and sustained  $Ca^{2+}$ -independent muscle contraction. Initial contraction by PAR1 and PAR2 receptors



was mediated by stimulation of PLC- $\beta$  activity, generation of IP<sub>3</sub>, IP<sub>3</sub>-dependent Ca<sup>2+</sup> release, Ca<sup>2+</sup>/calmodulin-dependent activation of MLC kinase and phosphorylation of MLC<sub>20</sub> at Ser<sup>19</sup>. Sustained contraction by PAR1 was mediated by sequential activation of G<sub>12</sub>, RhoA, and PKC, and PKC-dependent phosphorylation of CPI-17 at Thr<sup>38</sup> and inhibition of MLC phosphatase. In contrast, sustained contraction by PAR2 was mediated by sequential activation of G<sub>13</sub>, RhoA, and Rho kinase, and Rho kinase-dependent phosphorylation of MYPT1 at Thr<sup>696</sup> and inhibition of MLC phosphatase. Thus, these studies have demonstrated, for the first time, the expression of PAR1 and PAR2 in smooth muscle cells and identified the receptor-specific signal transduction pathways that mediate smooth muscle contraction.

Of all the body systems, the gastrointestinal tract is the most exposed to proteases. Under physiological conditions, digestive proteases are released into the GI tract during and after meals. Under pathophysiological conditions, proteases are released by infectious agents and by tissue injury. PARs are expressed in most cell types in the GI tract. Activation of PARs, particularly PAR1 and PAR2, modulates intestinal functions, such as epithelial functions (intestinal secretion and permeability), visceral nociception, inflammatory responses and gastrointestinal motility. Thus the importance of signaling pathways activated by proteases appears to be particularly important for the physiology and pathophysiology of the GI tract. As the physiological and/or pathophysiological significance of PARs modulation of the gastrointestinal smooth muscle motility is largely open to question, the challenges for the future are to identify the physiologically relevant proteases that activate smooth muscle PARs and to determine whether PAR expression in

smooth muscle is influenced during pathological conditions. In this regard the use of PAR-activating peptides, selective PAR antagonists and studies of model murine systems from animals deficient in one or more PARs will be of particular value.

## **List of References**

## List of References

1. **Alvarez C, Regan JP, Merianos D, and Bass BL.** Protease-activated receptor-2 regulates bicarbonate secretion by pancreatic duct cells in vitro. *Surgery* 136: 669-676, 2004.
2. **Amadesi S and Bunnett N.** Protease-activated receptors: protease signaling in the gastrointestinal tract. *Curr Opin Pharmacol* 4: 551-556, 2004.
3. **Asokanathan N, Graham PT, Fink J, Knight DA, Bakker AJ, McWilliam AS, Thompson PJ, and Stewart GA.** Activation of protease-activated receptor (PAR)-1, PAR-2, and PAR-4 stimulates IL-6, IL-8, and prostaglandin E2 release from human respiratory epithelial cells. *J Immunol* 168: 3577-3585, 2002.
4. **Bachli EB, Pech CM, Johnson KM, Johnson DJ, Tuddenham EG, and McVey JH.** Factor Xa and thrombin, but not factor VIIa, elicit specific cellular responses in dermal fibroblasts. *J Thromb Haemost* 1: 1935-1944, 2003.
5. **Barr AJ, Ali H, Haribabu B, Snyderman R, and Smrcka AV.** Identification of a region at the N-terminus of phospholipase C-beta 3 that interacts with G protein beta gamma subunits. *Biochemistry* 39: 1800-1806, 2000.
6. **Berridge MJ, Downes CP, and Hanley MR.** Lithium amplifies agonist-dependent phosphatidylinositol responses in brain and salivary glands. *Biochem J* 206: 587-595, 1982.
7. **Bleasdale JE, Thakur NR, Gremban RS, Bundy GL, Fitzpatrick FA, Smith RJ, and Bunting S.** Selective inhibition of receptor-coupled phospholipase C-dependent processes in human platelets and polymorphonuclear neutrophils. *J Pharmacol Exp Ther* 255: 756-768, 1990.
8. **Boger DL, Goldberg J, Silletti S, Kessler T, and Cheresh DA.** Identification of a novel class of small-molecule antiangiogenic agents through the screening of combinatorial libraries which function by inhibiting the binding and localization of proteinase MMP2 to integrin alpha(V)beta(3). *J Am Chem Soc* 123: 1280-1288, 2001.
9. **Bohm SK, Khitin LM, Grady EF, Aponte G, Payan DG, and Bunnett NW.** Mechanisms of desensitization and resensitization of proteinase-activated receptor-2. *J Biol Chem* 271: 22003-22016, 1996.
10. **Bohm SK, Kong W, Bromme D, Smeekens SP, Anderson DC, Connolly A, Kahn M, Nelken NA, Coughlin SR, Payan DG, and Bunnett NW.** Molecular cloning, expression and potential functions of the human proteinase-activated receptor-2. *Biochem J* 314 ( Pt 3): 1009-1016, 1996.
11. **Bretschneider E, Spanbroek R, Lotzer K, Habenicht AJ, and Schror K.** Evidence for functionally active protease-activated receptor-3 (PAR-3) in human vascular smooth muscle cells. *Thromb Haemost* 90: 704-709, 2003.

12. **Buresi MC, Buret AG, Hollenberg MD, and MacNaughton WK.** Activation of proteinase-activated receptor 1 stimulates epithelial chloride secretion through a unique MAP kinase- and cyclo-oxygenase-dependent pathway. *Faseb J* 16: 1515-1525, 2002.
13. **Buresi MC, Vergnolle N, Sharkey KA, Keenan CM, Andrade-Gordon P, Cirino G, Cirillo D, Hollenberg MD, and MacNaughton WK.** Activation of proteinase-activated receptor-1 inhibits neurally evoked chloride secretion in the mouse colon in vitro. *Am J Physiol Gastrointest Liver Physiol* 288: G337-345, 2005.
14. **Cairns JA and Walls AF.** Mast cell tryptase is a mitogen for epithelial cells. Stimulation of IL-8 production and intercellular adhesion molecule-1 expression. *J Immunol* 156: 275-283, 1996.
15. **Camerer E, Huang W, and Coughlin SR.** Tissue factor- and factor X-dependent activation of protease-activated receptor 2 by factor VIIa. *Proc Natl Acad Sci U S A* 97: 5255-5260, 2000.
16. **Cao T, Gerard NP, and Brain SD.** Use of NK(1) knockout mice to analyze substance P-induced edema formation. *Am J Physiol* 277: R476-481, 1999.
17. **Cao T, Pinter E, Al-Rashed S, Gerard N, Houtt JR, and Brain SD.** Neurokinin-1 receptor agonists are involved in mediating neutrophil accumulation in the inflamed, but not normal, cutaneous microvasculature: an in vivo study using neurokinin-1 receptor knockout mice. *J Immunol* 164: 5424-5429, 2000.
18. **Caunt M, Huang YQ, Brooks PC, and Karparkin S.** Thrombin induces neoangiogenesis in the chick chorioallantoic membrane. *J Thromb Haemost* 1: 2097-2102, 2003.
19. **Chambers RC, Dabbagh K, McAnulty RJ, Gray AJ, Blanc-Brude OP, and Laurent GJ.** Thrombin stimulates fibroblast procollagen production via proteolytic activation of protease-activated receptor 1. *Biochem J* 333 ( Pt 1): 121-127, 1998.
20. **Chan GH and Fiscus RR.** Severe impairment of CGRP-induced hypotension in vivo and vasorelaxation in vitro in elderly rats. *Eur J Pharmacol* 434: 133-139, 2002.
21. **Chen J, Ishii M, Wang L, Ishii K, and Coughlin SR.** Thrombin receptor activation. Confirmation of the intramolecular tethered liganding hypothesis and discovery of an alternative intermolecular liganding mode. *J Biol Chem* 269: 16041-16045, 1994.
22. **Chin AC, Vergnolle N, MacNaughton WK, Wallace JL, Hollenberg MD, and Buret AG.** Proteinase-activated receptor 1 activation induces epithelial apoptosis and increases intestinal permeability. *Proc Natl Acad Sci U S A* 100: 11104-11109, 2003.
23. **Chow JM, Moffatt JD, and Cocks TM.** Effect of protease-activated receptor (PAR)-1, -2 and -4-activating peptides, thrombin and trypsin in rat isolated airways. *Br J Pharmacol* 131: 1584-1591, 2000.
24. **Cocks TM, Sozzi V, Moffatt JD, and Selemidis S.** Protease-activated receptors mediate apamin-sensitive relaxation of mouse and guinea pig gastrointestinal smooth muscle. *Gastroenterology* 116: 586-592, 1999.
25. **Collins LR, Ricketts WA, Olefsky JM, and Brown JH.** The G12 coupled thrombin receptor stimulates mitogenesis through the Shc SH2 domain. *Oncogene* 15: 595-600, 1997.

26. **Colotta F, Sciacca FL, Sironi M, Luini W, Rabiet MJ, and Mantovani A.** Expression of monocyte chemotactic protein-1 by monocytes and endothelial cells exposed to thrombin. *Am J Pathol* 144: 975-985, 1994.
27. **Compton SJ, Cairns JA, Holgate ST, and Walls AF.** The role of mast cell tryptase in regulating endothelial cell proliferation, cytokine release, and adhesion molecule expression: tryptase induces expression of mRNA for IL-1 beta and IL-8 and stimulates the selective release of IL-8 from human umbilical vein endothelial cells. *J Immunol* 161: 1939-1946, 1998.
28. **Compton SJ, Cairns JA, Palmer KJ, Al-Ani B, Hollenberg MD, and Walls AF.** A polymorphic protease-activated receptor 2 (PAR2) displaying reduced sensitivity to trypsin and differential responses to PAR agonists. *J Biol Chem* 275: 39207-39212, 2000.
29. **Corvera CU, Dery O, McConalogue K, Gamp P, Thoma M, Al-Ani B, Caughey GH, Hollenberg MD, and Bunnett NW.** Thrombin and mast cell tryptase regulate guinea-pig myenteric neurons through proteinase-activated receptors-1 and -2. *J Physiol* 517 ( Pt 3): 741-756, 1999.
30. **Cottrell GS, Amadesi S, Grady EF, and Bunnett NW.** Trypsin IV, a novel agonist of protease-activated receptors 2 and 4. *J Biol Chem* 279: 13532-13539, 2004.
31. **D'Andrea MR, Derian CK, Leturcq D, Baker SM, Brunmark A, Ling P, Darrow AL, Santulli RJ, Brass LF, and Andrade-Gordon P.** Characterization of protease-activated receptor-2 immunoreactivity in normal human tissues. *J Histochem Cytochem* 46: 157-164, 1998.
32. **D'Andrea MR, Rogahn CJ, and Andrade-Gordon P.** Localization of protease-activated receptors-1 and -2 in human mast cells: indications for an amplified mast cell degranulation cascade. *Biotech Histochem* 75: 85-90, 2000.
33. **Darmoul D, Gratio V, Devaud H, Lehy T, and Laburthe M.** Aberrant expression and activation of the thrombin receptor protease-activated receptor-1 induces cell proliferation and motility in human colon cancer cells. *Am J Pathol* 162: 1503-1513, 2003.
34. **Darmoul D, Gratio V, Devaud H, Peiretti F, and Laburthe M.** Activation of proteinase-activated receptor 1 promotes human colon cancer cell proliferation through epidermal growth factor receptor transactivation. *Mol Cancer Res* 2: 514-522, 2004.
35. **de Garavilla L, Vergnolle N, Young SH, Ennes H, Steinhoff M, Ossovskaya VS, D'Andrea MR, Mayer EA, Wallace JL, Hollenberg MD, Andrade-Gordon P, and Bunnett NW.** Agonists of proteinase-activated receptor 1 induce plasma extravasation by a neurogenic mechanism. *Br J Pharmacol* 133: 975-987, 2001.
36. **Dery O, Corvera CU, Steinhoff M, and Bunnett NW.** Proteinase-activated receptors: novel mechanisms of signaling by serine proteases. *Am J Physiol* 274: C1429-1452, 1998.
37. **Dery O, Thoma MS, Wong H, Grady EF, and Bunnett NW.** Trafficking of proteinase-activated receptor-2 and beta-arrestin-1 tagged with green fluorescent protein. beta-Arrestin-dependent endocytosis of a proteinase receptor. *J Biol Chem* 274: 18524-18535, 1999.

38. **Fang Q, Liu X, Abe S, Kobayashi T, Wang XQ, Kohyama T, Hashimoto M, Wyatt T, and Rennard SI.** Thrombin induces collagen gel contraction partially through PAR1 activation and PKC-epsilon. *Eur Respir J* 24: 918-924, 2004.
39. **Frungieri MB, Weidinger S, Meineke V, Kohn FM, and Mayerhofer A.** Proliferative action of mast-cell tryptase is mediated by PAR2, COX2, prostaglandins, and PPARgamma : Possible relevance to human fibrotic disorders. *Proc Natl Acad Sci U S A* 99: 15072-15077, 2002.
40. **Fyfe M, Bergstrom M, Aspengren S, and Peterson A.** PAR-2 activation in intestinal epithelial cells potentiates interleukin-1beta-induced chemokine secretion via MAP kinase signaling pathways. *Cytokine* 31: 358-367, 2005.
41. **Gao C, Liu S, Hu HZ, Gao N, Kim GY, Xia Y, and Wood JD.** Serine proteases excite myenteric neurons through protease-activated receptors in guinea pig small intestine. *Gastroenterology* 123: 1554-1564, 2002.
42. **Garrido R, Segura B, Zhang W, and Mulholland M.** Presence of functionally active protease-activated receptors 1 and 2 in myenteric glia. *J Neurochem* 83: 556-564, 2002.
43. **Gerszten RE, Chen J, Ishii M, Ishii K, Wang L, Nanevich T, Turck CW, Vu TK, and Coughlin SR.** Specificity of the thrombin receptor for agonist peptide is defined by its extracellular surface. *Nature* 368: 648-651, 1994.
44. **Green BT, Bunnnett NW, Kulkarni-Narla A, Steinhoff M, and Brown DR.** Intestinal type 2 proteinase-activated receptors: expression in opioid-sensitive secretomotor neural circuits that mediate epithelial ion transport. *J Pharmacol Exp Ther* 295: 410-416, 2000.
45. **Greenberg DL, Mize GJ, and Takayama TK.** Protease-activated receptor mediated RhoA signaling and cytoskeletal reorganization in LNCaP cells. *Biochemistry* 42: 702-709, 2003.
46. **Guyonnet Duperat V, Jacquelin B, Boisseau P, Arveiler B, and Nurden AT.** Protease-activated receptor genes are clustered on 5q13. *Blood* 92: 25-31, 1998.
47. **Henriksen RA and Hanks VK.** PAR-4 agonist AYPGKF stimulates thromboxane production by human platelets. *Arterioscler Thromb Vasc Biol* 22: 861-866, 2002.
48. **Hersch E, Huang J, Grider JR, and Murthy KS.** Gq/G13 signaling by ET-1 in smooth muscle: MYPT1 phosphorylation via ETA and CPI-17 dephosphorylation via ETB. *Am J Physiol Cell Physiol* 287: C1209-1218, 2004.
49. **Hirota Y, Osuga Y, Hirata T, Harada M, Morimoto C, Yoshino O, Koga K, Yano T, Tsutsumi O, and Taketani Y.** Activation of protease-activated receptor 2 stimulates proliferation and interleukin (IL)-6 and IL-8 secretion of endometriotic stromal cells. *Hum Reprod* 20: 3547-3553, 2005.
50. **Hu W, Mahavadi S, Huang J, Li F, and Murthy KS.** Characterization of S1P1 and S1P2 receptor function in smooth muscle by receptor silencing and receptor protection. *Am J Physiol Gastrointest Liver Physiol* 291: G605-610, 2006.
51. **Huang J, Mahavadi S, Sriwai W, Hu W, and Murthy KS.** Gi-coupled receptors mediate phosphorylation of CPI-17 and MLC20 via preferential activation of the PI3K/ILK pathway. *Biochem J* 396: 193-200, 2006.

52. **Huang J, Zhou H, Mahavadi S, Sriwai W, Lyall V, and Murthy KS.** Signaling pathways mediating gastrointestinal smooth muscle contraction and MLC20 phosphorylation by motilin receptors. *Am J Physiol Gastrointest Liver Physiol* 288: G23-31, 2005.
53. **Huang J, Zhou H, Mahavadi S, Sriwai W, and Murthy KS.** Inhibition of Galphaq-dependent PLC-beta1 activity by PKG and PKA is mediated by phosphorylation of RGS4 and GRK2. *Am J Physiol Cell Physiol* 292: C200-208, 2007.
54. **Huang YQ, Li JJ, Hu L, Lee M, and Karpatkin S.** Thrombin induces increased expression and secretion of angiopoietin-2 from human umbilical vein endothelial cells. *Blood* 99: 1646-1650, 2002.
55. **Hung DT, Vu TK, Wheaton VI, Ishii K, and Coughlin SR.** Cloned platelet thrombin receptor is necessary for thrombin-induced platelet activation. *J Clin Invest* 89: 1350-1353, 1992.
56. **Hung DT, Wong YH, Vu TK, and Coughlin SR.** The cloned platelet thrombin receptor couples to at least two distinct effectors to stimulate phosphoinositide hydrolysis and inhibit adenylyl cyclase. *J Biol Chem* 267: 20831-20834, 1992.
57. **Ishihara H, Connolly AJ, Zeng D, Kahn ML, Zheng YW, Timmons C, Tram T, and Coughlin SR.** Protease-activated receptor 3 is a second thrombin receptor in humans. *Nature* 386: 502-506, 1997.
58. **Ishii K, Chen J, Ishii M, Koch WJ, Freedman NJ, Lefkowitz RJ, and Coughlin SR.** Inhibition of thrombin receptor signaling by a G-protein coupled receptor kinase. Functional specificity among G-protein coupled receptor kinases. *J Biol Chem* 269: 1125-1130, 1994.
59. **Jacob C, Yang PC, Darmoul D, Amadesi S, Saito T, Cottrell GS, Coelho AM, Singh P, Grady EF, Perdue M, and Bunnnett NW.** Mast cell tryptase controls paracellular permeability of the intestine. Role of protease-activated receptor 2 and beta-arrestins. *J Biol Chem* 280: 31936-31948, 2005.
60. **Jung U and Ley K.** Mice lacking two or all three selectins demonstrate overlapping and distinct functions for each selectin. *J Immunol* 162: 6755-6762, 1999.
61. **Kahn ML, Zheng YW, Huang W, Bigornia V, Zeng D, Moff S, Farese RV, Jr., Tam C, and Coughlin SR.** A dual thrombin receptor system for platelet activation. *Nature* 394: 690-694, 1998.
62. **Kaibuchi K, Kuroda S, and Amano M.** Regulation of the cytoskeleton and cell adhesion by the Rho family GTPases in mammalian cells. *Annu Rev Biochem* 68: 459-486, 1999.
63. **Kanke T, Macfarlane SR, Seatter MJ, Davenport E, Paul A, McKenzie RC, and Plevin R.** Proteinase-activated receptor-2-mediated activation of stress-activated protein kinases and inhibitory kappa B kinases in NCTC 2544 keratinocytes. *J Biol Chem* 276: 31657-31666, 2001.
64. **Kawabata A.** [Physiological functions of protease-activated receptor-2]. *Nippon Yakurigaku Zasshi* 121: 411-420, 2003.
65. **Kawabata A, Kinoshita M, Kuroda R, and Kakehi K.** Capsazepine partially inhibits neurally mediated gastric mucus secretion following activation of protease-activated receptor 2. *Clin Exp Pharmacol Physiol* 29: 360-361, 2002.



66. **Kawabata A, Kinoshita M, Nishikawa H, Kuroda R, Nishida M, Araki H, Arizono N, Oda Y, and Kakehi K.** The protease-activated receptor-2 agonist induces gastric mucus secretion and mucosal cytoprotection. *J Clin Invest* 107: 1443-1450, 2001.
67. **Kawabata A, Kubo S, Nakaya Y, Ishiki T, Kuroda R, Sekiguchi F, Kawao N, and Nishikawa H.** Distinct roles for protease-activated receptors 1 and 2 in vasomotor modulation in rat superior mesenteric artery. *Cardiovasc Res* 61: 683-692, 2004.
68. **Kawabata A, Kuroda R, Kuroki N, Nishikawa H, Kawai K, and Araki H.** Characterization of the protease-activated receptor-1-mediated contraction and relaxation in the rat duodenal smooth muscle. *Life Sci* 67: 2521-2530, 2000.
69. **Kawabata A, Kuroda R, Nakaya Y, Kawai K, Nishikawa H, and Kawao N.** Factor Xa-evoked relaxation in rat aorta: involvement of PAR-2. *Biochem Biophys Res Commun* 282: 432-435, 2001.
70. **Kawabata A, Kuroda R, Nishida M, Nagata N, Sakaguchi Y, Kawao N, Nishikawa H, Arizono N, and Kawai K.** Protease-activated receptor-2 (PAR-2) in the pancreas and parotid gland: Immunolocalization and involvement of nitric oxide in the evoked amylase secretion. *Life Sci* 71: 2435-2446, 2002.
71. **Kawabata A, Kuroda R, Nishikawa H, Asai T, Kataoka K, and Taneda M.** Enhancement of vascular permeability by specific activation of protease-activated receptor-1 in rat hindpaw: a protective role of endogenous and exogenous nitric oxide. *Br J Pharmacol* 126: 1856-1862, 1999.
72. **Kawabata A, Kuroda R, Nishikawa H, and Kawai K.** Modulation by protease-activated receptors of the rat duodenal motility in vitro: possible mechanisms underlying the evoked contraction and relaxation. *Br J Pharmacol* 128: 865-872, 1999.
73. **Kawabata A, Nakaya Y, Ishiki T, Kubo S, Kuroda R, Sekiguchi F, Kawao N, Nishikawa H, and Kawai K.** Receptor-activating peptides for PAR-1 and PAR-2 relax rat gastric artery via multiple mechanisms. *Life Sci* 75: 2689-2702, 2004.
74. **Kawabata A, Nishikawa H, Kuroda R, Kawai K, and Hollenberg MD.** Proteinase-activated receptor-2 (PAR-2): regulation of salivary and pancreatic exocrine secretion in vivo in rats and mice. *Br J Pharmacol* 129: 1808-1814, 2000.
75. **Kawabata A, Nishikawa H, Saitoh H, Nakaya Y, Hiramatsu K, Kubo S, Nishida M, Kawao N, Kuroda R, Sekiguchi F, Kinoshita M, Kakehi K, Arizono N, Yamagishi H, and Kawai K.** A protective role of protease-activated receptor 1 in rat gastric mucosa. *Gastroenterology* 126: 208-219, 2004.
76. **Kawao N, Hiramatsu K, Inoi N, Kuroda R, Nishikawa H, Sekiguchi F, and Kawabata A.** The PAR-1-activating peptide facilitates pepsinogen secretion in rats. *Peptides* 24: 1449-1451, 2003.
77. **Kawao N, Sakaguchi Y, Tagome A, Kuroda R, Nishida S, Irimajiri K, Nishikawa H, Kawai K, Hollenberg MD, and Kawabata A.** Protease-activated receptor-2 (PAR-2) in the rat gastric mucosa: immunolocalization and facilitation of pepsin/pepsinogen secretion. *Br J Pharmacol* 135: 1292-1296, 2002.
78. **Kim CG, Park D, and Rhee SG.** The role of carboxyl-terminal basic amino acids in Gqalpha-dependent activation, particulate association, and nuclear localization of phospholipase C-beta1. *J Biol Chem* 271: 21187-21192, 1996.

79. **Kong W, McConalogue K, Khitin LM, Hollenberg MD, Payan DG, Bohm SK, and Bunnnett NW.** Luminal trypsin may regulate enterocytes through proteinase-activated receptor 2. *Proc Natl Acad Sci U S A* 94: 8884-8889, 1997.
80. **Koo BH, Chung KH, Hwang KC, and Kim DS.** Factor Xa induces mitogenesis of coronary artery smooth muscle cell via activation of PAR-2. *FEBS Lett* 523: 85-89, 2002.
81. **Kozasa T, Jiang X, Hart MJ, Sternweis PM, Singer WD, Gilman AG, Bollag G, and Sternweis PC.** p115 RhoGEF, a GTPase activating protein for Galpha12 and Galpha13. *Science* 280: 2109-2111, 1998.
82. **Krupnick JG and Benovic JL.** The role of receptor kinases and arrestins in G protein-coupled receptor regulation. *Annu Rev Pharmacol Toxicol* 38: 289-319, 1998.
83. **Kudahl K, Fisker S, and Sonne O.** A thrombin receptor in resident rat peritoneal macrophages. *Exp Cell Res* 193: 45-53, 1991.
84. **Kuemmerle JF and Makhlof GM.** Agonist-stimulated cyclic ADP ribose. Endogenous modulator of Ca(2+)-induced Ca<sup>2+</sup> release in intestinal longitudinal muscle. *J Biol Chem* 270: 25488-25494, 1995.
85. **Kuemmerle JF, Martin DC, Murthy KS, Kellum JM, Grider JR, and Makhlof GM.** Coexistence of contractile and relaxant 5-hydroxytryptamine receptors coupled to distinct signaling pathways in intestinal muscle cells: convergence of the pathways on Ca<sup>2+</sup> mobilization. *Mol Pharmacol* 42: 1090-1096, 1992.
86. **KUMAR V, ABBAS AK, and FAUSTO N.** Robbins and Cotran pathologic basis of disease. (7 ed.). Philadelphia: Elsevier Saunders, 2005.
87. **Kunzelmann K, Schreiber R, Konig J, and Mall M.** Ion transport induced by proteinase-activated receptors (PAR2) in colon and airways. *Cell Biochem Biophys* 36: 209-214, 2002.
88. **Laposata M, Dohnarsky DK, and Shin HS.** Thrombin-induced gap formation in confluent endothelial cell monolayers in vitro. *Blood* 62: 549-556, 1983.
89. **Lerner DJ, Chen M, Tram T, and Coughlin SR.** Agonist recognition by proteinase-activated receptor 2 and thrombin receptor. Importance of extracellular loop interactions for receptor function. *J Biol Chem* 271: 13943-13947, 1996.
90. **Linden DR, Manning BP, Bunnnett NW, and Mawe GM.** Agonists of proteinase-activated receptor 2 excite guinea pig ileal myenteric neurons. *Eur J Pharmacol* 431: 311-314, 2001.
91. **Lipsky JJ and Lietman PS.** Aminoglycoside inhibition of a renal phosphatidylinositol phospholipase C. *J Pharmacol Exp Ther* 220: 287-292, 1982.
92. **Liu Y, Gilcrease MZ, Henderson Y, Yuan XH, Clayman GL, and Chen Z.** Expression of protease-activated receptor 1 in oral squamous cell carcinoma. *Cancer Lett* 169: 173-180, 2001.
93. **Ma L, Perini R, McKnight W, Dickey M, Klein A, Hollenberg MD, and Wallace JL.** Proteinase-activated receptors 1 and 4 counter-regulate endostatin and VEGF release from human platelets. *Proc Natl Acad Sci U S A* 102: 216-220, 2005.
94. **Mall M, Gonska T, Thomas J, Hirtz S, Schreiber R, and Kunzelmann K.** Activation of ion secretion via proteinase-activated receptor-2 in human colon. *Am J Physiol Gastrointest Liver Physiol* 282: G200-210, 2002.

95. **Matsumoto J, Takeuchi K, Ueshima K, and Okabe S.** Role of capsaicin-sensitive afferent neurons in mucosal blood flow response of rat stomach induced by mild irritants. *Dig Dis Sci* 37: 1336-1344, 1992.
96. **McLean K, Schirm S, Johns A, Morser J, and Light DR.** FXa-induced responses in vascular wall cells are PAR-mediated and inhibited by ZK-807834. *Thromb Res* 103: 281-297, 2001.
97. **Milia AF, Salis MB, Stacca T, Pinna A, Madeddu P, Trevisani M, Geppetti P, and Emanuelli C.** Protease-activated receptor-2 stimulates angiogenesis and accelerates hemodynamic recovery in a mouse model of hindlimb ischemia. *Circ Res* 91: 346-352, 2002.
98. **Mirza H, Schmidt VA, Derian CK, Jesty J, and Bahou WF.** Mitogenic responses mediated through the proteinase-activated receptor-2 are induced by expressed forms of mast cell alpha- or beta-tryptases. *Blood* 90: 3914-3922, 1997.
99. **Misra S, Murthy KS, Zhou H, and Grider JR.** Coexpression of Y1, Y2, and Y4 receptors in smooth muscle coupled to distinct signaling pathways. *J Pharmacol Exp Ther* 311: 1154-1162, 2004.
100. **Molino M, Barnathan ES, Numerof R, Clark J, Dreyer M, Cumashi A, Hoxie JA, Schechter N, Woolkalis M, and Brass LF.** Interactions of mast cell tryptase with thrombin receptors and PAR-2. *J Biol Chem* 272: 4043-4049, 1997.
101. **Molino M, Blanchard N, Belmonte E, Tarver AP, Abrams C, Hoxie JA, Cerletti C, and Brass LF.** Proteolysis of the human platelet and endothelial cell thrombin receptor by neutrophil-derived cathepsin G. *J Biol Chem* 270: 11168-11175, 1995.
102. **Mule F, Baffi MC, and Cerra MC.** Dual effect mediated by protease-activated receptors on the mechanical activity of rat colon. *Br J Pharmacol* 136: 367-374, 2002.
103. **Murthy KS.** Activation of phosphodiesterase 5 and inhibition of guanylate cyclase by cGMP-dependent protein kinase in smooth muscle. *Biochem J* 360: 199-208, 2001.
104. **Murthy KS.** Signaling for contraction and relaxation in smooth muscle of the gut. *Annu Rev Physiol* 68: 345-374, 2006.
105. **Murthy KS, Coy DH, and Makhlof GM.** Somatostatin receptor-mediated signaling in smooth muscle. Activation of phospholipase C-beta3 by Gbetagamma and inhibition of adenylyl cyclase by Galphai1 and Galphao. *J Biol Chem* 271: 23458-23463, 1996.
106. **Murthy KS, Grider JR, Kuemmerle JF, and Makhlof GM.** Sustained muscle contraction induced by agonists, growth factors, and Ca(2+) mediated by distinct PKC isozymes. *Am J Physiol Gastrointest Liver Physiol* 279: G201-210, 2000.
107. **Murthy KS, Grider JR, and Makhlof GM.** InsP3-dependent Ca2+ mobilization in circular but not longitudinal muscle cells of intestine. *Am J Physiol* 261: G937-944, 1991.
108. **Murthy KS, Jin JG, Grider JR, and Makhlof GM.** Characterization of PACAP receptors and signaling pathways in rabbit gastric muscle cells. *Am J Physiol* 272: G1391-1399, 1997.

109. **Murthy KS, Kuemmerle JF, and Makhlof GM.** Agonist-mediated activation of PLA2 initiates Ca<sup>2+</sup> mobilization in intestinal longitudinal smooth muscle. *Am J Physiol* 269: G93-102, 1995.
110. **Murthy KS and Makhlof GM.** Adenosine A1 receptor-mediated activation of phospholipase C-beta 3 in intestinal muscle: dual requirement for alpha and beta gamma subunits of Gi3. *Mol Pharmacol* 47: 1172-1179, 1995.
111. **Murthy KS and Makhlof GM.** cGMP-mediated Ca<sup>2+</sup> release from IP3-insensitive Ca<sup>2+</sup> stores in smooth muscle. *Am J Physiol* 274: C1199-1205, 1998.
112. **Murthy KS and Makhlof GM.** Coexpression of ligand-gated P2X and G protein-coupled P2Y receptors in smooth muscle. Preferential activation of P2Y receptors coupled to phospholipase C (PLC)-beta1 via Galphaq/11 and to PLC-beta3 via Gbetagamma3. *J Biol Chem* 273: 4695-4704, 1998.
113. **Murthy KS and Makhlof GM.** Differential coupling of muscarinic m2 and m3 receptors to adenylyl cyclases V/VI in smooth muscle. Concurrent M2-mediated inhibition via Galphai3 and m3-mediated stimulation via Gbetagammaq. *J Biol Chem* 272: 21317-21324, 1997.
114. **Murthy KS and Makhlof GM.** Differential regulation of phospholipase A2 (PLA2)-dependent Ca<sup>2+</sup> signaling in smooth muscle by cAMP- and cGMP-dependent protein kinases. Inhibitory phosphorylation of PLA2 by cyclic nucleotide-dependent protein kinases. *J Biol Chem* 273: 34519-34526, 1998.
115. **Murthy KS and Makhlof GM.** Identification of the G protein-activating domain of the natriuretic peptide clearance receptor (NPR-C). *J Biol Chem* 274: 17587-17592, 1999.
116. **Murthy KS and Makhlof GM.** Opioid mu, delta, and kappa receptor-induced activation of phospholipase C-beta 3 and inhibition of adenylyl cyclase is mediated by Gi2 and G(o) in smooth muscle. *Mol Pharmacol* 50: 870-877, 1996.
117. **Murthy KS and Makhlof GM.** Phosphoinositide metabolism in intestinal smooth muscle: preferential production of Ins(1,4,5)P3 in circular muscle cells. *Am J Physiol* 261: G945-951, 1991.
118. **Murthy KS and Makhlof GM.** Regulation of adenylyl cyclase type V/VI in smooth muscle: interplay of inhibitory G protein and Ca<sup>2+</sup> influx. *Mol Pharmacol* 54: 122-128, 1998.
119. **Murthy KS, McHenry L, Grider JR, and Makhlof GM.** Adenosine A1 and A2b receptors coupled to distinct interactive signaling pathways in intestinal muscle cells. *J Pharmacol Exp Ther* 274: 300-306, 1995.
120. **Murthy KS, Yee YS, Grider JR, and Makhlof GM.** Phorbol-stimulated Ca(2+) mobilization and contraction in dispersed intestinal smooth muscle cells. *J Pharmacol Exp Ther* 294: 991-996, 2000.
121. **Murthy KS, Zhou H, Grider JR, Brautigan DL, Eto M, and Makhlof GM.** Differential signalling by muscarinic receptors in smooth muscle: m2-mediated inactivation of myosin light chain kinase via Gi3, Cdc42/Rac1 and p21-activated kinase 1 pathway, and m3-mediated MLC20 (20 kDa regulatory light chain of myosin II) phosphorylation via Rho-associated kinase/myosin phosphatase targeting subunit 1 and protein kinase C/CPI-17 pathway. *Biochem J* 374: 145-155, 2003.

122. **Murthy KS, Zhou H, Grider JR, and Makhlof GM.** Inhibition of sustained smooth muscle contraction by PKA and PKG preferentially mediated by phosphorylation of RhoA. *Am J Physiol Gastrointest Liver Physiol* 284: G1006-1016, 2003.
123. **Murthy KS, Zhou H, Grider JR, and Makhlof GM.** Sequential activation of heterotrimeric and monomeric G proteins mediates PLD activity in smooth muscle. *Am J Physiol Gastrointest Liver Physiol* 280: G381-388, 2001.
124. **Murthy KS, Zhou H, Huang J, and Pentyala SN.** Activation of PLC-delta1 by Gi/o-coupled receptor agonists. *Am J Physiol Cell Physiol* 287: C1679-1687, 2004.
125. **Nakanishi-Matsui M, Zheng YW, Sulciner DJ, Weiss EJ, Ludeman MJ, and Coughlin SR.** PAR3 is a cofactor for PAR4 activation by thrombin. *Nature* 404: 609-613, 2000.
126. **Naldini A, Sower L, Bocci V, Meyers B, and Carney DH.** Thrombin receptor expression and responsiveness of human monocytic cells to thrombin is linked to interferon-induced cellular differentiation. *J Cell Physiol* 177: 76-84, 1998.
127. **Nanevich T, Ishii M, Wang L, Chen M, Chen J, Turck CW, Cohen FE, and Coughlin SR.** Mechanisms of thrombin receptor agonist specificity. Chimeric receptors and complementary mutations identify an agonist recognition site. *J Biol Chem* 270: 21619-21625, 1995.
128. **Nguyen C, Coelho AM, Grady E, Compton SJ, Wallace JL, Hollenberg MD, Cenac N, Garcia-Villar R, Bueno L, Steinhoff M, Bunnett NW, and Vergnolle N.** Colitis induced by proteinase-activated receptor-2 agonists is mediated by a neurogenic mechanism. *Can J Physiol Pharmacol* 81: 920-927, 2003.
129. **Nguyen TD, Moody MW, Steinhoff M, Okolo C, Koh DS, and Bunnett NW.** Trypsin activates pancreatic duct epithelial cell ion channels through proteinase-activated receptor-2. *J Clin Invest* 103: 261-269, 1999.
130. **Nishikawa H.** Role of protease-activated receptor-1 in modulation gastric acid secretion in rats. *Journal of Pharmacological Sciences* 91 (Suppl I): 259P, 1993.
131. **Nishikawa H, Kawai K, Nishimura S, Tanaka S, Araki H, Al-Ani B, Hollenberg MD, Kuroda R, and Kawabata A.** Suppression by protease-activated receptor-2 activation of gastric acid secretion in rats. *Eur J Pharmacol* 447: 87-90, 2002.
132. **Nystedt S, Emilsson K, Wahlestedt C, and Sundelin J.** Molecular cloning of a potential proteinase activated receptor. *Proc Natl Acad Sci U S A* 91: 9208-9212, 1994.
133. **Nystedt S, Larsson AK, Aberg H, and Sundelin J.** The mouse proteinase-activated receptor-2 cDNA and gene. Molecular cloning and functional expression. *J Biol Chem* 270: 5950-5955, 1995.
134. **Okamoto T, Ikezu T, Murayama Y, Ogata E, and Nishimoto I.** Measurement of GTP gamma S binding to specific G proteins in membranes using G-protein antibodies. *FEBS Lett* 305: 125-128, 1992.
135. **Olejar T, Matej R, Zadinova M, and Pouckova P.** Proteinase-activated receptor-2 expression on cerebral neurones after radiation damage: immunohistochemical observation in Wistar rats. *Int J Tissue React* 24: 81-88, 2002.
136. **Paing MM, Stutts AB, Kohout TA, Lefkowitz RJ, and Trejo J.** beta -Arrestins regulate protease-activated receptor-1 desensitization but not internalization or Down-regulation. *J Biol Chem* 277: 1292-1300, 2002.

137. **Parry MA, Myles T, Tschopp J, and Stone SR.** Cleavage of the thrombin receptor: identification of potential activators and inactivators. *Biochem J* 320 ( Pt 1): 335-341, 1996.
138. **Rahman A, Anwar KN, True AL, and Malik AB.** Thrombin-induced p65 homodimer binding to downstream NF-kappa B site of the promoter mediates endothelial ICAM-1 expression and neutrophil adhesion. *J Immunol* 162: 5466-5476, 1999.
139. **Rahman A, True AL, Anwar KN, Ye RD, Voyno-Yasenetskaya TA, and Malik AB.** Galpha(q) and Gbetagamma regulate PAR-1 signaling of thrombin-induced NF-kappaB activation and ICAM-1 transcription in endothelial cells. *Circ Res* 91: 398-405, 2002.
140. **Rasmussen UB, Vouret-Craviari V, Jallat S, Schlesinger Y, Pages G, Pavirani A, Lecocq JP, Pouyssegur J, and Van Obberghen-Schilling E.** cDNA cloning and expression of a hamster alpha-thrombin receptor coupled to Ca<sup>2+</sup> mobilization. *FEBS Lett* 288: 123-128, 1991.
141. **Reed DE, Barajas-Lopez C, Cottrell G, Velazquez-Rocha S, Dery O, Grady EF, Bunnett NW, and Vanner SJ.** Mast cell tryptase and proteinase-activated receptor 2 induce hyperexcitability of guinea-pig submucosal neurons. *J Physiol* 547: 531-542, 2003.
142. **Sabri A, Guo J, Elouardighi H, Darrow AL, Andrade-Gordon P, and Steinberg SF.** Mechanisms of protease-activated receptor-4 actions in cardiomyocytes. Role of Src tyrosine kinase. *J Biol Chem* 278: 11714-11720, 2003.
143. **Saifeddine M, al-Ani B, Cheng CH, Wang L, and Hollenberg MD.** Rat proteinase-activated receptor-2 (PAR-2): cDNA sequence and activity of receptor-derived peptides in gastric and vascular tissue. *Br J Pharmacol* 118: 521-530, 1996.
144. **Saifeddine M, Al-Ani B, Sandhu S, Wijesuriya SJ, and Hollenberg MD.** Contractile actions of proteinase-activated receptor-derived polypeptides in guinea-pig gastric and lung parenchymal strips: evidence for distinct receptor systems. *Br J Pharmacol* 132: 556-566, 2001.
145. **Schmidt VA, Nierman WC, Maglott DR, Cupit LD, Moskowitz KA, Wainer JA, and Bahou WF.** The human proteinase-activated receptor-3 (PAR-3) gene. Identification within a Par gene cluster and characterization in vascular endothelial cells and platelets. *J Biol Chem* 273: 15061-15068, 1998.
146. **Seeliger S, Derian CK, Vergnolle N, Bunnett NW, Nawroth R, Schmelz M, Von Der Weid PY, Buddenkotte J, Sunderkotter C, Metze D, Andrade-Gordon P, Harms E, Vestweber D, Luger TA, and Steinhoff M.** Proinflammatory role of proteinase-activated receptor-2 in humans and mice during cutaneous inflammation in vivo. *Faseb J* 17: 1871-1885, 2003.
147. **Shpacovitch VM, Brzoska T, Buddenkotte J, Stroh C, Sommerhoff CP, Ansel JC, Schulze-Osthoff K, Bunnett NW, Luger TA, and Steinhoff M.** Agonists of proteinase-activated receptor 2 induce cytokine release and activation of nuclear transcription factor kappaB in human dermal microvascular endothelial cells. *J Invest Dermatol* 118: 380-385, 2002.

148. **Somasundaram P, Ren G, Nagar H, Kraemer D, Mendoza L, Michael LH, Caughey GH, Entman ML, and Frangogiannis NG.** Mast cell tryptase may modulate endothelial cell phenotype in healing myocardial infarcts. *J Pathol* 205: 102-111, 2005.
149. **Steinhoff M, Vergnolle N, Young SH, Tognetto M, Amadesi S, Ennes HS, Trevisani M, Hollenberg MD, Wallace JL, Caughey GH, Mitchell SE, Williams LM, Geppetti P, Mayer EA, and Bunnett NW.** Agonists of proteinase-activated receptor 2 induce inflammation by a neurogenic mechanism. *Nat Med* 6: 151-158, 2000.
150. **Strigrow F, Riek-Burchardt M, Kiesel A, Schmidt W, Henrich-Noack P, Breder J, Krug M, Reymann KG, and Reiser G.** Four different types of protease-activated receptors are widely expressed in the brain and are up-regulated in hippocampus by severe ischemia. *Eur J Neurosci* 14: 595-608, 2001.
151. **Sugama Y, Tiruppathi C, offakidevi K, Andersen TT, Fenton JW, 2nd, and Malik AB.** Thrombin-induced expression of endothelial P-selectin and intercellular adhesion molecule-1: a mechanism for stabilizing neutrophil adhesion. *J Cell Biol* 119: 935-944, 1992.
152. **Tache Y, Pappas T, Lauffenburger M, Goto Y, Walsh JH, and Debas H.** Calcitonin gene-related peptide: potent peripheral inhibitor of gastric acid secretion in rats and dogs. *Gastroenterology* 87: 344-349, 1984.
153. **Takeeda M, Hayashi Y, Yamato M, Murakami M, and Takeuchi K.** Roles of endogenous prostaglandins and cyclooxygenase isoenzymes in mucosal defense of inflamed rat stomach. *J Physiol Pharmacol* 55: 193-205, 2004.
154. **Teng B, Murthy KS, Kuemmerle JF, Grider JR, Sase K, Michel T, and Makhlof GM.** Expression of endothelial nitric oxide synthase in human and rabbit gastrointestinal smooth muscle cells. *Am J Physiol* 275: G342-351, 1998.
155. **Teng BQ, Grider JR, and Murthy KS.** Identification of a VIP-specific receptor in guinea pig tenia coli. *Am J Physiol Gastrointest Liver Physiol* 281: G718-725, 2001.
156. **Tiruppathi C, Yan W, Sandoval R, Naqvi T, Pronin AN, Benovic JL, and Malik AB.** G protein-coupled receptor kinase-5 regulates thrombin-activated signaling in endothelial cells. *Proc Natl Acad Sci U S A* 97: 7440-7445, 2000.
157. **Toothill VJ, Van Mourik JA, Niewenhuis HK, Metzelaar MJ, and Pearson JD.** Characterization of the enhanced adhesion of neutrophil leukocytes to thrombin-stimulated endothelial cells. *J Immunol* 145: 283-291, 1990.
158. **Toyoda N, Gabazza EC, Inoue H, Araki K, Nakashima S, Oka S, Taguchi Y, Nakamura M, Suzuki Y, Taguchi O, Imoto I, Suzuki K, and Adachi Y.** Expression and cytoprotective effect of protease-activated receptor-1 in gastric epithelial cells. *Scand J Gastroenterol* 38: 253-259, 2003.
159. **Ubl JJ, Vohringer C, and Reiser G.** Co-existence of two types of [Ca<sup>2+</sup>]<sub>i</sub>-inducing protease-activated receptors (PAR-1 and PAR-2) in rat astrocytes and C6 glioma cells. *Neuroscience* 86: 597-609, 1998.
160. **Vartanian KB, Chen HY, Kennedy J, Beck SK, Ryaby JT, Wang H, and Hoying JB.** The non-proteolytically active thrombin peptide TP508 stimulates angiogenic sprouting. *J Cell Physiol* 206: 175-180, 2006.
161. **Vergnolle N.** Proteinase-activated receptor-2-activating peptides induce leukocyte rolling, adhesion, and extravasation in vivo. *J Immunol* 163: 5064-5069, 1999.

162. **Vergnolle N, Derian CK, D'Andrea MR, Steinhoff M, and Andrade-Gordon P.** Characterization of thrombin-induced leukocyte rolling and adherence: a potential proinflammatory role for proteinase-activated receptor-4. *J Immunol* 169: 1467-1473, 2002.
163. **Vergnolle N, Macnaughton WK, Al-Ani B, Saifeddine M, Wallace JL, and Hollenberg MD.** Proteinase-activated receptor 2 (PAR2)-activating peptides: identification of a receptor distinct from PAR2 that regulates intestinal transport. *Proc Natl Acad Sci U S A* 95: 7766-7771, 1998.
164. **Vu TK, Hung DT, Wheaton VI, and Coughlin SR.** Molecular cloning of a functional thrombin receptor reveals a novel proteolytic mechanism of receptor activation. *Cell* 64: 1057-1068, 1991.
165. **Vu TK, Wheaton VI, Hung DT, Charo I, and Coughlin SR.** Domains specifying thrombin-receptor interaction. *Nature* 353: 674-677, 1991.
166. **Wang H, Ubl JJ, and Reiser G.** Four subtypes of protease-activated receptors, co-expressed in rat astrocytes, evoke different physiological signaling. *Glia* 37: 53-63, 2002.
167. **Xu WF, Andersen H, Whitmore TE, Presnell SR, Yee DP, Ching A, Gilbert T, Davie EW, and Foster DC.** Cloning and characterization of human protease-activated receptor 4. *Proc Natl Acad Sci U S A* 95: 6642-6646, 1998.
168. **Yu Z, Ahmad S, Schwartz JL, Banville D, and Shen SH.** Protein-tyrosine phosphatase SHP2 is positively linked to proteinase-activated receptor 2-mediated mitogenic pathway. *J Biol Chem* 272: 7519-7524, 1997.
169. **Zhao A and Shea-Donohue T.** PAR-2 agonists induce contraction of murine small intestine through neurokinin receptors. *Am J Physiol Gastrointest Liver Physiol* 285: G696-703, 2003.
170. **Zhou H, Das S, and Murthy KS.** Erk1/2- and p38 MAP kinase-dependent phosphorylation and activation of cPLA2 by m3 and m2 receptors. *Am J Physiol Gastrointest Liver Physiol* 284: G472-480, 2003.
171. **Zhou H, Huang J, and Murthy K.** Lysophosphatidic acid (LPA) interacts with LPA3 receptors to activate selectively Gq and induce initial and sustained MLC20 phosphorylation and contraction (Abstract). *Gastroenterology* 126: A278, 2004.
172. **Zhou H and Murthy KS.** Distinctive G protein-dependent signaling in smooth muscle by sphingosine 1-phosphate receptors S1P1 and S1P2. *Am J Physiol Cell Physiol* 286: C1130-1138, 2004.
173. **Zhu WJ, Yamanaka H, Obata K, Dai Y, Kobayashi K, Kozai T, Tokunaga A, and Noguchi K.** Expression of mRNA for four subtypes of the proteinase-activated receptor in rat dorsal root ganglia. *Brain Res* 1041: 205-211, 2005.